

NASA TECHNICAL NOTE



NASA TN D-4741

NASA TN D-4741



LOAN COPY: RETURN TO  
AI WL (WLIL-2)  
KIRTLAND AFB, N MEX

# INFRARED HORIZON PROFILES FOR SUMMER CONDITIONS FROM PROJECT SCANNER

*by Thomas B. McKee, Ruth I. Whitman, and Richard E. Davis*

*Langley Research Center*

*Langley Station, Hampton, Va.*



0131270

✓  
INFRARED HORIZON PROFILES FOR SUMMER CONDITIONS

FROM PROJECT SCANNER

By Thomas B. McKee, Ruth I. Whitman,  
and Richard E. Davis

Langley Research Center  
Langley Station, Hampton, Va.

✓  
NATIONAL AERONAUTICS AND SPACE ADMINISTRATION

For sale by the Clearinghouse for Federal Scientific and Technical Information  
Springfield, Virginia 22151 - CFSTI price \$3.00



## CONTENTS

SUMMARY . . . . .	1
INTRODUCTION . . . . .	1
SYMBOLS . . . . .	2
BACKGROUND . . . . .	4
Theoretical Work . . . . .	6
Experimental Work . . . . .	7
PROJECT SCANNER EXPERIMENT . . . . .	8
DATA REDUCTION . . . . .	8
Dual Radiometer Data . . . . .	8
Radiance data . . . . .	10
Time delays . . . . .	12
Mirror angle . . . . .	13
Radar Data . . . . .	13
Tangent Height Calculation . . . . .	14
Reference spheroid . . . . .	14
Transformations . . . . .	14
Tangent height . . . . .	15
Radiance profiles . . . . .	15
Resultant Data Accuracy . . . . .	16
DATA PRESENTATION AND DISCUSSION . . . . .	18
Meteorological Rocket Network Support . . . . .	18
Analytical Profiles for CO <sub>2</sub> Spectral Band . . . . .	19
Radiative transfer equation . . . . .	19
Solution of transfer equation . . . . .	19
Factors affecting calculation of transfer equation . . . . .	20
Measured Profiles for CO <sub>2</sub> Spectral Band . . . . .	21
Measured Profiles for H <sub>2</sub> O Spectral Band . . . . .	23
Analytical Profiles for H <sub>2</sub> O Spectral Band . . . . .	24
Determination of Water-Vapor Mixing Ratio . . . . .	25
CONCLUDING REMARKS . . . . .	26
APPENDIX A – PROJECT SCANNER EXPERIMENT AND INSTRUMENTATION . . .	28
Operational Description . . . . .	28
Dual Radiometer Assembly . . . . .	29
Star Mapper . . . . .	33
Star-Mapper Data . . . . .	34

Telemetry . . . . .	34
Radar Tracking . . . . .	35
APPENDIX B – METEOROLOGICAL DATA . . . . .	36
Temperature and Pressure . . . . .	36
Water Vapor . . . . .	37
Nephanalysis . . . . .	38
Accuracy . . . . .	38
REFERENCES . . . . .	40
TABLES . . . . .	44
FIGURES . . . . .	94

# INFRARED HORIZON PROFILES FOR SUMMER CONDITIONS

## FROM PROJECT SCANNER

By Thomas B. McKee, Ruth I. Whitman,  
and Richard E. Davis  
Langley Research Center

### SUMMARY

Measured horizon radiance profiles in spectral bands of  $615\text{ cm}^{-1}$  to  $715\text{ cm}^{-1}$  ( $\text{CO}_2$ ) and  $315\text{ cm}^{-1}$  to  $475\text{ cm}^{-1}$  ( $\text{H}_2\text{O}$ ) from Project Scanner flight of August 16, 1966, are shown. Data cover a latitude range from  $10^\circ\text{ N}$  to  $57^\circ\text{ N}$ . Excellent agreement between measured and independently analytically predicted radiance profiles in the  $\text{CO}_2$  region confirms that the analytical technique is within the experimental accuracy. The agreement of measured with predicted profiles and the lack of dependence on the presence of clouds indicate that the  $615\text{ cm}^{-1}$  to  $715\text{ cm}^{-1}$  spectral region is a leading choice for attitude determination applications. Horizon profiles in the  $315\text{ cm}^{-1}$  to  $475\text{ cm}^{-1}$  spectral region show a strong dependence on the presence of clouds; therefore this spectral region would be a poor choice for attitude determination applications. Mixing ratios of water vapor deduced from the radiance measurements indicate little latitudinal variation and are less than  $0.017\text{ g/kg}$  at altitudes between  $16\text{ km}$  and  $33\text{ km}$ .

### INTRODUCTION

Throughout the space era to the present time manned and unmanned spacecraft have employed horizon sensing systems by which the earth's limb or horizon was sensed to determine and sometimes control the attitude of the spacecraft. The desire for these devices to operate both day and night led to sensors in the infrared region of the spectrum where the horizon characteristics are produced by the contrast of the "cold" of space with the thermal emissions of the earth and its atmosphere.

Flight experiences have revealed operational problems with the first-generation horizon scanners which were identified as being due to high cold clouds and not due to basic instrument limitations. Thus, there was added emphasis for increased knowledge and understanding of the characteristics of the input to these devices, the horizon itself, or, more particularly, the horizon radiance profile. Indeed, it is evident that a perfect instrument reflects the variabilities of the input. Therefore, the NASA Project Scanner

has been directed to the study of the radiance profiles of the earth's horizon, or horizon definition research.

The purpose of this report is to describe the Project Scanner experiment and to present the horizon radiance profiles measured during the first flight in August 1966. The relation of this experiment and the results to previous theoretical and experimental data is described as are the pertinent details of the instruments used. The meteorological situation existing as the flight measurements were made is described since these atmospheric conditions are the inputs to the theoretical methods used to calculate radiance profiles for comparison with the measured data. The measured and analytical profiles are presented as tabular data as well as graphs for increased utility in possible future analyses.

## SYMBOLS

A	amplitude ratio, dimensionless
b	intercept of line equation
B	coefficient in Fourier series, volts
$C_1$	constant, $1.1909 \times 10^{-5}$ erg-centimeter <sup>2</sup> /second-steradian
$C_2$	constant, 1.4389 centimeters-degrees
DEH	coordinate transformation matrix
e	partial pressure of water vapor, millibars
f	input to radiometer, volts
g	output of radiometer, volts
$GHA_\gamma$	Greenwich hour angle of Aries, degrees
GMT	Greenwich mean time
h	altitude, kilometers
H	tangent height, kilometers

$i,j$	integers
$J_\nu$	source function, watts/meter <sup>2</sup> -steradian-centimeter <sup>-1</sup>
$k$	radiance responsivity, volts-meters <sup>2</sup> -steradian/watt
$l$	period for Fourier series
$L$	latitude, degrees
$m$	slope in line equation
$M$	coordinate transformation matrix
$n$	number of term in Fourier series
$N$	radiance, watts/meter <sup>2</sup> -steradian
$N_\nu$	spectral radiance, watts/meter <sup>2</sup> -steradian-centimeter <sup>-1</sup>
$p$	pressure, millibars
$r$	radius, kilometers
$r_e$	equatorial radius, kilometers
$r_p$	polar radius, kilometers
$\vec{R}_1$	vector from center of earth to spacecraft
$\vec{R}_2$	vector from center of earth normal to $\vec{S}$
$s$	distance along line of sight, kilometers
$\vec{S}$	radiometer line of sight vector from spacecraft
$t$	time, seconds
$t_0$	reference time for each mirror scan, seconds

$\Delta t$	time delay, seconds
$T$	temperature, degrees Kelvin
$V$	voltage, volts
$\Delta V$	voltage difference, volts
$w$	water-vapor mixing ratio, grams/kilogram
$W_\nu$	spectral radiant emittance, watts/meter <sup>2</sup> -centimeter <sup>-1</sup>
$x,y,z$	Cartesian coordinates, kilometers
$\alpha,\beta,\gamma$	direction angles, degrees
$\eta$	mirror angle, degrees
$\Delta\eta$	angular spacing of elemental fields of view, degrees
$\theta$	reflectance of calibration optics, dimensionless
$\lambda$	longitude, degrees
$\nu$	wave number, centimeter <sup>-1</sup>
$\rho$	spherical coordinate, kilometers
$\sigma$	standard deviation
$\tau$	transmittance, dimensionless
$\varphi$	spectral response of radiometer, dimensionless
$\Phi$	phase angle, degrees

## BACKGROUND

Even the most cursory look at the earth's horizon reveals that what is seen is not necessarily the true solid-earth horizon. Man's experience from aircraft and in space

indicates that in the visible region of the spectrum to which the eye is sensitive the solid-earth boundary is not always discernible. Clouds and scattering of solar radiation by the atmosphere are the most important factors in this region and cause the indistinctness of the horizon. And, of course, at night even under conditions of moonlight the aforementioned factors still exist but have a much reduced contrast with the space reference. Since earth satellites experience day and night effects during each orbit, it was recognized that infrared sensors would be required if horizon scanners were to be of significant value in furnishing information on the attitude of a spacecraft. The infrared region at wavelengths greater than about  $5\mu$  is the part of the spectrum of interest since the thermal emission of the warm earth is at these wavelengths and also there is very little reflected solar radiation. After some of the flight experiences with the early horizon scanners, it became quite evident that the infrared region is not immune to disturbing factors. Again, what is "seen" is not the solid-earth—space interface but a view which is very strongly influenced by the atmosphere. The high cold cloud problem, mentioned previously, results from this influence. The infrared horizon is therefore characterized by no sharp thermal discontinuity between the warm earth and the cold space. The characterization is rather one of a gradient which has been termed the "horizon radiance profile" or the "earth limb radiance profile."

The usefulness of a horizon sensor does not necessarily require the detection of the solid-earth horizon. The detection of a characteristic of the radiance profile could provide and indeed does provide the necessary information for the tasks assigned to the horizon scanner device. Therefore, a meaningful measurement effort not only must measure the radiance accurately but also must determine accurately the positioning of the measured profile to the solid earth. The variability of the profile characteristic which is detected by a horizon sensor is a direct input-induced error to that system. (Ref. 1 defines many of the profile characteristics that are sensed by present-day horizon scanners.)

Recognition of the atmospheric effects just noted and exemplified by the operational problems of early horizon scanners led to an increased emphasis in the study of those atmospheric processes which give rise to the radiance profile and to how horizon scanner design should evolve to overcome the identified problems. For example, it was recognized that selection of the spectral region for the instrument sensitivity could reduce the effects of clouds and other variabilities in horizon profile characteristics. Spectral regions related to two strong absorption bands of atmospheric constituents were identified as the most promising. These bands were the  $665\text{ cm}^{-1}$   $\text{CO}_2$  band ( $15\mu$ ) and part of the extensive rotational water vapor band (wavelengths greater than about  $17\mu$ ). Emphasis was in these bands rather than at shorter wavelengths since the various atmospheric windows (at  $10\mu$  to  $12\mu$  and less) were avoided and also more energy might be available inasmuch as the effective blackbody temperatures associated with these atmospheric

radiations tended to give maximum radiance at wavelengths greater than about  $12\mu$ . Theoretical studies indicated that the  $\text{CO}_2$  band should be more promising since  $\text{CO}_2$  has a known constant mixing ratio in the atmosphere and absorbs strongly enough to limit the effects of clouds and the variable lower atmosphere. Water vapor is considered because it is a strong absorber and is active over a wide spectral range. However, the water-vapor mixing ratio is variable with altitude and time; these variations could cause significant changes in the horizon profile. Techniques were rapidly developed to predict the radiance profiles associated with various atmospheric representations. Beginnings were also made in the experimental investigations to support the theoretical predictions. These activities are discussed briefly herein. The most recent and comprehensive state-of-the-art summary in this topical area is reference 2.

### Theoretical Work

Considerable activity has been generated with regard to the analytical prediction of the infrared horizon radiance profile. Required for this effort is the well-founded theory of radiative transfer. Thermal radiation from the earth and the atmosphere has been the only source of energy considered in these calculations. The atmosphere is considered to be divided into an arbitrary number of spherical shells for which the temperature, pressure, and density are known. From a point outside the atmosphere it is necessary to sum the contributions of the various shell elements along different lines of sight through the atmosphere. These individual contributions are determined by a source function dependent on temperature and frequency (or wavelength) and by the spectral transmissivity which is a function of the particular gas and its effective pressure, temperature, and optical path. The factor that is most uncertain in such an analysis is the spectral transmissivity of the atmospheric gases since laboratory measurements on which to base such calculations do not exist for the combinations of pressures and optical paths which exist in the upper atmosphere. Various transmissivity models have been developed for use in these calculations.

References 3 to 13 are sources listed chronologically which contain radiance profile calculations. Various infrared wavelength regions and atmospheric conditions are presented in these sources, as well as different ways of handling the transmissivity representations for the different atmospheric constituents considered. References 11 and 13 present the most systematic collections of radiance profiles available. Reference 11 uses climatological data to represent latitudinal variations over a year's period. Reference 13 is more comprehensive in that eight synoptic situations as well as climatological data are used over a somewhat more extensive longitude range to depict the latitudinal results over a year's period. The method described in reference 12 was used for the results presented in reference 13 and for the theoretical profiles which are compared with the

experimental measurements reported herein. A more complete description of this method is contained in the section entitled "Analytical Profiles for CO<sub>2</sub> Band."

### Experimental Work

From the point of view of horizon definition research the experimental approaches capable of verifying the theory have been few indeed. However, several experiments have been conducted with at least a strong emphasis in their planning related to horizon sensor problems, especially the problem of cloud effects. In particular, various spectral regions have been investigated to determine the gross contrast between earth and space and the effects of clouds while viewing the earth. References 14 to 17, presented chronologically, are illustrative in this respect. In particular, references 15 and 16 illustrate the impact that the theoretical studies had with respect to the potential advantages of the 15 $\mu$  CO<sub>2</sub> band to overcome some of the experienced horizon scanner problems. A review of these experiments is presented in reference 2.

Only three experimental efforts have been directed primarily toward horizon definition research in the infrared in the sense of angular resolution sufficient to define the radiance profile and to measure the positioning of the profile with respect to the solid earth. These experiments are as follows:

- (1) The NASA-LRC flights of a radiometer aboard the X-15 research airplane (ref. 18)
- (2) The DOD-AFCRL flights of a multichannel radiometer on an Aerobee rocket probe (ref. 19)
- (3) The NASA-LRC flights of Project Scanner

The NASA-LRC work in horizon definition is described in references 20 and 21 with some results from the initial Project Scanner flight being given in references 21 and 22.

Table I is presented as a means of relating the experimental results referenced herein to the topic of horizon definition. In this table the term "vertical spatial resolution" means the vertical distance subtended by the field at the distance of the horizon from the instrument. The term "spatial positioning" is the accuracy to which the radiometer line-of-sight tangent height is known with respect to the solid earth. In some of the experiments no positioning data were available. Also, the Tiros reference data are omitted from the table because of the very large field of view (5<sup>0</sup>). The details of the Project Scanner values are presented in subsequent sections. As indicated in table I, the NASA-LRC data represent the best measurements of the horizon radiance profiles currently available.

## PROJECT SCANNER EXPERIMENT

The Project Scanner experiment was conducted on a suborbital rocket vehicle launched from Wallops Island, Virginia, at 0618 GMT on August 16, 1966. Peak altitude attained in the flight was 620 km. An operational schematic of the flight experiment is shown in figure 1. After the spacecraft was erected near the local vertical, scanning mirrors in the radiometer provided the vertical scan motion for horizon crossings and spacecraft spin allowed the horizon crossings to be at different azimuths. The necessary inertial orientation information was obtained from the star mapper. Development and testing of the star mapper are described in reference 23, and a detailed discussion of the determination of inertial orientation by using star-mapper data is presented in reference 24. A very limited description of the star mapper and associated data reduction are given in appendix A of this report. The dual radiometer used in the present experiment was actually two radiometers mounted back to back; one was sensitive in a spectral band ( $\text{CO}_2$ ) of  $615\text{ cm}^{-1}$  to  $715\text{ cm}^{-1}$  ( $16.3\mu$  to  $14.0\mu$ ) and the other was sensitive in a spectral band ( $\text{H}_2\text{O}$ ) of  $315\text{ cm}^{-1}$  to  $475\text{ cm}^{-1}$  ( $31.8\mu$  to  $21.1\mu$ ). Development and testing of the dual radiometer are described in reference 25. A detailed description of the instrument and the characteristics needed to interpret the radiometric data, which includes spectral response, frequency response, field of view, scan mirror operation, and preflight calibration, are included in appendix A. Also included in appendix A is a brief description of the telemetry and radar tracking used for the experiment.

## DATA REDUCTION

All data were transmitted to ground based receivers and recorded as a function of time during flight. A ground-based time generator provided the time code which was recorded on magnetic tapes along with flight data in real time. In data reduction the primary data of the star mapper, dual radiometer, and radar were first processed as a function of time and then combined to determine radiance as a function of tangent height. A block diagram of the data reduction process is shown in figure 2. The processing of the dual radiometer and radar data and the calculation of tangent height are described in this section. A brief description of star-mapper data reduction is given in appendix A.

### Dual Radiometer Data

Reduction of the dual radiometer data follows two separate paths. The upper path in figure 2 indicates the processing of radiance data. The lower path describes the handling of mirror angle data which is telemetered for brief periods through one of the radiance data channels.

Radiance data were taken continuously during flight. However, only data periods of 0.5 sec during a 3.2 sec scan period which record the horizon crossings were useful. These periods were hand selected from oscillograph records, filtered for high-frequency noise, converted to digital form, processed to obtain radiometer output voltage as a function of time, stored on magnetic tape, and listed. The list was then hand edited to select three data points within the 0.5-sec period needed for conversion from voltage to radiance.

Mirror angle data were transmitted from each side of the radiometer through one of the radiometer channels. The information was a series of eight coded pulses for each cycle of the scan mirrors. Radiance data were interrupted for 4 msec for each coded pulse. Data from the dual radiometer data tape were passed through a 5000-Hz linear phase filter, which preserves the steep slopes of the coded pulses, to a position pulse recognition scheme which determined the time and amplitude of each pulse. Time and amplitude data were then listed so that the list could be hand edited to eliminate bad data. Mirror angle calibration data are combined with the time and amplitude data to form a history of time  $t_i$  and mirror angle  $\eta_i$ . Each group of eight points defines a scan period and each group of four defines the linear portion of the up and down scans. All the down scan groups of four are put together and a straight line is fitted to each group of four points with the following form:

$$\eta = m(t - t_0) + b \quad (1)$$

where

$$m = \frac{4 \sum_{i=1}^4 (t_i - t_0) \eta_i - \sum_{i=1}^4 (t_i - t_0) \sum_{i=1}^4 \eta_i}{4 \sum_{i=1}^4 (t_i - t_0)^2 - \left[ \sum_{i=1}^4 (t_i - t_0) \right]^2} \quad (2)$$

and

$$b = \frac{\sum_{i=1}^4 (t_i - t_0)^2 \sum_{i=1}^4 \eta_i - \sum_{i=1}^4 (t_i - t_0) \sum_{i=1}^4 (t_i - t_0) \eta_i}{4 \sum_{i=1}^4 (t_i - t_0)^2 - \left[ \sum_{i=1}^4 (t_i - t_0) \right]^2} \quad (3)$$

The slope, intercept, and reference time  $t_0$  for each scan are used with voltage and time data as inputs to the dual radiometer data reduction program (fig. 2). The dual

radiometer data reduction program must convert voltage to radiance, compensate time for time delays, and compute a mirror angle for each data point for all five detectors.

Radiance data.- Radiometric calibration (appendix A) relates effective radiance to a voltage difference; thus a voltage difference from a known reference must be determined. A zero radiance source is assumed when the radiometer is pointed away from the earth at space. One cycle of the radiometer voltage output as a function of time is shown in figure 3. The scan proceeds from earth across the horizon to space, then back across the horizon to the earth again. While the radiometer looks at space, the output voltage is decaying to a steady-state level. The decay is interrupted briefly for an internal flight calibration of the radiometer. If a time period of 1 second is allowed between one horizon and the next, the slope of the output function becomes small enough so that a straight line provides a very good description of the output. Consequently, a straight line is fitted to the output from  $t_1$  to  $t_2$  (the first and last times used in line fit). A slope and an intercept are determined in a manner similar to that used in equations (2) and (3). The resulting equation is

$$V = m(t - t_1) + b \quad (4)$$

For  $t_2 \leq t_i \leq t_3$  ( $t_2$  and  $t_3$  being the first and last times used for radiance data), the voltage difference of the signal from the space reference is

$$\Delta V = V_i - m(t_i - t_1) - b \quad (5)$$

where at any time  $t_i$  there is a voltage  $V_i$ .

Next the  $\Delta V$ 's must be converted to radiance. In radiometric calibration each detector was calibrated with the blackbody sources, and a radiance responsivity  $k$  was determined from the following equation:

$$\Delta V = k \int_0^{\infty} [N_{\nu}(T) - N_{\nu}(77^{\circ} \text{ K})] \varphi(\nu) \theta(\nu) d\nu \quad (6)$$

In flight a value of  $\Delta V$  is measured which is given by

$$\Delta V = k \int_0^{\infty} N_{\nu}(H) \varphi(\nu) d\nu \quad (7)$$

where  $k$  is determined in preflight calibration. The purpose of the experimental measurement was to deduce the radiance of the horizon profile in a spectral band given by

$$N(H) = \int_{\nu_1}^{\nu_2} N_{\nu}(H) d\nu \quad (8)$$

and not by the integral expression in equation (7) which contains the effect of the spectral response of the measuring instrument. Unfortunately, the spectral shape of the source measured in flight  $N_{\nu}(H)$  is not the same as that of the source used in calibration  $N_{\nu}(T)$ .

To determine  $N(H)$ , an assumption must be made of the spectral shape of  $N_{\nu}(H)$ . The assumption is made that the analytically computed shape of  $N_{\nu}(H)$  is correct which

allows one to calculate the useful integral ratio  $\frac{\int_{\nu_1}^{\nu_2} N_{\nu}(H) d\nu}{\int N_{\nu}(H) \varphi(\nu) d\nu}$ . Now, rearrange equation (7) to be

$$\int N_{\nu}(H) \varphi(\nu) d\nu = \frac{\Delta V}{k} \quad (9)$$

Multiply both sides of equation (9) by the integral ratio to get

$$\int N_{\nu}(H) \varphi(\nu) d\nu \left[ \frac{\int_{\nu_1}^{\nu_2} N_{\nu}(H) d\nu}{\int N_{\nu}(H) \varphi(\nu) d\nu} \right] = \frac{\Delta V}{k} \left[ \frac{\int_{\nu_1}^{\nu_2} N_{\nu}(H) d\nu}{\int N_{\nu}(H) \varphi(\nu) d\nu} \right] \quad (10)$$

Then

$$\int_{\nu_1}^{\nu_2} N_{\nu}(H) d\nu = \frac{\Delta V}{k} \left[ \frac{\int_{\nu_1}^{\nu_2} N_{\nu}(H) d\nu}{\int N_{\nu}(H) \varphi(\nu) d\nu} \right] \quad (11)$$

But by definition of  $N(H)$  in equation (8)

$$N(H) = \frac{\Delta V}{k} \left[ \frac{\int_{\nu_1}^{\nu_2} N_{\nu}(H) d\nu}{\int N_{\nu}(H) \varphi(\nu) d\nu} \right] \quad (12)$$

The 1962 U.S. Standard Atmosphere (ref. 26) was used in evaluating the integral ratio. A change in the ratio of less than 2 percent is found as tangent height changes from 20 km to 50 km for the 615  $\text{cm}^{-1}$  to 715  $\text{cm}^{-1}$  band. For the present work the integral ratio value for a tangent height of 20 km is used; the change in radiance due to this effect at higher tangent heights is much smaller than the experimental accuracy.

In the 315  $\text{cm}^{-1}$  to 475  $\text{cm}^{-1}$  spectral region the problem of radiance determination is more serious because the water-vapor mixing ratio is variable and must be specified in addition to temperature and pressure. Both dry (ref. 7) and wet mixing ratios, given in table II, were investigated with the 1962 U.S. Standard Atmosphere in evaluating the integral ratio for  $\text{H}_2\text{O}$ . The atmosphere labeled wet is saturated up to  $h = 33$  km with a constant mixing ratio above this altitude. Also given in table II are the integral ratios normalized to the value at  $h = 15$  km for the dry atmosphere. Notice that the integral ratio is quite stable for both atmospheres up to an altitude of 30 km. Above this altitude the conversion for voltage to radiance is strongly dependent on tangent height. The value of the integral ratio at  $h = 15$  km for the dry atmosphere was used for all data to be presented.

Time delays.- Two time delays are introduced into the radiometric data; these delays must be removed. The first time delay is introduced through the electrical filters of the telemetry system and is easily determined since the filters are linear phase filters. Values differ slightly from channel to channel but 4.3 msec is typical. The second time delay is caused by the dual radiometer. Both the thermistor bolometer detectors and the amplifiers contribute. No simple definition exists of this time delay because the radiometer phase response is not linear. However, a quantitative determination of the effective time delay is possible.

Consider an idealization of the periodic waveform which is the input to the radiometer during the flight condition. One cycle of the near square wave is completed in 3.2 sec, which is in accord with the scan period of the radiometer. The horizon crossings are one-half cycle of a sine wave which take 50 msec. This time is typical of the flight experience. By inspection the ideal input function  $f(t)$  can be made antisymmetric about  $t = 0$ . The function  $f(t)$  may be represented by a Fourier sine series

$$f(t) = \sum_{n=1}^{\infty} B_n \sin \frac{n\pi t}{l} \quad (13)$$

where

$$B_n = \frac{2}{l} \int_0^l f(t) \sin \frac{n\pi t}{l} dt \quad (14)$$

When  $f(t)$  is processed through the radiometer with frequency characteristics given in appendix A, the output  $g(t)$  is a sine series having modified amplitude and phase; the output is given by

$$g(t) = \sum_{n=1}^{\infty} A_n B_n \sin\left(\frac{n\pi t}{l} + \Phi_n\right) \quad (15)$$

In figure 4(a), the input curve  $f(t)$  and the output curve  $g(t)$  are shown for the time of the horizon crossing. Apply a time delay  $\Delta t$  to make the two curves coincident at a time 25 msec into the horizon crossing; the result is noted in figure 4(b). An estimate of errors introduced in the experiment due to the frequency response is the difference in the curves shown in figure 4(b) with the exception that the difference at the peak amplitude of 2.0 is nearly accounted for in the radiometric calibration. In practice the time delay is determined by using a straight line for a horizon crossing instead of a sine wave; however, the time delays are nearly identical and the sine wave representation gives a much better view of the errors introduced by the frequency response. These time delays are determined for each detector channel and are added to the time delay due to telemetry and subtracted from the time  $t_i$  stored with the radiance data.

Mirror angle.— A mirror angle is needed for each detector at each time. An angle  $\Delta\eta$  which defines the location of each detector relative to the center one is measured in the laboratory. This  $\Delta\eta$  is incorporated along with time delay in equation (1) to yield

$$\eta = m(t - t_0 - \Delta t) + b + \Delta\eta \quad (16)$$

For each scan from space to earth the values of  $m$ ,  $b$ , and  $t_0$  are constant so that the angle data at the  $i$ th time for the  $j$ th detector is given by

$$\eta_{i,j} = m(t_{i,j} - t_0 - \Delta t_j) + b + \Delta\eta_j \quad (17)$$

### Radar Data

Radar data reduction is accomplished at the NASA Wallops Station as a service to the range user. Pertinent data, which include latitude and longitude of subspacecraft point, altitude, and time, are stored on magnetic tape. All position data are based on a Fischer spheroid (ref. 27).

### Tangent Height Calculation

All information necessary for a calculation of tangent height has been discussed. Tangent height  $H$  is defined (fig. 5) as the distance along a geocentric radius vector from the surface of the earth to the point where the radius vector is normal to the line of sight  $\vec{S}$ . In practice the known parameters in figure 5 are  $\vec{R}_1$  through the radar data and earth model and the direction of  $\vec{S}$  in a star-mapper-oriented coordinate system through the mirror angle  $\eta$ . Time is also known. In solving the problem for  $H$  and  $L, \lambda$  of the vector  $\vec{R}_2$ , the total vector  $\vec{S}$  must be found in an earth centered system and then  $\vec{R}_2$  may be determined. Once  $\vec{R}_2$  is found  $H$ ,  $L$ , and  $\lambda$  are computed for each set of  $N_i$ ,  $\eta_i$ , and  $t_i$  for each detector.

Reference spheroid.- For the calculation the relationship of radius as a function of geocentric latitude must be known and is given by

$$r = \frac{r_p}{\left[ 1 - \left( \frac{r_e^2 - r_p^2}{r_e^2} \right) \cos^2 L \right]^{1/2}} \quad (18)$$

In the present work the Fischer spheroid (ref. 27) has been used; the radii are  $r_e = 6378.166$  km and  $r_p = 6356.784$  km.

Transformations.- Transformation of the  $\vec{S}$  vector from a star-mapper coordinate system to an inertial system is already available. It is the inverse of the transformation needed to solve the spacecraft orientation problem with the star mapper and is given in equation (25) in reference 24. Direction of  $\vec{S}$  is

$$\underbrace{\left( \frac{\vec{S}}{|\vec{S}|} \right)}_{\text{Inertial}} = (DEH)^{-1} \underbrace{\left( \frac{\vec{S}}{|\vec{S}|} \right)}_{\text{Star mapper}} \quad (19)$$

One rotation of the inertial axis by the  $GHA_\gamma$  aligns the X-axis with Greenwich, England, and thus the system is earth centered. The transformation is

$$M = \begin{pmatrix} \cos GHA_\gamma & \sin GHA_\gamma & 0 \\ -\sin GHA_\gamma & \cos GHA_\gamma & 0 \\ 0 & 0 & 1 \end{pmatrix} \quad (20)$$

Now the direction of the  $\vec{S}$  vector is

$$\left( \frac{\vec{S}}{|\vec{S}|} \right)_{\text{Earth}} = M(\text{DEH})^{-1} \left( \frac{\vec{S}}{|\vec{S}|} \right)_{\text{Star mapper}} \quad (21)$$

Orientation of the  $\vec{S}$  vector in the star-mapper system is known through the mirror angle  $\eta$ ; thus, the orientation in the earth system is available from equation (21). The x,y,z coordinates of the earth system are related to latitude, longitude, and direction cosines by the following equations:

$$\left. \begin{aligned} x &= \rho \cos L \cos \lambda = \rho \cos \alpha \\ y &= -\rho \cos L \sin \lambda = \rho \cos \beta \\ z &= \rho \sin L = \rho \cos \gamma \end{aligned} \right\} \quad (22)$$

Once x, y, and z are determined, then  $\rho$ , L,  $\lambda$ ,  $\alpha$ ,  $\beta$ , and  $\gamma$  can also be determined.

Tangent height.- From the right triangle involving  $\vec{R}_1$ ,  $\vec{R}_2$ , and  $\vec{S}$  in figure 5, the magnitude of  $\vec{S}$  is given by

$$|\vec{S}| = -\vec{R}_1 \cdot \left( \frac{\vec{S}}{|\vec{S}|} \right) \quad (23)$$

Now the vector  $\vec{R}_2$  may be found by

$$\vec{R}_2 = \vec{R}_1 + \vec{S} \quad (24)$$

From  $\frac{\vec{R}_2}{|\vec{R}_2|}$  the latitude and longitude are found by using equation (22). Then the radius

at the tangent point is found from equation (18). Finally tangent height is given by

$$H = |\vec{R}_2| - r_2 \quad (25)$$

Radiance profiles.- When H, L, and  $\lambda$  are computed, a complete description of the horizon profile is contained in the set of  $H_i$ ,  $L_i$ ,  $\lambda_i$ , and  $N_i$ . To make following analyses simpler, these four parameters are linearly interpolated to yield tangent height at even 1-km increments.

Since signal-to-noise ratio for the  $615\text{ cm}^{-1}$  to  $715\text{ cm}^{-1}$  data is about 40:1, individual radiance profiles appear noisy. A significant improvement is possible if the profiles for one scan are averaged to produce one radiance profile instead of four profiles. The data presented have been averaged; however, one detector channel was not included due to a calibration error.

Signal-to-noise ratio for the  $315\text{ cm}^{-1}$  to  $475\text{ cm}^{-1}$  data is about 80:1; thus, averaging was not as necessary as for the  $\text{CO}_2$  data. Both averaged and not averaged data are presented.

### Resultant Data Accuracy

The intent of this section is to identify the principal error sources, to estimate an error for each source, and to combine these errors to yield an estimate of total system accuracy. Error sources are conveniently separated as error sources for the radiance measurement and error sources for the tangent height determination. Error sources and estimated errors for radiance are shown in the following table:

Error source	Error		Radiance accuracy, %, of -	
	$\text{CO}_2$	$\text{H}_2\text{O}$	$\text{CO}_2$ at $6\text{ W/m}^2\text{-sr}$	$\text{H}_2\text{O}$ at $12\text{ W/m}^2\text{-sr}$
Preflight calibration:				
Temperature of source . . . . .	$\pm 1^\circ\text{ K}$	$\pm 1^\circ\text{ K}$	$\pm 1.5$	$\pm 0.9$
Emissivity of source . . . . .	0 to $-0.5\%$	0 to $-0.5\%$	0 to $-0.5$	0 to $-0.5$
Spectral response of radiometer . .	$\pm 1\%$	$\pm 1\%$	$\pm 1$	$\pm 1$
Reflectance of calibration optics . .	$\pm\sqrt{3}\%$	$\pm\sqrt{3}\%$	$\pm\sqrt{3}$	$\pm\sqrt{3}$
Voltage readout ( $\pm 1\sigma$ ) . . . . .	$\pm 45\text{ mV}$	$\pm 25\text{ mV}$	$\pm 2$	$\pm 1$
System operation:				
Telemetry ( $\pm 1\sigma$ ) . . . . .	$\pm 60\text{ mV}$	$\pm 60\text{ mV}$	$\pm 3$	$\pm 3$
Frequency response . . . . .	0 to $-2\%$	0 to $-2\%$	0 to $-2$	0 to $-2$
Voltage readout ( $\pm 1\sigma$ ) . . . . .	$\pm 45\text{ mV}$	$\pm 25\text{ mV}$	$\pm 2$	$\pm 1$
Data reduction:				
Assumed spectral source . . . . .	$\pm 1\%$	$\pm 1\%$	$\pm 1$	$\pm 1$
Space zero determination . . . . .	$\pm 20\text{ mV}$	$\pm 10\text{ mV}$	$\pm 1$	$\pm 0.5$

Further subdivisions of sources are preflight calibration, system operation, and data reduction. Under the error heading the only difference in the  $\text{CO}_2$  and  $\text{H}_2\text{O}$  sides of the radiometer is the voltage errors which are a function of the signal-to-noise ratio for each radiometer. The last two columns in the table indicate the radiance accuracy associated

with each error at a particular radiance level which is near the maximum radiances measured. As the radiance level changes, the voltage and temperature errors cause the percent accuracy of radiance to change.

A similar description of errors in tangent height are contained in the following table:

Error source	Error	Tangent height accuracy, km
Radiometer mirror position ( $\pm 1\sigma$ ) . . .	$\pm 0.02^\circ$	$\pm 1.0$
Radiometer time delay . . . . .	$\pm 0.001$ sec	$\pm 0.5$
Star mapper ( $\pm 1\sigma$ ) . . . . .	$\pm 0.008^\circ$	$\pm 0.4$
Alinement of instruments . . . . .	$\pm 0.005^\circ$	$\pm 0.25$
Altitude ( $\pm 1\sigma$ ) . . . . .	$\pm 0.5$ km	$\pm 0.45$
Total system error		$\pm 1.3$

The radiometer mirror position contributed the largest error which was caused by a jitter in the mirror drive system in the radiometer. Conversion from time and angle to altitude in tangent height is dependent on spacecraft altitude; a typical value was used to obtain the values shown. A total system tangent height accuracy, the square root of the sum of the squares of each contributor, is  $\pm 1.3$  km.

Measured radiance profiles presented for the CO<sub>2</sub> and H<sub>2</sub>O spectral regions were obtained by averaging the radiance data from four detectors; in addition, profiles for the H<sub>2</sub>O region are presented by individual detector. Since averaged data are presented, consideration must be given to the effect of averaging on radiance accuracy. When data are averaged, the error sources under preflight calibration are not improved with the exception of voltage readout. As a conservative estimate, assume no improvement in preflight calibration. The errors from telemetry, voltage readout, and space zero determination are random errors which are improved by the square root of the number of readings averaged; thus, an improvement of a factor of 2 is realized by averaging radiances from four detectors. Further averaging into geographic cells provides better accuracy depending on the number of profiles in the cell.

Relative accuracy, which is the accuracy of one profile relative to another or of one point to another within one profile, is another accuracy of interest. The preflight calibration does not affect the relative accuracy since the calibration is described by a straight line through the origin. Thus, only the system operation and data reduction errors need to be considered.

Estimates of resultant data accuracy for CO<sub>2</sub> and H<sub>2</sub>O data at several radiance levels are shown in the following table:

Radiance, W/m <sup>2</sup> -sr	Absolute accuracy (1 $\sigma$ ), percent			Relative accuracy (1 $\sigma$ ), percent		
	CO <sub>2</sub>	H <sub>2</sub> O	Averaged H <sub>2</sub> O	CO <sub>2</sub>	H <sub>2</sub> O	Averaged H <sub>2</sub> O
12		4	4		4	3
6	4	7	5	3	6	4
3	6	12	8	4	11	6
1	17	35	21	11	33	17

## DATA PRESENTATION AND DISCUSSION

Horizon radiance profiles include measured and analytically predicted profiles for the spectral region 615 cm<sup>-1</sup> to 715 cm<sup>-1</sup> (CO<sub>2</sub>). Predicted profiles for the CO<sub>2</sub> region are derived independently of the measured profiles. Measured radiance profiles are presented for the spectral region 315 cm<sup>-1</sup> to 475 cm<sup>-1</sup> (H<sub>2</sub>O). Predicted profiles for the H<sub>2</sub>O region are not presented due to a lack of independent knowledge of H<sub>2</sub>O mixing ratio. Mixing ratio of water vapor has been deduced from the measured radiance profiles in the 315 cm<sup>-1</sup> to 475 cm<sup>-1</sup> region.

Geographical locations of horizon radiance profiles are shown for 615 cm<sup>-1</sup> to 715 cm<sup>-1</sup> spectral interval in figure 6 and for 315 cm<sup>-1</sup> to 475 cm<sup>-1</sup> spectral interval in figure 7. Locations of measured radiance profiles are shown as solid dots. Circles with a cross inside denote the locations of analytical profiles. Since the radiance profiles are measured from a spinning spacecraft, the radiance data that contribute to a single profile are gathered over a geographic region which defines the spatial resolution of the data. This spatial resolution is indicated by bars for a few profiles in figures 6 and 7. Latitude coverage of the experiment is seen to be from 10° N to 57° N.

### Meteorological Rocket Network Support

An attempt to predict the horizon radiance profiles in the 615 cm<sup>-1</sup> to 715 cm<sup>-1</sup> region independently of the measured profiles has been made. In order to do so a knowledge of the meteorological parameters (temperature and pressure) as a function of altitude must be obtained. In support of the experiment special launchings were made to measure temperature, wind speed, and wind direction from four Meteorological Rocket Network (MRN) sites. All MRN data were taken within 2 hours of the radiance profile measurements. The meteorological data and analysis of that data which resulted in temperature and pressure distributions in geographical areas of the horizon profile measurements are presented in detail as appendix B of this report. An error analysis of effects of temperature accuracies on radiance profiles is also included.

## Analytical Profiles for CO<sub>2</sub> Spectral Band

The atmospheric data discussed in appendix B were used to predict radiance profiles which can be compared with the measured radiance profiles. The analytical profiles were calculated by using a modified version of the computer program described in detail in reference 12. This section contains a brief description of the calculation and the principal factors involved.

Radiative transfer equation.- Any technique used to calculate the radiance profile of the earth's limb (refs. 3 to 13) has as a goal the solution of the radiative transfer problem in a curved atmosphere. The equation for radiance at a tangent height  $H$  is

$$N(H) = - \int_{\nu_1}^{\nu_2} \int_0^{s_0} J_{\nu}(T) \frac{\partial \tau}{\partial s} ds d\nu + \int_{\nu_1}^{\nu_2} J_{\nu}(T_0) \tau_0 d\nu \quad (26)$$

where  $s_0$ ,  $T_0$ , and  $\tau_0$  are the values at a boundary or for the last layer of the atmosphere when no boundary is present. As long as the assumption of local thermodynamic equilibrium is valid, the source function  $J_{\nu}(T)$  is related to the Planck blackbody equation  $W_{\nu}(T)$  as follows:

$$J_{\nu}(T) = \frac{W_{\nu}(T)}{\pi} = N_{\nu}(T) = \frac{C_1 \nu^3}{\exp\left(\frac{C_2 \nu}{T}\right) - 1} \quad (27)$$

Thus equation (26) can be rewritten as

$$N(H) = - \int_{\nu_1}^{\nu_2} \int_0^{s_0} N_{\nu}(T) \frac{\partial \tau}{\partial s} ds d\nu + \int_{\nu_1}^{\nu_2} N_{\nu}(T_0) \tau_0 d\nu \quad (28)$$

The second term of equation (28) represents a boundary condition determined by the temperature of the boundary and the fractional amount of that surface induced radiance transmitted to the observer. In the radiance profile calculations the boundaries considered are clouds and the earth's surface.

Solution of transfer equation.- In the transfer equation (eq. (28)) temperature is dependent on altitude, and transmittance is dependent on temperature, pressure, path length, concentration of absorbing gas, and wave number. Since neither temperature nor transmittance is expressible in a closed form, the integrals of equation (28) are normally solved by numerical integration. It is convenient in solving equation (28) to rewrite it as

$$N(H) = - \int_{\nu_1}^{\nu_2} \int_0^{s_0} N_{\nu}(T) d\tau d\nu + \int_{\nu_1}^{\nu_2} N(T_0) \tau_0 d\nu \quad (29)$$

Since a valid assumption is a spherical earth and a spherical atmosphere, a solution of equation (29) for a given tangent height is determined in the following manner:

- (1) Divide the atmosphere into concentric spherical shells and find a mean temperature and a pressure representative of each shell.
- (2) Calculate a transmittance from the top of the atmosphere to each shell boundary for each band interval  $\Delta\nu$ .
- (3) Form the  $\Delta\tau$  for each shell by subtracting one value of  $\tau$  from the next value of  $\tau$ .
- (4) Compute the blackbody radiance  $N_\nu(T)$  for each shell by using the average temperature in the shell.
- (5) Sum the products  $N_\nu(T)\Delta\tau\Delta\nu$  for the shells; this completes the solution.

Factors affecting calculation of transfer equation.- In the  $615\text{ cm}^{-1}$  to  $715\text{ cm}^{-1}$  spectral region the factors considered in the computation of the transfer equation are temperature, pressure, mixing ratio of  $\text{CO}_2$ , transmittance, absence of thermodynamic equilibrium, Doppler broadening, refraction, clouds, and other gases ( $\text{H}_2\text{O}$  and  $\text{O}_3$ ). Temperature and pressure were the meteorological data described previously. The  $\text{CO}_2$  mixing ratio was taken to be 314 parts per million in the sensible atmosphere (0 km to 80 km) and is given in reference 12. Effects of  $\text{H}_2\text{O}$  and  $\text{O}_3$  on the radiance from  $615\text{ cm}^{-1}$  to  $715\text{ cm}^{-1}$  have been estimated and found negligible (ref. 12). Clouds were included in the computer program as blackbody boundaries; however, none were evident at altitudes high enough to have an effect on measured data.

In the  $\text{CO}_2$  spectral region the transmittance model used was the data computed by Stull, Wyatt, and Plass (ref. 28). This work assumed a Benedict modification of the Lorentz line shape. These data are published as tables which contain transmittance computed for a range of pressure, temperature, and path length. Rather than use the tables which would require a very time-consuming table look-up, the data were curve fitted in the regions of interest so that transmittance can be computed directly. Effective temperature, effective pressure, and optical depth are the essential elements in the computation of transmittance for slant paths in a real atmosphere.

Optional modifications of the radiance and transmittance functions in equation (28) can be made to account for effects due to Doppler broadening of spectral lines and the absence of local thermodynamic equilibrium. In the lower atmosphere the Doppler half-width is masked by the stronger Lorentz line shape, but at  $h \approx 30\text{ km}$  in the earth's atmosphere the half-widths for the Doppler and the Lorentz line shapes are equal. Above this altitude the Lorentz line shape is narrower near the center of the line than is the Doppler shape. The behavior of the Doppler and the Lorentz line shapes away from the center, in the wings of the line, is markedly different. The Doppler line shape at a given

altitude falls from the more strongly absorbing center in an exponential manner but the Lorentz line shape at the same altitude falls from the less strongly absorbing center according to an inverse square law. Therefore, at altitudes above 30 km it is desirable to assume a mixed Doppler-Lorentz shape in which the line center takes account of the Doppler shape but the wings of the line follow the Lorentz shape.

As previously stated, the source function is related to the Planck blackbody function by equation (27) when local thermodynamic equilibrium exists. Local thermodynamic equilibrium can only be assumed when the vibrational and rotational energy levels of the gas molecule remain populated according to a Boltzmann distribution determined by the local kinetic temperature. This condition cannot be assumed to exist throughout the effective atmosphere. The modification of the source function used to approximate the Curtis and Goody nonequilibrium source function is discussed in detail in reference 12.

A constantly changing density exists along a line of sight so that Snell's law of refraction is relevant in the limb profile problem. A constantly changing index of refraction is as computationally impractical as a constantly changing temperature and pressure. A similar approximation to that employed for the temperatures and pressures was used whereby an effective density for each shell was used to compute the index of refraction for that shell. The distance that the line of sight traversed in each shell was then modified by the refraction of that shell. In this way the gas concentration, and thereby the transmission of each shell, was slightly changed.

Analytical profiles predicted for the present experiment are shown in figure 8 as dashed-line curves. The average of the analytical profiles weighted by the distribution of measured profiles is also given in figure 8. Figure 9 shows the temperature distributions and analytical radiance profiles at the extremes in geographical latitude of the experimental data. The radiance and tangent height have been reversed in this figure for ease in comparing radiance and temperature profiles. The analytically predicted radiance profiles have differences of  $0.7 \text{ W/m}^2\text{-sr}$  in peak radiance due to tropospheric temperature variations, but little difference in radiance levels is noted at larger tangent heights (fig. 9). The temperature variation with latitude is large at low altitudes but small at high altitudes. This condition is not unusual for the summer season.

#### Measured Profiles for CO<sub>2</sub> Spectral Band

Fifty measured radiance profiles in the  $615 \text{ cm}^{-1}$  to  $715 \text{ cm}^{-1}$  spectral interval are given in table III. Radiance profiles are tabulated at 1-km increments from  $H = 10 \text{ km}$  to  $60 \text{ km}$ . Geographic location is indicated by a mean latitude and longitude given at the bottom of the table, and the data are presented in order of increasing latitude.

To compare the measured radiance profiles with analytical radiance profiles, the measured profiles were divided into groups by geographic cells. Each geographic cell

contains one analytical profile. The cell designation for each measured profile is given in table III. Measured profiles in each cell were averaged together and compared with analytical profiles by cell in figure 8. A comparison of the average of all measured data with analytical data averaged and weighted according to measured data distribution is also shown in figure 8.

Numerical data used in figure 8 are given in tables IV to XII. In addition to average radiance the maximum, minimum, and standard deviations are also given. An examination of the standard deviations in tables IV to X reveals values consistent with those that the error analysis would predict. For example, at a radiance of  $6 \text{ W/m}^2\text{-sr}$  a  $1\sigma$  relative error of 3 percent is  $0.18 \text{ W/m}^2\text{-sr}$ . Standard deviations from  $H = 10 \text{ km}$  to  $19 \text{ km}$  for cell 6 vary from  $0.10$  to  $0.15 \text{ W/m}^2\text{-sr}$ . Cell 6 has the largest number of profiles of any cell, a total of 16.

Agreement between measured profiles from cell averages and analytical profiles is within experimental error in figure 8. The agreement confirms that the analytical technique of calculating radiance profiles is within the accuracy of the experiment.

These statements are made of course in the light of the error analyses previously discussed. In this regard it is well to remember that the analytical profiles have error bounds (due to meteorological data errors as described in appendix B) as have the measured profiles. Actually, the agreement is not as good in cells 2 and 3 (fig. 8) as in the other cells. Peak radiance differences in cell 1 are partly caused by the analytical profile being located at a higher latitude than any measured profile in cell 1. A noticeable trait of cells 2 and 3 is the consistent manner in which measured radiances are about  $0.15 \text{ W/m}^2\text{-sr}$  larger than predicted radiances at higher tangent heights. This difference is larger than the error due to meteorological effects in appendix B, but it is smaller than the combined errors of appendix A and appendix B.

Differences in radiance near  $H = 20 \text{ km}$  in cell 5 are an example of how the radiance data can reveal an error in interpolating the temperature field. Radiance values at  $H = 20 \text{ km}$  for cells 4, 5, and 6 are, respectively,  $5.66$ ,  $5.48$ , and  $5.44 \text{ W/m}^2\text{-sr}$  for the measured data and  $5.83$ ,  $5.79$ , and  $5.59 \text{ W/m}^2\text{-sr}$  for the analytical data (fig. 8). Both sets decrease from cell 4 to cell 6; however, the analytical profiles show that cell 5 is much more like cell 4 than cell 6, and the measured profiles show that cell 5 is more like cell 6 than cell 4. A temperature error of  $2^\circ \text{ K}$  in the lower stratosphere would account for the differences. Agreement in cells 6 and 7 is excellent.

Agreement between the measured and analytical profiles for the average of all data is excellent. Experimental confirmation of the analytical technique in predicting horizon radiance profiles in the  $615 \text{ cm}^{-1}$  to  $715 \text{ cm}^{-1}$  spectral region contributes significantly to the confidence in using this spectral band in horizon sensing for navigational purposes. First, if enough radiance profile measurements or atmospheric temperature and pressure

data are given, the horizon profiles characteristics are predictable. Second, the formation of the radiance profile, which reaches a peak or plateau at about  $H = 15$  km, indicates little sensitivity to clouds at and below the tropopause and to temperature variations in the lower atmosphere.

### Measured Profiles for H<sub>2</sub>O Spectral Band

Fifty measured radiance profiles in the  $315\text{ cm}^{-1}$  to  $475\text{ cm}^{-1}$  spectral interval are given in tables XIII and XIV. Table XIII presents radiance data by individual detectors which are identified at the bottom of the table. Latitude and longitude are also given at the bottom of the table; the data are arranged in order of increasing latitude for each detector.

All the measured radiance profiles in the  $315\text{ cm}^{-1}$  to  $475\text{ cm}^{-1}$  interval have been influenced by a radiometer limitation which must be understood before the data can be used. A typical radiance profile from a low cloud geographical area is the solid-line curve in figure 10. Radiance changes rather slowly from  $H = 35$  km to 20 km. Then the slope becomes very steep from  $H = 15$  km to 10 km. When the radiometer is scanned across the steep portion of this radiance profile, the frequency response of the radiometer has been exceeded. Measured radiance values in the region of the steep slope will be too small. Data affected the most are between radiance levels of  $5\text{ W/m}^2\text{-sr}$  and  $10\text{ W/m}^2\text{-sr}$ . Radiance values below  $H = 5$  km should be quite good. The error analysis for the data presented in appendix A does not include the effects of this frequency limitation.

Radiance profiles in the  $315\text{ cm}^{-1}$  to  $475\text{ cm}^{-1}$  spectral region are dependent on cloud cover. Consequently, large radiance differences are observed from one detector to another in the presence of clouds. Cloud effects are seen more clearly in the data from individual detectors (table XIII) than in the averaged data (table XIV) because averaging has reduced cloud effects. Radiance profiles from clear and cloudy areas are shown in figure 10. Two of the profiles at latitudes  $13.2^\circ\text{ N}$  and  $57.4^\circ\text{ N}$  are from relatively clear or low cloud areas near the extremes of latitudes of the experiment, whereas the profile from latitude  $38.9^\circ\text{ N}$  is from a region of high clouds. A cloud at  $h = 10$  km to 12 km has resulted in a radiance of  $5.7\text{ W/m}^2\text{-sr}$  at  $H = 5$  km compared with radiances greater than  $10\text{ W/m}^2\text{-sr}$  for the other profiles. Cloud effects of this magnitude are highly undesirable for applications in horizon sensing for attitude determination and make the  $315\text{ cm}^{-1}$  to  $475\text{ cm}^{-1}$  spectral region a poor one to use for high-accuracy attitude determination.

A nephalanalysis of the region in which radiance profiles were measured for the evening of August 15-16, 1966, is given in figure 11. The northern and southern profiles occur in areas with clouds at  $h < 3$  km which have a much smaller effect. Radiance

profiles that exhibit cloud effects are evident in table XIII in two geographical areas. One area (fig. 11) between latitudes  $37^{\circ}$  N and  $41^{\circ}$  N at about longitude  $45^{\circ}$  W has clouds estimated to be at  $h = 9.5$  km. The short-dash-line curve in figure 10 represents profiles in this area. The other area (fig. 11) between latitudes  $52^{\circ}$  N and  $57^{\circ}$  N from approximately longitudes  $55^{\circ}$  W to  $80^{\circ}$  W is affected by clouds estimated to be at altitudes from 6.1 km to 7.6 km in the region nearby.

In figure 10, the small oscillations at tangent heights greater than 15 km are caused by detector noise in the radiometer. This random noise is significantly reduced by averaging the radiance values. The average radiances for the four detectors for each horizon crossing are given in table XIV. These data are best used to illustrate the change in radiance with tangent height above 15 km. Since profiles with cloud effects are in some instances averaged with profiles with no cloud effects, care must be taken in use of the averaged profiles at tangent heights less than 12 km.

Latitudinal variation of the radiance profiles is illustrated in figures 10 and 12. Figure 10 indicates that the radiance profiles are quite similar, with the profile of latitude  $13.2^{\circ}$  N having a slightly larger radiance near a tangent height of 1 km. A comparison at tangent heights above 15 km is better seen in figure 12 where the northern profile has larger radiances from  $H = 15$  km to 30 km. The northern profile has been formed by averaging the data in table XIV for latitudes  $51.9^{\circ}$ ,  $52.3^{\circ}$ ,  $52.3^{\circ}$ ,  $52.6^{\circ}$ ,  $53.7^{\circ}$ , and  $54.5^{\circ}$  N. The southern profile has been formed by averaging the data for latitudes  $10.9^{\circ}$ ,  $12.2^{\circ}$ ,  $12.8^{\circ}$ ,  $13.5^{\circ}$ ,  $13.5^{\circ}$ ,  $15.5^{\circ}$ ,  $15.6^{\circ}$ ,  $17.4^{\circ}$ , and  $18.6^{\circ}$  N.

These radiance profiles have a good correlation with the temperature field which is shown in figure 9. In the northern area, from  $h = 35$  km to 15 km the temperature is higher and the radiance is larger than in the southern area and below  $h = 12$  km the temperatures are lower and the radiances are smaller. This correlation of temperature and radiance indicates that the mixing ratio of water vapor does not vary a great deal with latitude above  $h \approx 15$  km.

#### Analytical Profiles for H<sub>2</sub>O Spectral Band

The calculations of horizon radiance profiles in the rotational water-vapor band present two significant problems not encountered in the CO<sub>2</sub> band. First, much less work has been done in the study of transmission or absorption in the rotational water-vapor band. Elsasser's transmission model (ref. 29) was incorporated into the computer program previously discussed because of its availability. Second, the mixing ratio of water vapor is highly variable in the troposphere and there are very little authoritative data on the mixing ratio and its changes above  $h = 10$  km. No attempt was made to measure the mixing ratio of H<sub>2</sub>O independent of the radiance profile measurements. The

analytical profiles in table XV for the H<sub>2</sub>O band have not included the effects of refraction, Doppler broadening, and the lack of thermodynamic equilibrium.

#### Determination of Water-Vapor Mixing Ratio

If temperature and pressure were known, the mixing ratio could be deduced from the measured radiance profiles. Mixing ratio is the ratio by weight of water vapor to dry air. The temperature and pressure data for the geographic cells given in appendix B are assumed to be valid. This assumption is made with confidence since the measured radiance profiles in the 615 cm<sup>-1</sup> to 715 cm<sup>-1</sup> spectral region indicated excellent agreement with the analytical radiance profiles based on these pressure and temperature data. Since no boundaries are included, consider again equation (28) without the boundary term, namely,

$$N(H) = - \int_{\nu_1}^{\nu_2} \int_0^{s_0} N_{\nu}(T) \frac{\partial \tau}{\partial s} ds d\nu \quad (30)$$

The only term dependent on mixing ratio is  $\partial \tau / \partial s$ . The procedure used to determine mixing ratio is as follows:

- (1) Start with the highest tangent height for which measured data are available (35 km) and assume that the mixing ratio above that altitude is constant.
- (2) Compare the radiance computed from equation (30) with the measured radiance and change the mixing ratio until the radiance difference is small.
- (3) Change the line of sight to a lower tangent height (34 km) and make a guess at the mixing ratio in the new altitude layer from 34 km to 35 km.
- (4) Compare the radiance computed from equation (30) with the measured radiance and change the mixing ratio in the new layer until the radiance difference is small.
- (5) Repeat steps (3) and (4) to determine the mixing ratio in each new layer. This process is only valid of course when the line of sight does not intersect any boundaries such as clouds or the earth.

Mixing ratios have been determined for the two radiance profiles shown in figure 12 which were formed by averaging several radiance profiles to smooth the radiance variations at larger tangent heights. The measured profiles and analytical profiles are given in table XV. Analytical radiances were terminated at heights of 11 km and 13 km because the data below these heights have been affected by the frequency limitations of the radiometer.

The inferred water-vapor mixing ratios and relative humidities are given in table XVI. A comparison of the Scanner deduced mixing ratios with those from other

investigations is shown in figure 13. The present data (solid- and short-dash-line curves) show little variation above  $h = 28$  km. Above  $h = 35$  km constant values of 0.0155 g/kg and 0.0170 g/kg yield radiances in agreement with experimental data at  $H = 35$  km. At altitudes below 18 km the mixing ratios diverge and are a factor of 3 apart by  $h = 15$  km. From the temperatures discussed in appendix B the tropopause occurs at altitudes of 16 km for latitude  $17^\circ$  N and between 10 and 12 km for latitude  $53^\circ$  N. Mixing ratios increase rapidly in the lower atmosphere and must reach an independently measured value at the surface of 19.0 g/kg at latitude  $17^\circ$  N and of 6.68 g/kg at latitude  $53^\circ$  N. The present data show that the variability with latitude at altitudes larger than 18 km is small. Comparative data in figure 13 have been taken from references 30, 31, and 32. Previous measurements of mixing ratio above  $h = 15$  km have been either by hygrometry (ref. 31), by absorption spectroscopy using the sun as a source (ref. 32), or by measuring thermally emitted radiation from the nadir (ref. 33). The present method is a different technique by which thermally emitted radiation is measured in the rotational band from the horizon. Presently determined mixing ratios indicate a drier stratosphere above  $H = 25$  km than do those obtained in references 30 and 31 but not as dry as the spectroscopic measurement in reference 32. Below  $h = 15$  km all measurements show a rapid increase in mixing ratio.

#### CONCLUDING REMARKS

Horizon radiance profiles have been measured in two spectral bands of the strongly absorbing atmospheric constituents  $\text{CO}_2$  ( $615\text{ cm}^{-1}$  to  $715\text{ cm}^{-1}$ ) and  $\text{H}_2\text{O}$  ( $315\text{ cm}^{-1}$  to  $475\text{ cm}^{-1}$ ). Data were obtained in the summer and cover a latitude range from  $10^\circ$  N to  $57^\circ$  N. The measured data include 50 radiance profiles for the  $\text{CO}_2$  region and for the  $\text{H}_2\text{O}$  region.

Temperature and pressure conditions in the atmosphere were determined independently in the geographical regions of measured horizon profiles and were used to calculate radiance profiles in the  $\text{CO}_2$  band which were compared with the measured radiance profiles. The comparison of analytical and measured radiance profiles shows excellent agreement; thus, the analytical technique is verified within the experimental accuracy.

Measured horizon radiance profiles in the  $615\text{ cm}^{-1}$  to  $715\text{ cm}^{-1}$  spectral region ( $\text{CO}_2$ ) are formed high enough in the atmosphere to be affected little by tropospheric weather variations. The  $\text{CO}_2$  spectral band is a leading choice for attitude determination applications.

Measured radiance profiles in the  $315\text{ cm}^{-1}$  to  $475\text{ cm}^{-1}$  spectral region ( $\text{H}_2\text{O}$ ) show a strong dependence on clouds; therefore, this spectral region would not be a good choice for attitude determination applications.

Mixing ratio of water vapor has been deduced from the radiance measurements for horizon profiles in the regions of latitudes  $17^{\circ}$  N and  $53^{\circ}$  N. The present technique of measuring thermally emitted radiation in the rotational band at different tangent heights to determine mixing ratio is a different method. Mixing ratios have been determined up to an altitude of 35 km and show little variation with latitude above an altitude of 18 km.

Langley Research Center,  
National Aeronautics and Space Administration,  
Langley Station, Hampton, Va., May 17, 1968,  
715-02-00-01-23.

## APPENDIX A

### PROJECT SCANNER EXPERIMENT AND INSTRUMENTATION

#### Operational Description

The Project Scanner experiment was conducted on a suborbital rocket vehicle launched from Wallops Island, Virginia, at 0618 GMT on August 16, 1966. A three-stage, solid-rocket vehicle propelled the payload to a peak altitude of 620 km. An operational schematic of the flight experiment is shown in figure 1. The launch vehicle was aerodynamically stabilized and the spacecraft containing the instrumentation was spin stabilized as it exited the atmosphere. The spacecraft was despun to a nominal  $3/4$  Hz following burnout of the third-stage motor and was erected so that the spin axis was near the local vertical. This spacecraft orientation was accomplished by a reaction jet system deriving information from a horizon sensor and a rate gyroscope (ref. 34). Data gathering began after the reaction jet system was shut down following attainment of the near vertical attitude. Since the spacecraft retains this spin-stabilized inertial attitude and since the direction of the local (earth) vertical changes as the spacecraft goes down range, a programmer initiated three other orientations to new local verticals by actuating the reaction jet system for three 20-sec periods of operation which were interspersed with data periods of about 130-sec duration each. This sequence resulted in four data periods totaling approximately 525 sec. Data gathering began at an altitude of 430 km and continued through apogee (620 km) and down to an altitude of 350 km, below which mirror scans did not cross the horizon.

Two radiometers were mounted back to back as shown in figure 14(a). Filters are provided so that one radiometer responds in the  $\text{CO}_2$  spectral region and the other responds in the rotational water-vapor region. Two cyclically scanning mirrors in these radiometers cause the fields of view of the detectors to scan up and down across the horizon. This near vertical scanning gives the basic measurement of the radiance profile, and the spin of the spacecraft permits measurement of various azimuth locations on the horizon.

The precise spacecraft attitude information needed to position the radiance profiles relative to the earth was obtained from the star mapper. This star mapper (refs. 23 and 24) was aligned with the dual radiometer to an accuracy of  $0.005^\circ$  and allowed inertial attitude to be obtained to an accuracy of  $1\sigma$  of  $0.008^\circ$ . All spacecraft data are transmitted on a real-time basis to ground stations and are later combined with radar tracking information to reconstruct the measured horizon radiance profiles.

## APPENDIX A

### Dual Radiometer Assembly

General description.- The basic instrument in the Project Scanner horizon definition experiment was the dual radiometer assembly. This unit consisted of two nearly identical radiometers mounted as a single assembly. Sketches of this instrument are given in figure 14. A single motor drove the two planar scan mirrors each of which directs the incoming radiation into a Cassegrain optical system. In the converging beam, within appropriate baffling and just prior to the focal plane, filters were placed to define the spectral interval. At the focal plane a mask or field stop defined five elemental fields of view in each radiometer. Behind each field aperture was an immersed thermistor bolometer as the detector. Signal processing electronics were mounted nearby. A complete description of this instrument and its development is contained in reference 25. An abbreviated description of pertinent features follows.

Optics.- The flat scan mirrors were fabricated of electroless nickel-plated beryllium with a reflective coating of aluminum applied to the polished nickel. A protective coating of SiO was used on the mirror on the carbon dioxide side, and a coating of  $\text{MgF}_2$  was used on the water-vapor side.

The primary and secondary mirrors of the Cassegrain system were a matched pair of aspheric surfaces. The optical system had an aperture diameter of 23 cm and a focal length of 33 cm. After figuring the primary mirror the secondary mirror was final polished to achieve proper system performance. The primary mirror was fabricated of electroless nickel-plated beryllium with a selective coating of aluminum on the final figured nickel and a protective coating of SiO. The required aspheric curve was machined in the beryllium before plating. The same plating and coatings were used for the secondary mirror as for the primary mirror but the blank material was silicon instead of beryllium.

Filters.- The primary spectral interval for each radiometer was defined by a filter which was positioned in the converging beam just ahead of the focal plane. The filter for the carbon dioxide band was an interference filter with substrates of germanium and press-sintered zinc selenide. The filter for the water-vapor side used an interference coating on silicon for the cut-on wavelength and potassium bromide for the cut-off wavelength.

Immersed detectors.- Behind the field stop in each radiometer was a housing containing the five-element array of immersed thermistor bolometers. For the carbon dioxide radiometer the immersion lenses were antireflection coated germanium; for the water-vapor side the immersion lenses were antireflection coated silicon. Both were hyperhemisphere-type lenses 1 mm in diameter. The individual detectors were 0.1 mm by 0.1 mm in size and of thermistor material #1 with a thickness of about  $8\mu$  and a resistance of 4 M $\Omega$ . The active bolometers did not have the usual black absorber applied to

## APPENDIX A

the flakes. This blackening had been shown effective in improving the spectral response of these detectors at shorter infrared wavelengths; however, for this application it was proved unnecessary. These results and others about these immersed detectors are presented in reference 35. The resistance-matched compensating bolometers were also mounted inside the stainless-steel housing and feedthrough pins were potted in place. Tests with the housing evacuated revealed noise problems which were attributed to leakage currents across the feedthrough insulation. The final configuration flown had the interior cavity of the housing made larger, used glass to metal feedthroughs, and was backfilled with krypton. These changes did not eliminate the noise problems but did reduce them to tolerable values.

Another noise problem, probably related in some way to that previously noted, was that some individual detectors did deteriorate over a period of time and became increasingly noisy and unusable. Normal bolometers exhibit a ratio of rms noise voltage with bias applied to that without bias of 1.15 to 1.20. The observed effect of a detector going bad was usually a gradual increase or occasionally a sudden increase in this ratio to 2, 3, or 5 or more. This problem was faced by requiring a 200-hr burn-in test with the ratio not exceeding 1.50. Documentation of the details of these particular experiences is contained in reference 25.

The bolometers exhibited time constants of between 2.3 msec and 2.5 msec and were operated at bias voltages of 43 V per flake. This bias voltage was supplied by mercury batteries.

Spectral responses.- Typical normalized spectral responses of the two radiometer channels are presented in figure 15. These spectral intervals have been characterized as  $615\text{ cm}^{-1}$  to  $715\text{ cm}^{-1}$  ( $16.3\mu$  to  $14.0\mu$ ) for the carbon dioxide band and as the  $315\text{ cm}^{-1}$  to  $475\text{ cm}^{-1}$  ( $31.8\mu$  to  $21.1\mu$ ) part of the rotational water-vapor band. These wave-number intervals are not precisely the half-power points but are nearly so and are those intervals most readily available for computation of the analytical profiles used for comparisons.

Fields of view.- The elemental field of view of each of the five detectors in each array is determined by the field stop located in the focal plane. Each field of view is nominally  $0.025^\circ$  in the vertical and  $0.100^\circ$  in the horizontal and is separated by  $0.15^\circ$  in the vertical. Representative field-of-view contours are presented for the carbon dioxide and water-vapor regions in figure 16.

Electronics.- The radiometer signal-processing electronics consists of a preamplifier followed by two additional amplifiers for each of the 10 detectors. Total system voltage gain for each detector-amplifier system was approximately 20 000. Output voltage of up to  $\pm 2.5\text{ V}$  was fed with proper impedance matching to the FM-FM telemetry equipment. The design features stressed low noise, gain stability with temperature, and

## APPENDIX A

closely controlled frequency response characteristics. The complete radiometer frequency response must include those detector characteristics also. Typical measurements of the total radiometer frequency responses are presented in figure 17.

Scan-mirror operation.- The two scan mirrors for the dual radiometer assembly were driven by a single drive motor as shown in figure 14(a). This operation was accomplished through reduction gearing driving a cam and follower mechanism. The total angular motion of these mirrors was  $15^{\circ}$ . The mirror motion was about a center position represented by a depression angle of  $24^{\circ}$  from the instrument base plane with the scan motion in an orthogonal plane. The two mirrors scanned in the same plane, that is, the look planes were separated  $180^{\circ}$  azimuthally. The scan motion about the mean depression angle had a saw-toothed waveform with a basic sweep rate of  $10^{\circ}$  per sec. This sweep rate over the  $15^{\circ}$  range and a reversal time of 0.1 sec resulted in a scan cycle period of 3.2 sec.

Scan-mirror position was determined by four mirror-position pick-offs located through the scan range. The four position readout points were coded as follows: zero output for 1 msec, rise to coded output voltage in 0.1 msec, and hold of output code voltage for 2 msec. The coded output voltages were 1, 2, 3, and 4 V. These coded pulses were combined with two detector channel outputs to the telemeter; one from each side of the radiometer. Therefore, at each scan-mirror position indication, less than 4 msec of radiance information was lost. The ability to interpolate scan-mirror position between pick-off indications is of course directly related to the repeatability of the waveform. This repeatability was verified through extensive testing before and after various environmental tests. The resulting accuracy estimated for this mirror-position measurement was  $\pm 0.02^{\circ}$ .

Radiometer calibration.- The method chosen to calibrate the dual radiometer was one that closely simulated the manner in which the dual radiometer was used in the flight experiment. A complete description of this calibration is contained in reference 25. Reference 36 contains a discussion of several calibration procedures. An optical relay system was employed to make the calibration sources appear at infinity and extended, that is, fill the radiometer aperture and field of view. A chopping mirror operating at 5 Hz allowed the radiometer to view alternately two blackbody sources at different temperatures, and the voltage difference thus generated was measured.

A schematic of the calibration optical system is shown in figure 18. Radiant energy from the blackbody sources enters the optical system by reflection from the chopping mirror for one source and from the fixed mirror for the second source, which maintains the same number of reflections for each source. The Cassegrain system has an entrance aperture larger than that of the radiometer and a central obscuration smaller than the central obscuration of the radiometer.

## APPENDIX A

Each blackbody source is a 16° right circular cone fabricated from copper and painted with black velvet. The sources can be heated or cooled but temperature control and stabilization are not provided. In calibration the temperatures of the blackbodies were measured for each calibration point.

Radiometric calibration is conducted in a vacuum to prevent absorption by atmospheric CO<sub>2</sub> and H<sub>2</sub>O. Since the responsivity of the radiometer is dependent on operating temperature, the radiometer was calibrated at the five operating temperatures 10.0° C, 15.6° C, 21.1° C, 26.7° C, and 32.2° C. Temperature was adjusted by flowing liquids through heater plates clamped to the sides of the dual radiometer. When a desired temperature was achieved, the flow was stopped and the mass of the radiometer was such that little variation occurred during a calibration test. In the flight experiment the temperature was so close to 21.1° C that the 21.1° C calibration curve was used with no modifications.

To start the calibration both blackbody sources were cooled to liquid nitrogen temperature (77° K) to assure that a proper zero voltage difference existed when alternately viewing the two sources. This zero check assured that all alignments of the radiometer with the calibration optics were proper and that zero output for zero input is indeed a true point on the calibration curve. Next the liquid nitrogen supply was cut off to one blackbody and the blackbody was allowed to warm up. As the source slowly warms up, eight or nine calibration points are recorded. The technique used to read the output voltage of the radiometer is described in reference 25. Results for a calibration test for one detector are shown in figure 19. The abscissa is an effective radiance which is defined as

$$\int_0^{\infty} [N_{\nu}(T) - N_{\nu}(77^{\circ} \text{ K})] \varphi(\nu) \theta(\nu) d\nu$$

and is produced by alternately viewing two sources. Effective radiance is computed for each data point and the integration limits are practically determined by the spectral response  $\varphi(\nu)$ . This effective radiance is directly proportional to the total power received by the detector and varies linearly with the voltage differences measured. Data points are shown in figure 19, and a solid line illustrates the results of fitting a straight line to the measured data points in a least squares sense. The point of zero radiance at zero voltage has not been included in the straight-line determination.

The fitted line in figure 19 passes within the rms noise of the radiometer ( $\approx 45$  mV) of each data point; however, the line misses the origin. In all calibrations the line fit is of comparable quality; however, the determined intercepts vary considerably. The intercepts have been found to be both positive and negative to values larger than the rms noise of the radiometer. No pattern or reason for the variation has been found. The zero-zero

## APPENDIX A

point is known to be a valid point and is checked at the beginning of each calibration. The authors' opinion is that the intercept wandering is due to a characteristic of the person who reads the output voltage (technique described in ref. 25). Consequently, the slopes of the fitted lines have been used and the intercepts have been arbitrarily set to zero. The linear equation which relates the effective radiance to voltage is

$$\Delta V = k \int [N_{\nu}(T) - N_{\nu}(77^{\circ} \text{ K})] \phi(\nu) \theta(\nu) d\nu \quad (31)$$

There is one such equation for each detector in the dual radiometer.

### Star Mapper

The inertial attitude of the spin-stabilized spacecraft was determined by measurements furnished by a star mapper which is a wide-angle, high-resolution star telescope. A sketch of the star mapper is shown as figure 20, and a more complete description of this instrument is presented in reference 23. In operation, light entering the entrance aperture is imaged on a coded reticle in the focal plane. On passing through the reticle the light is diffused over the surface of the cathode of a photomultiplier tube. On the opaque reticle are two groups of transparent slits, the spacing or coding of which is a necessary aid in star detection. One group of slits is parallel to the vehicle spin axis and the other group is at an angle of about  $43^{\circ}$ . As the spacecraft spins, the star image moves across the reticle; this forms a pulse train which is telemetered to the ground. The measurement of times when stars transit the vertical and slanted slits together with the identification of the stars provides enough information to deduce the inertial orientation of the spacecraft.

The star mapper has an optical field of  $6^{\circ}$  by  $6^{\circ}$ . The effective focal length is 38.10 cm (15 in.) at  $f/3.0$ . The optical system is of a modified Petzval design with the optical path being folded for compactness. A field flattener is located immediately before the reticle with two field lenses between the reticle and photomultiplier. The photomultiplier tube has an S-11 spectral response. The optical quality is such that a 36 arc-sec circle contains 66 percent of the total effective energy on axis and 56 percent at the maximum off-axis angle. The system will detect stars down to a visual magnitude of about +3.0.

The star mapper in the flight experiment was mounted directly atop the radiometer, and the alinement with the radiometer was measured to  $0.005^{\circ}$ . For the present experiment the star mapper has allowed inertial attitude to be obtained to an accuracy ( $1\sigma$ ) of  $0.008^{\circ}$ .

## APPENDIX A

### Star-Mapper Data

Data reduction for the star mapper starts by operating on the raw data (star-mapper data tape) with a pulse pattern recognition scheme to determine a transit time and signal amplitude for each star as it transits both the vertical and slanted slits. This operation (fig. 2) results in a listing and punched cards of transit times and output voltage of the star mapper. The cards and transit times are the input data for the star identification program (ref. 24); however, the transit times must be paired such that the times each star transited the vertical and slanted slits are paired. Since more than one star may be in the  $6^\circ$  by  $6^\circ$  field of the star mapper at once, the transit times for each star are not necessarily in sequence. A hand editing utilizing time differences and voltage data is used to pair the proper transit times. The output of the star identification program is a listing and punched cards containing transit times and an identification number from a star analog which has the right ascension and declination of the stars updated to the nearest 0.1 day in time of the flight experiment. At this point all the data for the flight are in one batch.

The last step in the star-mapper data reduction is to use the transit times of identified stars to determine a set of nine constants which can be used to calculate inertial orientation of the spacecraft as a function of time. Reference 24 (in parameter identification) contains a detailed treatment of the orientation problem for a symmetric rigid body with no external torques. Since the transit times are not perfect, the time period for which a single group of nine constants apply has limitations. Too short a time period has too few star transits to yield an accurate set of constants, and too long a time period shows a buildup of error in the predicted orientation. Selection of time periods for determination of sets of constants is the star window choice. In the present experiment, 23 groups of stars were processed to give required constants. Time periods varied from 7 sec to 15 sec. The groups of nine constants and the time periods for which they apply are put on cards as an input to the tangent height calculation.

### Telemetry

An FM-FM telemetry system was used for data transmission from the Project Scanner spacecraft. The system consisted of two FM-FM transmitters, one direct FM transmitter, two wide-band mixing amplifiers, an antenna triplexer, and a power divider. Two FM-FM transmitters were utilized so that the upper five highest frequency response channels of each could be used with the 10 radiometer detectors to assure sufficient bandwidth. These transmitters operated with center carrier frequencies of 231.40 and 240.20 MHz. Frequency bandwidth requirements for the transmission of the pulse trains from the star mapper precluded the use of a subcarrier oscillator; therefore, the direct FM transmitter was modulated directly by the star-mapper output signal. The center

## APPENDIX A

carrier frequency of this transmitter was 244.30 MHz. Outputs of the three transmitters were combined into a single antenna feed by the triplexer with the feed line terminating in a set of four external antennas on the spacecraft nose cone. Real-time telemetry data reception was at NASA Wallops Station.

Extensive preflight tests and calibrations of the flight telemeter and preflight and postflight tests of the ground equipment were performed to insure that proper corrections and time correlations (to less than 0.5 msec) were known so that the positioning of the radiance data with respect to the solid earth would not be compromised.

### Radar Tracking

An accurate spacecraft track is required for combination with celestial attitude data to position accurately the measured radiance profile with respect to the solid earth and to determine the geographic location of the measured profile. A transponder in the spacecraft provided a C-band tracking signal so that the AN/FPQ-6 radar at NASA Wallops Station could maintain precise location of the spacecraft. This equipment provided trajectory positional information to an accuracy estimated to be  $\pm 0.5$  km. Spacecraft altitude and subvehicle point latitude and longitude were furnished with respect to the reference Fischer spheroid (ref. 27).

## APPENDIX B

### METEOROLOGICAL DATA

By Richard E. Davis

In order to attempt to verify the analytical technique used to compute radiance profiles by experimental observation, it is necessary to have a good estimate of the behavior of atmospheric variables (pressure, temperature, and density) as a function of altitude in the volume of atmosphere being sampled by the dual radiometer. Model atmospheres for climatological means and extremes serve to define the range of variability for instrument design purposes but are inadequate to allow the rigorous testing of atmospheric transfer theory. Therefore, it is desirable to have measurements of these variables coincident in time with and over as much as possible of the physical volume of atmosphere being sampled in the experiment.

In support of Project Scanner, then, it was decided to make full use of the meteorological data routinely available and to request additional meteorological support where it could be provided practically.

#### Temperature and Pressure

Specification of the atmospheric state over the continental areas of the earth is made possible through the rawinsonde balloon network at altitudes up to 31 km (ref. 37). Pressure and temperature are measured directly throughout this altitude range. Dew-point observations are also made; however, these usually cease before a 10-km altitude is reached with present instrumentation. By means of visual or radar tracking, the variation of wind velocity with altitude can be derived.

Balloon soundings are made twice daily at 0000 and 1200 GMT. These soundings provide atmospheric data good enough to support the Project Scanner analysis up to  $h = 31$  km. Above the peak altitude of rawinsonde balloons, the frequency of data is low in both time and space. The North American land mass, with adjacent waters, is the only area of the globe which has the semblance of a regular sounding program above an altitude of 30 km; this is the Meteorological Rocket Network or MRN (ref. 38). This network, consisting of several stations in North America, takes routine soundings by means of small sounding rockets of the atmosphere above  $h = 30$  km. These soundings are usually taken each Monday, Wednesday, and Friday near local noon. Inasmuch as the circulation studies are of prime interest to MRN users, wind velocity variation with altitude (radar-determined) constitutes a large part of the data. However, temperature and density payloads may be fitted to the sounding rockets.

## APPENDIX B

It was decided to request the MRN stations nearest the geographic locations of Scanner measurements to undertake atmospheric soundings of temperature and wind velocity closely following the launch of the Scanner vehicle. For the support of the Project Scanner experiment, soundings were obtained from the four MRN sites shown in figure 6. Unfortunately, White Sands was unable to obtain wind data due to tracking radar malfunction. (Antigua, B.W.I., was unable to launch a rocket due to excessive low altitude winds.) All sites obtained wind and temperature data as follows:

Site	Launch time, GMT	Peak altitude of temperature data, km	Wind
Fort Churchill, Canada	0730	57.6	Yes
Wallops Island, Virginia	0706	57.5	Yes
Eglin Air Force Base, Florida	0750	54.9	Yes
White Sands Missile Range, New Mexico	0730	61.0	No

The MRN data are presented in tables XVII to XX.

The goal of the meteorological support is the construction of model atmospheres near enough together to sample the variability which may be caused by the meteorological condition existing at the time of flight. The first step is to inspect the stratospheric temperature field. Where the isotherms are close together, model atmospheres are placed closer together; where temperature gradients in the stratosphere are weak, fewer model atmospheres are needed. The stratospheric temperature field was drawn at 5-km intervals for altitudes from 30 km to 55 km by using the thermal wind technique for a constant-altitude surface (refs. 39 and 40). Wind shears were computed for 4-km-thick slabs. The constant-altitude isothermal analyses are given in figure 21.

It is also necessary to specify the variation of pressure with altitude for a model atmosphere; unfortunately, the MRN payload capability does not include pressure measuring instruments. The pressure values for these model atmospheres were derived through hydrostatic buildup as given by equation (3) in reference 40. The model atmospheres derived by these procedures are listed in table XXI.

### Water Vapor

Derivation of the variation of water-vapor mixing ratio with altitude was done separately for those altitudes above and below the maximum altitude of radiosonde dew-point data. The teletype radiosonde soundings for 0000 GMT, August 16, 1966, were collected and decoded for the locations of the model atmospheres selected. Part of such data includes dewpoint information up to that altitude over the station where the atmosphere becomes too dry and/or too cold for the moisture sensor to function. Such dewpoint data

## APPENDIX B

usually cease before a pressure altitude of 300 mb (nominal 9 km) is reached. In this range, the water-vapor mixing ratio  $w$  in grams of water vapor per kg of air is

$$w = \frac{0.621e}{p - e} \quad (32)$$

The partial pressure of water vapor  $e$  is obtained from reference 41. Vapor pressure over water is used for temperatures exceeding  $-40^{\circ}$  C and vapor pressure over ice is used for temperatures smaller than or equal to  $-40^{\circ}$  C.

Above a pressure altitude of 200 mb, the mixing ratio is unknown from the rawinsonde data and was deduced as described in the main body of the report in the section entitled "Determination of Water-Vapor Mixing Ratio."

### Nephanalysis

In order to evaluate better the effects of cloud cover on the measured radiance profiles, it is desirable to have a nephanalysis as near as possible to the time of the Scanner flight. It was fortunate that the Nimbus II medium resolution infrared radiometer (MRIR) data (ref. 42) were available near the area covered and the time of the Scanner mission. A mosaic was constructed of photographs processed from the MRIR data corresponding to the evening of August 15-16, 1966, and to the area North America, Western Atlantic, and South America (data orbits 1235, 1236, 1237, and 1238). From these photographs, the nephanalysis (cloud chart) of figure 11 was drawn. The numbers give the estimated heights of clouds in kilometers. Also, the positions of the fronts at the surface, obtained from standard Weather Bureau data, are shown. Photographs from Tiros by means of automatic picture transmission (APT) for 1200 to 1600 GMT on August 16 were used to check the persistence of the cloud patterns detected by the early morning Nimbus MRIR photographs. Also Radar Summary charts were used to check the heights of cloud build-ups over the United States and Caribbean Sea.

### Accuracy

The accuracy of the model atmospheres derived is determined by (1) the MRN data accuracy and (2) the error in placing the thermal-wind-derived isotherms on the constant-altitude isothermal analyses. In the approach to the accuracy problem, all rawinsonde data were assumed to be correct, and the effects of the aforementioned errors were studied only above  $h = 30$  km.

The correction of meteorological rocketsonde readings for the various effects is discussed at length in references 43 and 44. Briefly, some sources of error are solar radiation heating, dynamic heating, and sensor lag. The accuracy of the Arcasonde bead thermistor is  $\pm 0.5^{\circ}$  K. Estimates of error, including the effects of dynamic heating and radiation, are given in the following table:

## APPENDIX B

Altitude, km	Dynamic heating and radiation, °K		Sensor lag, °K	Total MRN error, °K
	Day	Night		
30	2	<1	1	1
40	3	2	1	3
50	6	4	1	5
60	9	7	1	8

It should be noted that the day correction applies to daytime soundings. The support for Project Scanner occurred during the hours of darkness at the surface and aloft. Therefore, the radiational heating error does not exist for the Scanner mission. The estimates for night launches appear in the column labeled "Night." In both the Day and Night columns, the indicated temperature errors are always positive. In addition, sensor lag in the stratosphere is estimated to be 1° K. When this lag error is added to the estimated night errors, the total estimated MRN errors given in the last column are obtained. These corrections were applied to the 1962 U.S. Standard Atmosphere up to an altitude of 60 km and the results are given in table XXII.

For the summer synoptic situation analyzed, where typically weak horizontal temperature gradients occurred, the worst error in placement of isotherms is assumed to be  $\pm 2^\circ$  K over the geographic area of interest. In an attempt to simulate this worst effect, the temperature of the 1962 U.S. Standard Atmosphere was increased by  $2^\circ$  K between altitudes of 30 and 80 km. These results are also given in table XXII.

As an estimate of the error in the radiance profile of a model atmosphere, due to errors in the meteorological data from which it was constructed, the root-sum-square error for selected tangent heights is formed for the aforementioned two sources of error. This error is not symmetric with respect to the unperturbed radiance profile. The existence of MRN errors means, essentially, lack of correction. Therefore, the resulting level of radiance at a given tangent height would be too high. Of course, the map analysis error may be uniformly positive or negative or a mixture of both.

The combination of the two errors is given in table XXII. Figure 22 shows the unperturbed radiance profile as a solid-line curve and the profile with errors as dash-line curves. The errors at  $H = 10$  km and  $20$  km are due to the temperature errors above  $h = 30$  km since no errors were introduced below  $h = 30$  km. These error bounds are only illustrative since they are derived from the perturbations applied to a standard atmosphere. However, the errors are smaller than the radiometric measurement errors (p. 18) for low radiance levels and of the same magnitude for larger radiance levels.

## REFERENCES

1. Thomas, John R.: Derivation and Statistical Comparison of Various Analytical Techniques Which Define the Location of Reference Horizons in the Earth's Horizon Radiance Profile. NASA CR-726, 1967.
2. Kirk, Raymond J.; Watson, Bruce F.; Brooks, Edward M.; and Carpenter, Robert O'B.: Infrared Horizon Definition — A State-of-the-Art Report. NASA CR-722, 1967.
3. Kondratiev, K. Y.; and Yakushevskaya, K. E.: Angular Distribution of the Outgoing Thermal Radiation in the Different Regions of the Spectrum. First International Symposium on Rocket and Satellite Meteorology, H. Wexler and J. E. Caskey, Jr., eds., John Wiley & Sons, Inc., 1963, pp. 254-277.
4. McGee, R. A.: An Analytical Infrared Radiation Model of the Earth. Appl. Opt., vol. 1, no. 5, Sept. 1962, pp. 649-653.
5. Hanel, R. A.; Bandeen, W. R.; and Conrath, B. J.: The Infrared Horizon of the Planet Earth. NASA TN D-1850, 1963. (Also published in J. Atmos. Sci., vol. 20, no. 2, Mar. 1963, pp. 73-86.)
6. Woestman, John W.: Earth Radiation Model for Infrared Horizon Sensor Applications. Infrared Phys., vol. 3, no. 2, July 1963, pp. 93-105.
7. Wark, D. Q.; Alishouse, J.; and Yamamoto, G.: Calculations of the Earth's Spectral Radiance for Large Zenith Angles. Meteorol. Satellite Lab. Rep. No. 21, Weather Bur., U.S. Dep. Com., Oct. 1963.
8. Wark, D. Q.; Alishouse, J.; and Yamamoto, G.: Variation of the Infrared Spectral Radiance Near the Limb of the Earth. Appl. Opt., vol. 3, no. 2, Feb., 1964, pp. 221-227.
9. Duncan, John; Wolfe, William; Oppel, George; and Burn, James: Infrared Horizon Sensors. 2389-80-T (Contract NONr 1224(12)), Inst. Sci. Technol., Univ. of Michigan, Apr. 1965. (Available from DDC as AD 466289.)
10. Burn, James W.: Infrared Horizons for Model Atmospheres of the Earth. Proceedings of the First Symposium on Infrared Sensors for Spacecraft Guidance & Control, Barnes Eng. Co., c.1965, pp. 3-14.
11. Burn, J. W.; Uplinger, W. G.; and Morris, P. P.: Earth Limb Radiance Profiles for the 15-Micron Carbon Dioxide Absorption Band — Data Computed by Month for Every 10 Degrees of Latitude in the Northern Hemisphere. LMSC-677318 (Contract AF 04(695)-1031, Subcontract 325), Lockheed Missiles & Space Co., Mar. 10, 1967.

12. Bates, Jerry C.; Hanson, David S.; House, Fred B.; Carpenter, Robert O'B.; and Gille, John C.: The Synthesis of  $15\mu$  Infrared Horizon Radiance Profiles From Meteorological Data Inputs. NASA CR-724, 1967.
13. Anon.: Compilation of Atmospheric Profiles and Synthesized  $15\mu$  Infrared Horizon Radiance Profiles Covering the Northern Hemisphere in the Longitude Region Between  $60^{\circ}$  W and  $160^{\circ}$  W From March 1964 Through February 1965. Honeywell, Inc., Oct. 1966.  
Part I. NASA CR-66184.  
Part II. NASA CR-66185.
14. Conrath, Barney J.: Earth Scan Analog Signal Relationships in the TIROS Radiation Experiment and Their Application to the Problem of Horizon Sensing. NASA TN D-1341, 1962.
15. Bradfield, L.: Horizon Sensor Infra-Red Flight Test Program. Rep. No. AO64189, Lockheed Missiles & Space Co., Oct. 19, 1962.
16. Collinge, J.; and Haynie, W.: Measurement of 15-Micron Horizon Radiance From a Satellite. EK/ARD ED-995 (Contract AFO4(695)-160), Eastman Kodak Co., Mar. 1, 1963. (Available from DDC as AD No. 437 804.)
17. McKee, Thomas B.; Whitman, Ruth I.; and Engle, Charles D.: Radiometric Observations of the Earth's Horizon From Altitudes Between 300 and 600 Kilometers. NASA TN D-2528, 1964.
18. Jalink, Antony, Jr.; Davis, Richard E.; and Hinton, Dwayne E.: Radiometric Measurements of the Earth's Infrared Horizon From the X-15 in Three Spectral Intervals. NASA TN D-4654, 1968.
19. Walker, R. G.; Cunniff, C. V.; and D'Agati, A. P.: Measurement of the Infrared Horizon of the Earth. AFCRL-66-631, U.S. Air Force, Sept. 1966.
20. Dodgen, John; and Curfman, Howard J.: Summary of Horizon Definition Studies Being Undertaken by Langley Research Center. Proceedings of the First Symposium on Infrared Sensors for Spacecraft Guidance & Control, Barnes Eng. Co., c.1965, pp. 233-239.
21. Dodgen, J. A.; McKee, T. B.; and Jalink, A.: NASA-LRC Program To Define Experimentally the Earth's IR Horizon. NASA paper presented at the Second Symposium on Infrared Horizon Sensors for Spacecraft Guidance and Control (El Segundo, Calif.), Mar. 14-15, 1967.
22. McKee, Thomas B.; Whitman, Ruth I.; and Davis, Richard E.: Preliminary Infrared Horizon Profiles From Project Scanner. NASA TM X-1483, 1967.

23. Walsh, T. M.; Dixon, William C., Jr.; Hinton, Dwayne E.; and Holland, James A.: A Celestial Attitude Measurement Instrument for Project Scanner. NASA TN D-4742, 1968.
24. Walsh, T. M.; Keating, Jean C.; and Hinton, Dwayne E.: Attitude Determination of Spin-Stabilized Project Scanner Spacecraft. NASA TN D-4740, 1968.
25. Chase, Stillman C.: Dual Radiometer Assembly for Project Scanner. NASA CR-1086, 1968.
26. Anon.: U.S. Standard Atmosphere, 1962. NASA, U.S. Air Force, and U.S. Weather Bur., Dec. 1962.
27. Fischer, Irene: An Astrogeodetic World Datum From Geoidal Heights Based on the Flattening  $f = 1/298.3$ . J. Geophys. Res., vol. 65, no. 7, July 1960, pp. 2067-2076.
28. Stull, V. R.; Wyatt, P. J.; and Plass, G. N.: Infrared Transmission Studies. Final Report, Volume III - The Infrared Absorption of Carbon Dioxide. SSD-TDR-62-127, Vol. III, U.S. Air Force, Jan. 31, 1963.
29. Elsasser, Walter M.; and Culbertson, Margaret F.: Atmospheric Radiation Tables. Meteorol. Monogr., vol. 4, no. 23, Aug. 1960.
30. Valley, Shea L., ed.: Handbook of Geophysics and Space Environments. Air Force Cambridge Res. Lab., 1965.
31. Mastenbrook, H. J.; and Dinger, J. E.: The Measurement of Water-Vapor Distribution in the Stratosphere. NRL Rep. 5551, U.S. Navy, Nov. 16, 1960. (Available from DDC as AD No. 247 760.)
32. Neporent, B. S.; Kiseleva, M. S.; Makogonenko, A. G.; and Shlyakhov, V. I.: Determination of Moisture in the Atmosphere From Absorption of Solar Radiation. Appl. Opt., vol. 6, no. 11, Nov. 1967, pp. 1845-1850.
33. Williamson, E. J.; and Houghton, J. T.: Radiometric Measurements of Emission From Stratospheric Water Vapour. Quart. J. Roy. Meteorol. Soc., vol. 91, no. 389, July 1965, pp. 330-338.
34. Garner, H. D.; and Reid, H. J. E., Jr.: Simulator Studies of Simple Attitude Control for Spin-Stabilized Vehicles. NASA TN D-1395, 1962.
35. De Waard, Russell; and Weiner, Seymour: Miniature Optically Immersed Thermistor Bolometer Arrays. Appl. Opt., vol. 6, no. 8, Aug. 1967, pp. 1327-1331.
36. Nicodemus, Fred E.; and Zissis, George J.: Methods of Radiometric Calibration. 4613-20-R (Contract SD-91), Inst. Sci. Technol., Univ. of Michigan, Oct. 1962.
37. Anon.: International Station Numbers for North and Central America. Third ed., Weather Bur., U.S. Dep. Com., 1954; Amendment No. 1, Feb. 1955.

38. Webb, Willis L.: Structure of the Stratosphere and Mesosphere. Academic Press, 1966.
39. Petterssen, Sverre: Weather Analysis and Forecasting. Volume I – Motion and Motion Systems. Second ed., McGraw-Hill Book Co., Inc., 1956, pp. 95-96.
40. Peterson, Roy E.; Schuetz, John; Shenk, William E.; and Tang, Wen: Derivation of a Meteorological Body of Data Covering the Northern Hemisphere in the Longitude Region Between 60° W and 160° W From March 1964 Through February 1965. NASA CR-723, 1967.
41. List, Robert J.: Smithsonian Meteorological Tables. Sixth revised ed., Smithsonian Inst., 1951.
42. Nordberg, W.; McCulloch, A. W.; Foshee, L. L.; and Bandeen, W. R.: Preliminary Results From Nimbus II. Bull. Amer. Meteorol. Soc., vol. 47, no. 11, Nov. 1966, pp. 857-872.
43. Clark, George Q.; and McCoy, John G.: Measurement of Stratospheric Temperature. J. Appl. Meteorol., vol. 4, no. 3, June, 1965, pp. 365-370.
44. Thompson, Donald C.; and Keily, D. P.: The Accuracy of Thermistors in the Measurement of Upper Air Temperature. J. Appl. Meteorol., vol. 6, no. 2, Apr. 1967, pp. 380-385.

**TABLE I**  
**HORIZON DEFINITION AND RELATED EXPERIMENTS**

Agency	Vehicle	Wavelengths of spectral regions, $\mu$	Vertical spatial resolution, km	Spatial positioning, km
DOD-Lockheed (ref. 15)	Satellite	$\left\{ \begin{array}{l} 5 \text{ to } 18 \\ 15 \text{ to } 18 \\ 12.5 \text{ to } 18 \\ 14 \text{ to } 16 \\ 15 \text{ to } 35 \end{array} \right.$	$\left. \begin{array}{c} \text{Not available} \end{array} \right\}$	None
DOD-Eastman Kodak (ref. 16)	Satellite	$\left\{ \begin{array}{l} 14.0 \text{ to } 15.2 \\ 13.7 \text{ to } 15.6 \\ 13.6 \text{ to } 16.5 \end{array} \right.$	$\left. \begin{array}{c} >5 \end{array} \right\}$	None
NASA-LRC (ref. 17)	Probe	$\begin{array}{l} 0.22 \text{ to } 0.29 \\ .35 \text{ to } 1.0 \\ .8 \text{ to } 2.5 \\ 1.8 \text{ to } 25.0 \end{array}$	$\begin{array}{c} 12 \\ 12 \\ 12 \\ 36 \end{array}$	None
NASA-LRC (ref. 18)	X-15 airplane	$\left\{ \begin{array}{l} 0.8 \text{ to } 2.8 \\ 10.5 \text{ to } 13.5 \\ 14.0 \text{ to } 20.0 \end{array} \right.$	$\left. \begin{array}{c} 2 \end{array} \right\}$	5
DOD-AFCRL (ref. 19)	Probe	$\begin{array}{l} 10.2 \text{ to } 11.8 \\ 14.0 \text{ to } 15.6 \\ 19.5 \text{ to } 31.8 \end{array}$	$\begin{array}{c} 6 \\ 9 \\ 6 \end{array}$	Not available
NASA-LRC Project Scanner	Probe	$\left\{ \begin{array}{l} 14.0 \text{ to } 16.3 \\ 21.0 \text{ to } 31.8 \end{array} \right.$	$\left. \begin{array}{c} <2 \end{array} \right\}$	<2

TABLE II  
CALIBRATION CONVERSION DATA FOR H<sub>2</sub>O

Altitude, km	Dry mixing ratio, g/kg	Integral ratio (eq. (12))	Wet mixing ratio, g/kg	Integral ratio (eq. (12))
0	5.500	0.991	10.650	1.020
2	2.500	-----	5.590	-----
4	1.100	-----	2.670	-----
6	.417	-----	1.170	-----
8	.181	-----	.453	-----
10	.0625	1.015	.093	1.036
12	.0190	-----	.055	-----
14	.0066	-----	.0755	-----
15	.0043	1.000	.088	1.050
16	.0020	-----	.103	-----
18	.0029	-----	.141	-----
20	.0037	.990	.194	1.052
22	.0052	-----	.338	-----
24	.0071	-----	.593	-----
26	.0093	-----	1.065	-----
28	.0125	-----	1.790	-----
30	.0174	.991	3.040	1.052
32	.0200	-----	5.270	-----
34	.0200	-----	8.040	-----
36	.0200	-----	8.040	-----
38	.0200	-----	8.040	-----
40	.0200	.915	8.040	1.044

**TABLE III**  
**MEASURED RADIANCE PROFILES FOR 615 cm<sup>-1</sup> TO 715 cm<sup>-1</sup>**

Tangent height, km	Radiance, W/m <sup>2</sup> -sr									
10.0		5.12	5.54	5.30	5.33	5.55	5.33	5.33	5.62	5.66
11.0		5.14	5.56	5.30	5.34	5.56	5.35	5.34	5.64	5.65
12.0		5.17	5.57	5.32	5.34	5.56	5.35	5.34	5.62	5.63
13.0	5.33	5.21	5.60	5.32	5.33	5.57	5.34	5.36	5.60	5.61
14.0	5.36	5.28	5.62	5.33	5.31	5.58	5.34	5.40	5.60	5.61
15.0	5.38	5.34	5.61	5.32	5.31	5.57	5.35	5.44	5.60	5.60
16.0	5.38	5.36	5.59	5.31	5.32	5.57	5.37	5.46	5.61	5.59
17.0	5.38	5.37	5.56	5.32	5.33	5.55	5.39	5.46	5.62	5.59
18.0	5.39	5.35	5.53	5.33	5.34	5.52	5.40	5.44	5.62	5.59
19.0	5.40	5.33	5.49	5.34	5.37	5.47	5.38	5.41	5.61	5.60
20.0	5.40	5.33	5.46	5.33	5.38	5.42	5.36	5.38	5.59	5.61
21.0	5.40	5.35	5.43	5.29	5.36	5.38	5.33	5.36	5.57	5.60
22.0	5.36	5.34	5.37	5.23	5.34	5.34	5.30	5.33	5.52	5.58
23.0	5.30	5.29	5.30	5.18	5.30	5.30	5.24	5.28	5.45	5.53
24.0	5.22	5.22	5.24	5.13	5.24	5.26	5.15	5.23	5.37	5.47
25.0	5.12	5.16	5.18	5.08	5.18	5.20	5.05	5.16	5.29	5.39
26.0	5.01	5.09	5.13	5.03	5.12	5.13	4.97	5.08	5.21	5.30
27.0	4.92	5.02	5.06	4.95	5.03	5.02	4.92	4.97	5.14	5.20
28.0	4.85	4.95	4.98	4.85	4.91	4.90	4.84	4.85	5.05	5.08
29.0	4.75	4.85	4.87	4.72	4.78	4.76	4.72	4.69	4.92	4.94
30.0	4.61	4.72	4.72	4.60	4.66	4.62	4.56	4.52	4.74	4.77
31.0	4.46	4.57	4.55	4.46	4.55	4.46	4.36	4.33	4.54	4.58
32.0	4.30	4.40	4.37	4.29	4.42	4.29	4.15	4.16	4.36	4.37
33.0	4.11	4.22	4.18	4.03	4.24	4.10	3.93	3.98	4.18	4.14
34.0	3.91	4.02	3.96	3.87	4.01	3.89	3.73	3.77	3.99	3.91
35.0	3.70	3.79	3.72	3.65	3.79	3.66	3.52	3.57	3.77	3.69
36.0	3.49	3.57	3.47	3.38	3.59	3.41	3.30	3.37	3.54	3.48
37.0	3.30	3.38	3.24	3.11	3.38	3.16	3.08	3.17	3.29	3.27
38.0	3.11	3.19	3.03	2.89	3.13	2.93	2.85	2.98	3.06	3.06
39.0	2.90	2.98	2.80	2.71	2.86	2.73	2.64	2.81	2.85	2.85
40.0	2.64	2.80	2.58	2.51	2.60	2.54	2.47	2.66	2.65	2.65
41.0	2.40	2.64	2.38	2.30	2.37	2.34	2.29	2.48	2.44	2.48
42.0	2.19	2.50	2.21	2.11	2.17	2.14	2.08	2.28	2.26	2.30
43.0	2.03	2.36	2.07	1.93	2.03	1.94	1.85	2.06	2.07	2.12
44.0	1.90	2.19	1.93	1.76	1.88	1.73	1.63	1.85	1.87	1.92
45.0	1.75	2.02	1.79	1.62	1.74	1.55	1.46	1.66	1.68	1.73
46.0	1.55	1.84	1.65	1.50	1.62	1.39	1.31	1.48	1.52	1.56
47.0	1.35	1.63	1.51	1.40	1.49	1.25	1.16	1.34	1.38	1.40
48.0	1.19	1.44	1.35	1.30	1.34	1.13	1.04	1.22	1.24	1.26
49.0	1.09	1.30	1.18	1.19	1.20	1.03	.92	1.09	1.11	1.12
50.0	.97	1.20	1.05	1.05	1.08	.93	.79	.96	1.00	.99
51.0	.82	1.10	.95	.89	.98	.83	.65	.85	.91	.89
52.0	.69	1.00	.88	.76	.88	.73	.50	.75	.84	.80
53.0	.62	.87	.81	.69	.75	.64	.38	.66	.77	.72
54.0	.59	.75	.74	.64	.60	.56	.31	.59	.69	.64
55.0	.52	.64	.66	.56	.49	.49	.30	.53	.61	.56
56.0	.43	.55	.59	.49	.39	.42	.33	.49	.54	.48
57.0	.35	.49	.54	.43	.32	.38	.34	.47	.46	.41
58.0	.29	.43	.48	.38	.28	.33		.44	.39	.35
59.0	.25	.34	.42	.35	.27	.27		.36	.34	.31
60.0	.22	.26	.38	.32	.26	.19		.28	.30	.28
LAT.	12.7	13.8	16.9	17.6	17.8	18.0	19.0	19.8	20.0	20.3
LONG.	58.5	56.3	52.9	53.2	61.9	51.7	51.8	51.4	50.7	49.9
Cell	7	7	6	6	7	6	6	6	6	6

TABLE III.- Continued

MEASURED RADIANCE PROFILES FOR 615  $\text{cm}^{-1}$  TO 715  $\text{cm}^{-1}$ 

Tangent height, km	Radiance, $\text{W/m}^2\text{-sr}$									
10.0	5.58	5.17	5.39		5.26	5.49		5.64	5.44	
11.0	5.59	5.15	5.41	5.49	5.27	5.52	5.51	5.64	5.44	
12.0	5.60	5.15	5.39	5.53	5.28	5.54	5.52	5.64	5.44	5.57
13.0	5.61	5.18	5.35	5.54	5.30	5.54	5.52	5.63	5.43	5.57
14.0	5.62	5.25	5.32	5.54	5.32	5.54	5.52	5.62	5.43	5.56
15.0	5.62	5.31	5.32	5.51	5.33	5.54	5.52	5.61	5.45	5.55
16.0	5.63	5.35	5.33	5.50	5.34	5.54	5.53	5.60	5.47	5.54
17.0	5.63	5.35	5.35	5.49	5.34	5.53	5.54	5.60	5.48	5.52
18.0	5.64	5.32	5.35	5.48	5.34	5.51	5.55	5.59	5.48	5.50
19.0	5.63	5.29	5.34	5.47	5.33	5.49	5.53	5.58	5.46	5.48
20.0	5.62	5.26	5.31	5.44	5.31	5.47	5.50	5.55	5.42	5.44
21.0	5.61	5.24	5.30	5.41	5.29	5.45	5.44	5.51	5.38	5.41
22.0	5.59	5.24	5.29	5.38	5.26	5.44	5.37	5.46	5.32	5.36
23.0	5.57	5.21	5.27	5.34	5.21	5.40	5.30	5.41	5.24	5.31
24.0	5.54	5.17	5.22	5.27	5.15	5.35	5.22	5.37	5.15	5.25
25.0	5.48	5.11	5.17	5.17	5.07	5.26	5.15	5.32	5.06	5.18
26.0	5.40	5.02	5.11	5.05	4.96	5.16	5.06	5.24	4.97	5.10
27.0	5.29	4.93	5.06	4.93	4.84	5.04	4.93	5.14	4.90	5.01
28.0	5.15	4.83	4.99	4.81	4.73	4.91	4.78	5.01	4.82	4.91
29.0	4.98	4.69	4.84	4.70	4.62	4.77	4.62	4.87	4.72	4.81
30.0	4.81	4.47	4.64	4.56	4.48	4.62	4.46	4.73	4.59	4.70
31.0	4.63	4.23	4.42	4.41	4.32	4.46	4.31	4.58	4.43	4.56
32.0	4.45	4.02	4.24	4.23	4.12	4.29	4.15	4.42	4.24	4.40
33.0	4.27	3.85	4.08	4.04	3.92	4.12	3.98	4.25	4.04	4.21
34.0	4.07	3.68	3.89	3.83	3.72	3.94	3.79	4.08	3.83	4.00
35.0	3.85	3.45	3.65	3.63	3.51	3.73	3.61	3.89	3.62	3.78
36.0	3.65	3.20	3.38	3.41	3.29	3.51	3.42	3.70	3.40	3.56
37.0	3.44	2.99	3.13	3.18	3.07	3.28	3.20	3.48	3.16	3.34
38.0	3.23	2.79	2.93	2.95	2.84	3.06	2.96	3.25	2.91	3.13
39.0	3.01	2.57	2.75	2.73	2.61	2.84	2.71	3.02	2.67	2.92
40.0	2.77	2.38	2.55	2.52	2.40	2.61	2.46	2.82	2.45	2.70
41.0	2.55	2.21	2.34	2.31	2.18	2.39	2.21	2.63	2.25	2.49
42.0	2.35	2.06	2.12	2.09	1.98	2.18	1.99	2.45	2.09	2.28
43.0	2.17	1.83	1.89	1.87	1.78	2.01	1.79	2.27	1.94	2.07
44.0	2.01	1.67	1.67	1.67	1.62	1.86	1.61	2.09	1.80	1.88
45.0	1.86	1.51	1.50	1.48	1.46	1.74	1.46	1.91	1.65	1.70
46.0	1.71	1.39	1.38	1.30	1.30	1.61	1.30	1.73	1.49	1.54
47.0	1.57	1.27	1.28	1.13	1.14	1.46	1.15	1.55	1.35	1.40
48.0	1.41	1.14	1.15	.98	1.01	1.30	.99	1.39	1.22	1.28
49.0	1.28	.98	.99	.86	.90	1.14	.87	1.25	1.11	1.16
50.0	1.16	.85	.84	.79	.81	1.01	.79	1.13	1.00	1.05
51.0	1.04	.70	.73	.76	.73	.91	.74	1.03	.91	.94
52.0	.92	.53	.64	.73	.68	.84	.70	.94	.82	.85
53.0	.80	.43	.56	.68	.64	.78	.60	.86	.74	.77
54.0	.70	.39	.49	.58	.60	.72	.45	.78	.67	.69
55.0	.61	.35	.42	.47	.55	.66	.29	.72	.59	.63
56.0	.53	.28	.33	.37	.48	.59	.18	.65	.51	.57
57.0	.47	.17	.25	.30	.39	.52	.16	.59	.43	.52
58.0	.43	.09	.21	.23	.29	.45	.17	.52	.37	.50
59.0	.39	.04	.21	.17	.21	.39	.18	.48	.31	.46
60.0	.36	-.01	.18	.12	.13	.33	.15	.44	.25	.42
LAT.	21.4	21.7	22.3	22.4	22.6	23.1	23.9	24.3	25.1	25.4
LCNG.	58.1	53.1	52.1	48.6	49.9	48.2	47.8	48.0	48.3	46.6
Cell	6	6	6	6	6	6	6	6	6	5

TABLE III.- Continued

MEASURED RADIANCE PROFILES FOR 615 cm<sup>-1</sup> TO 715 cm<sup>-1</sup>

Tangent height, km	Radiance, W/m <sup>2</sup> -sr									
10.0	5.57	5.42		5.36	5.55	5.51	5.30	5.77	5.48	5.44
11.0	5.62	5.44		5.37	5.59	5.55	5.34	5.76	5.51	5.45
12.0	5.63	5.44		5.37	5.60	5.57	5.39	5.75	5.54	5.49
13.0	5.63	5.44		5.38	5.60	5.57	5.43	5.75	5.55	5.54
14.0	5.61	5.44		5.39	5.56	5.56	5.46	5.76	5.57	5.59
15.0	5.60	5.45		5.40	5.53	5.52	5.48	5.76	5.58	5.61
16.0	5.58	5.43		5.40	5.53	5.48	5.47	5.76	5.58	5.62
17.0	5.58	5.50		5.40	5.58	5.45	5.44	5.74	5.57	5.60
18.0	5.58	5.49	5.40	5.42	5.65	5.44	5.41	5.72	5.55	5.59
19.0	5.57	5.45	5.39	5.45	5.70	5.45	5.36	5.68	5.52	5.58
20.0	5.56	5.40	5.37	5.44	5.71	5.47	5.32	5.63	5.48	5.56
21.0	5.53	5.33	5.35	5.41	5.63	5.48	5.23	5.57	5.44	5.54
22.0	5.48	5.25	5.32	5.36	5.61	5.46	5.23	5.51	5.40	5.50
23.0	5.41	5.17	5.27	5.28	5.54	5.39	5.13	5.44	5.36	5.42
24.0	5.32	5.10	5.21	5.21	5.45	5.31	5.11	5.37	5.32	5.33
25.0	5.22	5.04	5.13	5.15	5.35	5.21	5.03	5.29	5.26	5.25
26.0	5.11	4.93	5.03	5.09	5.24	5.11	4.93	5.20	5.17	5.16
27.0	5.01	4.90	4.93	5.00	5.13	5.00	4.81	5.10	5.06	5.08
28.0	4.90	4.80	4.81	4.87	5.01	4.86	4.69	5.00	4.92	4.96
29.0	4.78	4.66	4.66	4.69	4.87	4.72	4.55	4.87	4.78	4.80
30.0	4.63	4.48	4.48	4.50	4.71	4.59	4.39	4.73	4.63	4.61
31.0	4.46	4.27	4.29	4.31	4.53	4.45	4.21	4.58	4.48	4.42
32.0	4.24	4.05	4.07	4.14	4.35	4.29	4.02	4.41	4.32	4.24
33.0	4.01	3.85	3.86	3.98	4.18	4.12	3.81	4.23	4.14	4.08
34.0	3.77	3.63	3.65	3.80	3.99	3.93	3.60	4.02	3.94	3.92
35.0	3.52	3.42	3.45	3.59	3.77	3.73	3.39	3.80	3.73	3.74
36.0	3.30	3.20	3.24	3.36	3.54	3.54	3.16	3.58	3.51	3.52
37.0	3.10	2.99	3.04	3.14	3.33	3.33	2.94	3.37	3.28	3.28
38.0	2.90	2.79	2.85	2.92	3.13	3.11	2.72	3.17	3.06	3.03
39.0	2.70	2.61	2.66	2.71	2.92	2.88	2.50	2.96	2.87	2.78
40.0	2.49	2.41	2.48	2.48	2.70	2.66	2.29	2.76	2.69	2.56
41.0	2.27	2.22	2.29	2.26	2.46	2.44	2.09	2.56	2.49	2.36
42.0	2.06	2.03	2.11	2.06	2.24	2.23	1.90	2.36	2.28	2.17
43.0	1.88	1.84	1.95	1.92	2.04	2.03	1.72	2.17	2.07	1.97
44.0	1.73	1.68	1.79	1.80	1.85	1.83	1.54	1.97	1.86	1.77
45.0	1.53	1.52	1.63	1.66	1.67	1.64	1.37	1.78	1.65	1.56
46.0	1.45	1.37	1.47	1.50	1.48	1.47	1.22	1.59	1.46	1.37
47.0	1.32	1.21	1.31	1.32	1.30	1.33	1.03	1.41	1.28	1.20
48.0	1.19	1.04	1.14	1.16	1.17	1.20	.96	1.25	1.12	1.06
49.0	1.07	.89	.93	1.01	1.03	1.07	.85	1.11	.98	.93
50.0	.97	.76	.84	.90	1.00	.95	.75	.99	.87	.82
51.0	.87	.65	.73	.80	.91	.83	.67	.87	.76	.72
52.0	.76	.54	.63	.69	.80	.72	.59	.76	.65	.63
53.0	.65	.45	.55	.57	.68	.61	.52	.65	.53	.53
54.0	.56	.36	.49	.48	.57	.53	.45	.55	.43	.43
55.0	.43	.28	.43	.42	.48	.48	.40	.46	.34	.35
56.0	.41	.23	.38	.37	.40	.42	.32	.37	.27	.29
57.0	.34	.20	.34	.34	.32	.33	.23	.29	.22	.26
58.0	.28	.19	.31	.30	.28	.21	.14	.23	.18	.24
59.0	.24	.18	.27	.26	.27	.12	.06	.19	.14	.22
60.0	.21	.14	.24	.22	.25	.07	.01	.17	.11	.20
LAT.	28.0	30.3	30.6	32.0	32.8	32.9	35.9	37.7	38.2	38.9
LONG.	45.7	45.4	45.1	45.6	44.8	49.8	44.7	44.6	46.4	45.4
Cell	5	5	5	5	5	5	5	5	5	4

TABLE III. - Continued

MEASURED RADIANCE PROFILES FOR 615 cm<sup>-1</sup> TO 715 cm<sup>-1</sup>

Tangent height, km	Radiance, W/m <sup>2</sup> -sr									
10.0	5.82			5.68	5.93	5.80		5.84	5.95	
11.0	5.81	5.80		5.68	5.92	5.83		5.84	5.96	
12.0	5.81	5.83		5.71	5.92	5.85		5.83	5.96	
13.0	5.82	5.84		5.77	5.93	5.85		5.82	5.96	
14.0	5.81	5.83		5.81	5.94	5.84		5.82	5.95	
15.0	5.77	5.82	5.67	5.83	5.94	5.83	5.97	5.83	5.94	6.02
16.0	5.72	5.81	5.64	5.82	5.93	5.83	5.94	5.84	5.91	6.03
17.0	5.69	5.79	5.62	5.79	5.91	5.83	5.90	5.85	5.89	6.05
18.0	5.67	5.74	5.60	5.76	5.88	5.82	5.87	5.84	5.87	6.04
19.0	5.64	5.68	5.58	5.73	5.84	5.78	5.82	5.82	5.83	6.02
20.0	5.59	5.62	5.54	5.70	5.80	5.73	5.77	5.81	5.80	5.97
21.0	5.54	5.56	5.49	5.67	5.77	5.68	5.70	5.79	5.75	5.92
22.0	5.48	5.52	5.44	5.63	5.72	5.63	5.62	5.77	5.69	5.87
23.0	5.43	5.48	5.37	5.57	5.65	5.58	5.54	5.74	5.62	5.83
24.0	5.38	5.42	5.30	5.51	5.55	5.52	5.44	5.68	5.55	5.76
25.0	5.31	5.34	5.21	5.42	5.43	5.45	5.35	5.60	5.47	5.66
26.0	5.22	5.24	5.11	5.29	5.30	5.37	5.24	5.51	5.38	5.53
27.0	5.09	5.13	5.01	5.14	5.18	5.28	5.13	5.40	5.27	5.39
28.0	4.94	5.02	4.90	4.98	5.07	5.17	5.00	5.28	5.13	5.24
29.0	4.76	4.90	4.77	4.83	4.95	5.03	4.85	5.16	4.97	5.07
30.0	4.57	4.77	4.63	4.68	4.81	4.88	4.69	5.02	4.80	4.91
31.0	4.38	4.60	4.47	4.53	4.64	4.73	4.53	4.88	4.62	4.74
32.0	4.20	4.41	4.30	4.37	4.45	4.58	4.35	4.73	4.43	4.55
33.0	4.02	4.20	4.12	4.19	4.26	4.40	4.16	4.56	4.23	4.37
34.0	3.82	3.99	3.94	3.98	4.06	4.21	3.95	4.36	4.03	4.18
35.0	3.60	3.78	3.75	3.72	3.85	4.00	3.72	4.15	3.82	3.99
36.0	3.37	3.56	3.53	3.46	3.65	3.79	3.50	3.93	3.58	3.81
37.0	3.15	3.34	3.29	3.19	3.44	3.56	3.28	3.72	3.35	3.63
38.0	2.93	3.11	3.04	2.96	3.23	3.33	3.09	3.50	3.11	3.44
39.0	2.72	2.89	2.82	2.77	3.01	3.12	2.91	3.26	2.88	3.25
40.0	2.53	2.66	2.63	2.59	2.79	2.94	2.75	3.03	2.65	3.04
41.0	2.34	2.45	2.45	2.40	2.55	2.79	2.58	2.81	2.44	2.82
42.0	2.14	2.25	2.27	2.21	2.31	2.63	2.42	2.60	2.24	2.60
43.0	1.95	2.06	2.08	2.01	2.09	2.43	2.25	2.39	2.05	2.38
44.0	1.78	1.89	1.88	1.84	1.88	2.19	2.08	2.18	1.88	2.20
45.0	1.61	1.71	1.69	1.67	1.70	1.93	1.91	1.98	1.73	2.04
46.0	1.44	1.54	1.50	1.50	1.55	1.70	1.73	1.79	1.59	1.86
47.0	1.27	1.38	1.33	1.33	1.42	1.52	1.56	1.62	1.46	1.66
48.0	1.11	1.24	1.19	1.18	1.29	1.36	1.40	1.46	1.33	1.46
49.0	.98	1.09	1.08	1.02	1.18	1.21	1.24	1.31	1.20	1.28
50.0	.88	.95	.98	.88	1.05	1.06	1.09	1.17	1.08	1.12
51.0	.79	.81	.89	.77	.93	.93	.95	1.05	.97	.99
52.0	.68	.68	.80	.68	.82	.82	.83	.95	.88	.87
53.0	.58	.58	.71	.60	.71	.72	.73	.86	.79	.77
54.0	.52	.50	.61	.56	.63	.62	.65	.78	.69	.69
55.0	.48	.42	.52	.52	.57	.51	.58	.71	.58	.61
56.0	.44	.37	.44	.46	.52	.41	.52	.64	.49	.54
57.0	.39	.33	.39	.40	.47	.34	.46	.58	.41	.47
58.0	.34	.29	.35	.35	.41	.29	.42	.52	.36	.40
59.0	.30	.27	.32	.33	.35	.25	.39	.46	.30	.33
60.0	.26	.26	.28	.30	.30	.22	.36	.39	.25	.26
LAT.	40.2	40.4	40.5	43.0	44.0	44.2	44.9	46.3	48.9	50.8
LONG.	45.3	46.7	48.1	46.2	46.3	49.5	46.9	48.7	49.9	57.0
Cell	4	4	4	4	4	4	4	3	3	2

TABLE III.- Concluded

MEASURED RADIANCE PROFILES FOR 615 cm<sup>-1</sup> TO 715 cm<sup>-1</sup>

Tangent height, km	Radiance, W/m <sup>2</sup> -sr									
10.0	5.78	5.57	5.84	5.95	5.90	5.88	5.98	5.80		
11.0	5.76	5.99	5.85	5.98	5.92	5.93	5.99	5.82		
12.0	5.76	5.99	5.87	6.01	5.94	5.96	5.99	5.86		
13.0	5.78	5.57	5.90	6.01	5.95	5.96	6.00	5.90	5.95	5.86
14.0	5.80	5.96	5.93	5.99	5.95	5.93	6.01	5.95	5.97	5.90
15.0	5.82	5.55	5.94	5.97	5.93	5.92	6.00	5.98	5.99	5.91
16.0	5.85	5.94	5.92	5.96	5.90	5.94	6.00	5.98	6.02	5.92
17.0	5.87	5.95	5.88	5.96	5.88	5.96	6.00	5.97	6.04	5.93
18.0	5.88	5.96	5.85	5.95	5.89	5.95	5.99	5.94	6.04	5.94
19.0	5.87	5.97	5.82	5.92	5.89	5.91	5.98	5.92	6.00	5.94
20.0	5.86	5.97	5.78	5.89	5.88	5.89	5.96	5.89	5.94	5.90
21.0	5.83	5.95	5.75	5.87	5.85	5.89	5.93	5.86	5.88	5.86
22.0	5.79	5.88	5.71	5.88	5.81	5.85	5.89	5.81	5.80	5.82
23.0	5.74	5.79	5.66	5.86	5.75	5.80	5.83	5.73	5.72	5.76
24.0	5.67	5.69	5.60	5.82	5.68	5.74	5.75	5.64	5.65	5.70
25.0	5.58	5.59	5.53	5.74	5.59	5.70	5.67	5.52	5.57	5.62
26.0	5.47	5.48	5.45	5.63	5.49	5.64	5.56	5.39	5.47	5.52
27.0	5.34	5.35	5.35	5.48	5.38	5.53	5.44	5.24	5.37	5.41
28.0	5.20	5.20	5.24	5.32	5.24	5.40	5.30	5.09	5.26	5.30
29.0	5.06	5.05	5.10	5.16	5.07	5.26	5.15	4.94	5.13	5.18
30.0	4.92	4.87	4.95	5.00	4.90	5.12	5.00	4.79	4.98	5.04
31.0	4.76	4.69	4.79	4.83	4.73	4.96	4.84	4.64	4.82	4.91
32.0	4.59	4.50	4.59	4.65	4.55	4.76	4.67	4.46	4.64	4.75
33.0	4.42	4.30	4.36	4.47	4.34	4.57	4.49	4.27	4.44	4.56
34.0	4.26	4.08	4.11	4.28	4.14	4.40	4.30	4.06	4.23	4.34
35.0	4.08	3.87	3.89	4.09	3.93	4.21	4.11	3.82	4.02	4.09
36.0	3.88	3.67	3.67	3.88	3.73	3.99	3.89	3.57	3.80	3.84
37.0	3.65	3.47	3.47	3.67	3.52	3.79	3.65	3.33	3.58	3.62
38.0	3.43	3.25	3.27	3.46	3.30	3.60	3.41	3.13	3.36	3.44
39.0	3.22	3.02	3.06	3.23	3.09	3.41	3.19	2.97	3.12	3.22
40.0	3.02	2.78	2.85	2.99	2.86	3.21	2.98	2.80	2.88	2.97
41.0	2.79	2.55	2.63	2.75	2.62	2.98	2.78	2.61	2.64	2.71
42.0	2.55	2.34	2.41	2.55	2.38	2.70	2.56	2.40	2.42	2.50
43.0	2.29	2.12	2.21	2.36	2.15	2.43	2.34	2.19	2.24	2.28
44.0	2.06	1.91	2.01	2.18	1.93	2.20	2.12	2.00	2.08	2.07
45.0	1.86	1.71	1.82	1.98	1.73	2.01	1.93	1.81	1.92	1.88
46.0	1.70	1.56	1.64	1.78	1.56	1.83	1.78	1.63	1.75	1.70
47.0	1.55	1.45	1.46	1.58	1.40	1.65	1.63	1.45	1.61	1.53
48.0	1.41	1.34	1.30	1.41	1.26	1.47	1.49	1.29	1.49	1.37
49.0	1.26	1.22	1.13	1.25	1.12	1.32	1.33	1.14	1.36	1.20
50.0	1.13	1.07	.98	1.12	1.00	1.20	1.17	1.00	1.20	1.02
51.0	1.00	.92	.85	1.00	.87	1.06	1.03	.89	1.03	.88
52.0	.88	.78	.75	.89	.74	.91	.91	.80	.87	.77
53.0	.76	.69	.68	.78	.62	.81	.79	.72	.73	.69
54.0	.65	.63	.62	.68	.55	.77	.68	.65	.63	.60
55.0	.56	.58	.57	.61	.51	.71	.59	.58	.57	.52
56.0	.50	.53	.50	.54	.47	.60	.51	.53	.54	.47
57.0	.45	.46	.41	.48	.44	.47	.42	.47	.51	.42
58.0	.40	.39	.31	.41	.41	.37	.41	.41	.45	.36
59.0	.37	.32	.24	.36	.37	.29	.33	.33	.37	.29
60.0	.32	.25	.17	.31	.31	.25		.26	.26	.22
LAT.	51.7	52.2	52.4	52.9	53.0	54.5	55.5	56.2	56.7	57.0
LONG.	53.2	54.1	55.1	58.7	60.1	62.2	64.2	66.5	68.7	69.9
Cell	3	2	2	1	2	2	1	1	1	1

TABLE IV

AVERAGE OF MEASURED RADIANCE PROFILES FOR  
 615  $\text{cm}^{-1}$  TO 715  $\text{cm}^{-1}$  FOR GEOGRAPHIC  
 CELL 1 AT 58° N 68° W

Tangent height, km	Average radiance, $\text{W}/\text{m}^2\text{-sr}$	Maximum radiance, $\text{W}/\text{m}^2\text{-sr}$	Minimum radiance, $\text{W}/\text{m}^2\text{-sr}$	Standard deviation, $\text{W}/\text{m}^2\text{-sr}$
10.0	5.91	5.98	5.80	.08
11.0	5.93	5.99	5.82	.08
12.0	5.95	6.01	5.86	.07
13.0	5.95	6.01	5.86	.06
14.0	5.97	6.01	5.90	.04
15.0	5.97	6.00	5.91	.03
16.0	5.98	6.02	5.92	.03
17.0	5.98	6.04	5.93	.04
18.0	5.97	6.04	5.94	.04
19.0	5.95	6.00	5.92	.03
20.0	5.92	5.96	5.89	.03
21.0	5.88	5.93	5.86	.03
22.0	5.84	5.89	5.80	.04
23.0	5.78	5.86	5.72	.05
24.0	5.71	5.82	5.64	.07
25.0	5.62	5.74	5.52	.08
26.0	5.51	5.63	5.39	.08
27.0	5.39	5.48	5.24	.08
28.0	5.26	5.32	5.09	.08
29.0	5.11	5.18	4.94	.09
30.0	4.96	5.04	4.79	.09
31.0	4.81	4.91	4.64	.09
32.0	4.63	4.75	4.46	.09
33.0	4.45	4.56	4.27	.10
34.0	4.24	4.34	4.06	.10
35.0	4.02	4.11	3.82	.11
36.0	3.80	3.89	3.57	.12
37.0	3.57	3.67	3.33	.13
38.0	3.36	3.46	3.13	.12
39.0	3.15	3.23	2.97	.10
40.0	2.92	2.99	2.80	.07
41.0	2.70	2.78	2.61	.07
42.0	2.48	2.56	2.40	.07
43.0	2.28	2.36	2.19	.06
44.0	2.09	2.18	2.00	.06
45.0	1.90	1.98	1.81	.06
46.0	1.73	1.78	1.63	.06
47.0	1.56	1.63	1.45	.07
48.0	1.41	1.49	1.29	.08
49.0	1.25	1.36	1.14	.08
50.0	1.10	1.20	1.00	.08
51.0	.97	1.03	.88	.07
52.0	.85	.91	.77	.05
53.0	.74	.79	.69	.04
54.0	.65	.68	.60	.03
55.0	.57	.61	.52	.03
56.0	.52	.54	.47	.03
57.0	.46	.51	.42	.03
58.0	.41	.45	.36	.03
59.0	.34	.37	.29	.03
60.0	.26	.31	.22	.03

TABLE V

AVERAGE OF MEASURED RADIANCE PROFILES FOR  
 615  $\text{cm}^{-1}$  TO 715  $\text{cm}^{-1}$  FOR GEOGRAPHIC  
 CELL 2 AT 53° N 60° W

Tangent height, km	Average radiance, $\text{W/m}^2\text{-sr}$	Maximum radiance, $\text{W/m}^2\text{-sr}$	Minimum radiance, $\text{W/m}^2\text{-sr}$	Standard deviation, $\text{W/m}^2\text{-sr}$
10.0	5.90	5.97	5.84	.05
11.0	5.92	5.99	5.85	.05
12.0	5.94	5.99	5.87	.04
13.0	5.95	5.97	5.90	.03
14.0	5.94	5.96	5.93	.01
15.0	5.95	6.02	5.92	.04
16.0	5.95	6.03	5.90	.05
17.0	5.94	6.05	5.88	.06
18.0	5.94	6.04	5.85	.07
19.0	5.92	6.02	5.82	.07
20.0	5.90	5.97	5.78	.07
21.0	5.87	5.95	5.75	.07
22.0	5.82	5.88	5.71	.06
23.0	5.76	5.83	5.66	.06
24.0	5.69	5.76	5.60	.06
25.0	5.61	5.70	5.53	.06
26.0	5.52	5.64	5.45	.06
27.0	5.40	5.53	5.35	.07
28.0	5.26	5.40	5.20	.07
29.0	5.11	5.26	5.05	.08
30.0	4.95	5.12	4.87	.09
31.0	4.78	4.96	4.69	.09
32.0	4.59	4.76	4.50	.09
33.0	4.39	4.57	4.30	.09
34.0	4.18	4.40	4.08	.11
35.0	3.98	4.21	3.87	.12
36.0	3.77	3.99	3.67	.12
37.0	3.57	3.79	3.47	.12
38.0	3.37	3.60	3.25	.13
39.0	3.17	3.41	3.02	.15
40.0	2.95	3.21	2.78	.16
41.0	2.72	2.98	2.55	.16
42.0	2.49	2.70	2.34	.14
43.0	2.26	2.43	2.12	.13
44.0	2.05	2.20	1.91	.13
45.0	1.86	2.04	1.71	.14
46.0	1.69	1.86	1.56	.13
47.0	1.52	1.66	1.40	.11
48.0	1.36	1.47	1.26	.09
49.0	1.22	1.32	1.12	.08
50.0	1.07	1.20	.98	.08
51.0	.94	1.06	.85	.08
52.0	.81	.91	.74	.07
53.0	.71	.81	.62	.07
54.0	.65	.77	.55	.07
55.0	.60	.71	.51	.07
56.0	.53	.60	.47	.04
57.0	.45	.47	.41	.02
58.0	.38	.41	.31	.03
59.0	.31	.37	.24	.04
60.0	.25	.31	.17	.05

TABLE VI

AVERAGE OF MEASURED RADIANCE PROFILES FOR  
 615  $\text{cm}^{-1}$  TO 715  $\text{cm}^{-1}$  FOR GEOGRAPHIC  
 CELL 3 at 47° N 57° W

Tangent height, km	Average radiance, $\text{W}/\text{m}^2\text{-sr}$	Maximum radiance, $\text{W}/\text{m}^2\text{-sr}$	Minimum radiance, $\text{W}/\text{m}^2\text{-sr}$	Standard deviation, $\text{W}/\text{m}^2\text{-sr}$
10.0	5.85	5.95	5.78	.07
11.0	5.85	5.96	5.76	.08
12.0	5.85	5.96	5.76	.08
13.0	5.85	5.96	5.78	.08
14.0	5.85	5.95	5.80	.07
15.0	5.86	5.94	5.82	.05
16.0	5.87	5.91	5.84	.03
17.0	5.87	5.89	5.85	.02
18.0	5.86	5.88	5.84	.02
19.0	5.84	5.87	5.82	.02
20.0	5.82	5.86	5.80	.03
21.0	5.79	5.83	5.75	.03
22.0	5.75	5.79	5.69	.05
23.0	5.70	5.74	5.62	.06
24.0	5.63	5.68	5.55	.06
25.0	5.55	5.60	5.47	.06
26.0	5.45	5.51	5.38	.05
27.0	5.34	5.40	5.27	.05
28.0	5.21	5.28	5.13	.06
29.0	5.06	5.16	4.97	.08
30.0	4.91	5.02	4.80	.09
31.0	4.75	4.88	4.62	.11
32.0	4.58	4.73	4.43	.12
33.0	4.40	4.56	4.23	.13
34.0	4.22	4.36	4.03	.14
35.0	4.02	4.15	3.82	.14
36.0	3.80	3.93	3.58	.15
37.0	3.57	3.72	3.35	.16
38.0	3.35	3.50	3.11	.17
39.0	3.12	3.26	2.88	.17
40.0	2.90	3.03	2.65	.18
41.0	2.68	2.81	2.44	.17
42.0	2.46	2.60	2.24	.16
43.0	2.24	2.39	2.05	.14
44.0	2.04	2.18	1.88	.12
45.0	1.86	1.98	1.73	.10
46.0	1.69	1.79	1.59	.08
47.0	1.54	1.62	1.46	.07
48.0	1.40	1.46	1.33	.05
49.0	1.26	1.31	1.20	.04
50.0	1.13	1.17	1.08	.04
51.0	1.01	1.05	.97	.04
52.0	.90	.95	.88	.03
53.0	.80	.86	.76	.04
54.0	.71	.78	.65	.06
55.0	.62	.71	.56	.06
56.0	.54	.64	.49	.07
57.0	.48	.58	.41	.07
58.0	.43	.52	.36	.07
59.0	.38	.46	.30	.07
60.0	.32	.39	.25	.06

TABLE VII  
AVERAGE OF MEASURED RADIANCE PROFILES FOR  
615 cm<sup>-1</sup> TO 715 cm<sup>-1</sup> FOR GEOGRAPHIC  
CELL 4 AT 43° N 45° W

Tangent height, km	Average radiance, W/m <sup>2</sup> -sr	Maximum radiance, W/m <sup>2</sup> -sr	Minimum radiance, W/m <sup>2</sup> -sr	Standard deviation, W/m <sup>2</sup> -sr
10.0	5.73	5.93	5.44	.17
11.0	5.75	5.92	5.45	.15
12.0	5.77	5.92	5.49	.14
13.0	5.79	5.93	5.54	.12
14.0	5.80	5.94	5.59	.11
15.0	5.80	5.97	5.61	.11
16.0	5.79	5.94	5.62	.11
17.0	5.77	5.91	5.60	.11
18.0	5.74	5.88	5.59	.10
19.0	5.71	5.84	5.58	.10
20.0	5.66	5.80	5.54	.09
21.0	5.62	5.77	5.49	.09
22.0	5.57	5.72	5.44	.09
23.0	5.50	5.65	5.37	.09
24.0	5.43	5.55	5.30	.08
25.0	5.34	5.45	5.21	.08
26.0	5.24	5.37	5.11	.08
27.0	5.13	5.28	5.01	.07
28.0	5.00	5.17	4.90	.08
29.0	4.86	5.03	4.76	.09
30.0	4.71	4.88	4.57	.10
31.0	4.54	4.73	4.38	.11
32.0	4.36	4.58	4.20	.11
33.0	4.18	4.40	4.02	.11
34.0	3.98	4.21	3.82	.11
35.0	3.77	4.00	3.60	.11
36.0	3.55	3.79	3.37	.12
37.0	3.32	3.56	3.15	.12
38.0	3.09	3.33	2.93	.13
39.0	2.88	3.12	2.72	.13
40.0	2.68	2.94	2.53	.13
41.0	2.49	2.79	2.34	.14
42.0	2.30	2.63	2.14	.15
43.0	2.11	2.43	1.95	.15
44.0	1.91	2.19	1.77	.14
45.0	1.72	1.93	1.56	.12
46.0	1.54	1.73	1.37	.11
47.0	1.38	1.56	1.20	.11
48.0	1.23	1.40	1.06	.11
49.0	1.09	1.24	.93	.10
50.0	.96	1.09	.82	.09
51.0	.85	.95	.72	.08
52.0	.74	.83	.63	.08
53.0	.65	.73	.53	.07
54.0	.56	.65	.43	.07
55.0	.49	.58	.35	.07
56.0	.43	.52	.29	.07
57.0	.38	.47	.26	.06
58.0	.34	.42	.24	.06
59.0	.30	.39	.22	.05
60.0	.27	.36	.20	.05

TABLE VIII

AVERAGE OF MEASURED-RADIANCE PROFILES FOR  
 615  $\text{cm}^{-1}$  TO 715  $\text{cm}^{-1}$  FOR GEOGRAPHIC  
 CELL 5 AT 35° N 48° W

Tangent height, km	Average radiance, $\text{W}/\text{m}^2\text{-sr}$	Maximum radiance, $\text{W}/\text{m}^2\text{-sr}$	Minimum radiance, $\text{W}/\text{m}^2\text{-sr}$	Standard deviation, $\text{W}/\text{m}^2\text{-sr}$
10.0	5.49	5.77	5.30	.14
11.0	5.52	5.76	5.34	.13
12.0	5.54	5.75	5.37	.12
13.0	5.55	5.75	5.38	.11
14.0	5.55	5.76	5.39	.10
15.0	5.54	5.76	5.40	.10
16.0	5.53	5.76	5.40	.10
17.0	5.53	5.74	5.40	.10
18.0	5.52	5.72	5.40	.10
19.0	5.51	5.70	5.36	.11
20.0	5.48	5.71	5.32	.11
21.0	5.45	5.68	5.28	.11
22.0	5.40	5.61	5.23	.11
23.0	5.34	5.54	5.17	.11
24.0	5.26	5.45	5.10	.10
25.0	5.19	5.35	5.03	.10
26.0	5.10	5.24	4.93	.09
27.0	4.99	5.13	4.81	.09
28.0	4.88	5.01	4.69	.09
29.0	4.74	4.87	4.55	.10
30.0	4.58	4.73	4.39	.11
31.0	4.41	4.58	4.21	.13
32.0	4.23	4.41	4.02	.14
33.0	4.04	4.23	3.81	.15
34.0	3.83	4.02	3.60	.15
35.0	3.62	3.80	3.39	.16
36.0	3.40	3.58	3.16	.16
37.0	3.19	3.37	2.94	.16
38.0	2.98	3.17	2.72	.15
39.0	2.77	2.96	2.50	.15
40.0	2.56	2.76	2.29	.15
41.0	2.36	2.56	2.09	.14
42.0	2.16	2.36	1.90	.14
43.0	1.97	2.17	1.72	.13
44.0	1.79	1.97	1.54	.11
45.0	1.62	1.78	1.37	.11
46.0	1.45	1.59	1.22	.10
47.0	1.30	1.41	1.08	.09
48.0	1.15	1.23	.96	.09
49.0	1.02	1.16	.85	.09
50.0	.91	1.05	.75	.10
51.0	.80	.94	.65	.09
52.0	.70	.85	.54	.09
53.0	.60	.77	.45	.09
54.0	.51	.69	.36	.09
55.0	.44	.63	.28	.09
56.0	.37	.57	.23	.09
57.0	.31	.52	.20	.09
58.0	.26	.50	.14	.09
59.0	.22	.46	.06	.10
60.0	.18	.42	.01	.11

TABLE IX  
AVERAGE OF MEASURED RADIANCE PROFILES FOR  
615  $\text{cm}^{-1}$  TO 715  $\text{cm}^{-1}$  FOR GEOGRAPHIC  
CELL 6 AT 21° N 55° W

Tangent height, km	Average radiance, $\text{W}/\text{m}^2\text{-sr}$	Maximum radiance, $\text{W}/\text{m}^2\text{-sr}$	Minimum radiance, $\text{W}/\text{m}^2\text{-sr}$	Standard deviation, $\text{W}/\text{m}^2\text{-sr}$
10.0	5.45	5.66	5.17	.15
11.0	5.46	5.65	5.15	.14
12.0	5.47	5.64	5.15	.14
13.0	5.47	5.63	5.18	.14
14.0	5.48	5.62	5.25	.13
15.0	5.48	5.62	5.31	.12
16.0	5.49	5.63	5.31	.11
17.0	5.49	5.63	5.32	.10
18.0	5.48	5.64	5.32	.10
19.0	5.46	5.63	5.29	.10
20.0	5.44	5.62	5.26	.11
21.0	5.41	5.61	5.24	.11
22.0	5.38	5.59	5.23	.11
23.0	5.33	5.57	5.18	.11
24.0	5.27	5.54	5.13	.12
25.0	5.20	5.48	5.05	.12
26.0	5.11	5.40	4.96	.12
27.0	5.02	5.29	4.84	.12
28.0	4.91	5.15	4.73	.12
29.0	4.78	4.98	4.62	.11
30.0	4.62	4.81	4.46	.11
31.0	4.44	4.63	4.23	.11
32.0	4.26	4.45	4.02	.12
33.0	4.07	4.27	3.85	.12
34.0	3.87	4.08	3.68	.11
35.0	3.66	3.89	3.45	.12
36.0	3.43	3.70	3.20	.12
37.0	3.20	3.48	2.99	.12
38.0	2.98	3.25	2.79	.12
39.0	2.77	3.02	2.57	.12
40.0	2.56	2.82	2.38	.12
41.0	2.36	2.63	2.18	.12
42.0	2.17	2.45	1.98	.13
43.0	1.98	2.27	1.78	.13
44.0	1.79	2.09	1.61	.14
45.0	1.63	1.91	1.46	.14
46.0	1.48	1.73	1.30	.14
47.0	1.33	1.57	1.13	.14
48.0	1.20	1.41	.98	.14
49.0	1.06	1.28	.86	.13
50.0	.95	1.16	.79	.12
51.0	.84	1.04	.65	.11
52.0	.75	.94	.50	.12
53.0	.67	.86	.38	.13
54.0	.60	.78	.31	.13
55.0	.52	.72	.29	.12
56.0	.45	.65	.18	.12
57.0	.39	.59	.16	.12
58.0	.34	.52	.09	.12
59.0	.30	.48	.04	.11
60.0	.25	.44	-.01	.12

TABLE X

AVERAGE OF MEASURED RADIANCE PROFILES FOR  
615  $\text{cm}^{-1}$  TO 715  $\text{cm}^{-1}$  FOR GEOGRAPHIC  
CELL 7 AT 17° N 60° W

Tangent height, km	Average radiance, $\text{W}/\text{m}^2\text{-sr}$	Maximum radiance, $\text{W}/\text{m}^2\text{-sr}$	Minimum radiance, $\text{W}/\text{m}^2\text{-sr}$	Standard deviation, $\text{W}/\text{m}^2\text{-sr}$
10.0	5.23	5.33	5.12	.11
11.0	5.24	5.34	5.14	.10
12.0	5.25	5.34	5.17	.09
13.0	5.29	5.33	5.21	.05
14.0	5.32	5.36	5.28	.03
15.0	5.34	5.38	5.31	.03
16.0	5.36	5.38	5.32	.03
17.0	5.36	5.38	5.33	.02
18.0	5.36	5.39	5.34	.02
19.0	5.36	5.40	5.33	.03
20.0	5.37	5.40	5.33	.03
21.0	5.37	5.40	5.35	.02
22.0	5.35	5.36	5.34	.01
23.0	5.29	5.30	5.29	.00
24.0	5.23	5.24	5.22	.01
25.0	5.15	5.18	5.12	.02
26.0	5.07	5.12	5.01	.04
27.0	4.99	5.03	4.92	.05
28.0	4.90	4.95	4.85	.04
29.0	4.79	4.85	4.75	.04
30.0	4.66	4.72	4.61	.04
31.0	4.53	4.57	4.46	.05
32.0	4.37	4.42	4.30	.05
33.0	4.19	4.24	4.11	.06
34.0	3.98	4.02	3.91	.05
35.0	3.76	3.79	3.70	.04
36.0	3.55	3.59	3.49	.04
37.0	3.35	3.38	3.30	.04
38.0	3.14	3.19	3.11	.04
39.0	2.91	2.98	2.86	.05
40.0	2.68	2.80	2.60	.08
41.0	2.47	2.64	2.37	.12
42.0	2.29	2.50	2.17	.15
43.0	2.14	2.36	2.03	.15
44.0	1.99	2.19	1.88	.14
45.0	1.84	2.02	1.74	.13
46.0	1.67	1.84	1.55	.12
47.0	1.49	1.63	1.35	.11
48.0	1.32	1.44	1.19	.10
49.0	1.20	1.30	1.09	.09
50.0	1.08	1.20	.97	.09
51.0	.97	1.10	.82	.12
52.0	.86	1.00	.69	.13
53.0	.75	.87	.62	.10
54.0	.65	.75	.59	.07
55.0	.55	.64	.49	.07
56.0	.45	.55	.39	.07
57.0	.39	.49	.32	.07
58.0	.33	.43	.28	.07
59.0	.29	.34	.25	.04
60.0	.25	.26	.22	.02

TABLE XI  
AVERAGE OF ALL MEASURED RADIANCE PROFILES  
FOR 615  $\text{cm}^{-1}$  TO 715  $\text{cm}^{-1}$

Tangent height, km	Average radiance, $\text{W}/\text{m}^2\text{-sr}$	Maximum radiance, $\text{W}/\text{m}^2\text{-sr}$	Minimum radiance, $\text{W}/\text{m}^2\text{-sr}$	Standard deviation, $\text{W}/\text{m}^2\text{-sr}$
10.0	5.60	5.98	5.12	.24
11.0	5.61	5.99	5.14	.24
12.0	5.62	6.01	5.15	.23
13.0	5.63	6.01	5.18	.24
14.0	5.64	6.01	5.25	.23
15.0	5.66	6.02	5.31	.23
16.0	5.66	6.03	5.31	.22
17.0	5.65	6.05	5.32	.22
18.0	5.64	6.04	5.32	.22
19.0	5.62	6.02	5.29	.22
20.0	5.60	5.97	5.26	.21
21.0	5.57	5.95	5.24	.21
22.0	5.52	5.89	5.23	.21
23.0	5.47	5.86	5.17	.20
24.0	5.40	5.82	5.10	.20
25.0	5.32	5.74	5.03	.20
26.0	5.23	5.64	4.93	.19
27.0	5.13	5.53	4.81	.18
28.0	5.01	5.40	4.69	.17
29.0	4.87	5.26	4.55	.17
30.0	4.71	5.12	4.39	.17
31.0	4.55	4.96	4.21	.18
32.0	4.37	4.76	4.02	.19
33.0	4.18	4.57	3.81	.19
34.0	3.98	4.40	3.60	.19
35.0	3.76	4.21	3.39	.20
36.0	3.54	3.99	3.16	.20
37.0	3.32	3.79	2.94	.20
38.0	3.11	3.60	2.72	.21
39.0	2.89	3.41	2.50	.20
40.0	2.68	3.21	2.29	.20
41.0	2.43	2.98	2.09	.20
42.0	2.27	2.70	1.90	.19
43.0	2.08	2.43	1.72	.18
44.0	1.89	2.20	1.54	.17
45.0	1.72	2.04	1.37	.16
46.0	1.55	1.86	1.22	.16
47.0	1.40	1.66	1.08	.15
48.0	1.25	1.49	.96	.14
49.0	1.11	1.36	.85	.13
50.0	.99	1.20	.75	.12
51.0	.88	1.10	.65	.11
52.0	.77	1.00	.50	.11
53.0	.68	.87	.38	.11
54.0	.60	.78	.31	.11
55.0	.52	.72	.28	.11
56.0	.45	.65	.18	.10
57.0	.39	.59	.16	.10
58.0	.34	.52	.09	.10
59.0	.29	.48	.04	.10
60.0	.24	.44	-.01	.09

TABLE XII

ANALYTICAL RADIANCE PROFILES FOR 615  $\text{cm}^{-1}$  TO 715  $\text{cm}^{-1}$ 

Tangent height, km	Radiance, $\text{W/m}^2\text{-sr}$ , for --							Weighted average radiance, $\text{W/m}^2\text{-sr}$
	Cell 1	Cell 2	Cell 3	Cell 4	Cell 5	Cell 6	Cell 7	
0	6.14	5.96	5.93	5.79	5.68	5.47	5.43	5.70
1	6.14	5.96	5.93	5.79	5.68	5.47	5.43	5.70
2	6.15	5.97	5.93	5.80	5.69	5.48	5.44	5.71
3	6.15	5.97	5.94	5.80	5.69	5.48	5.44	5.71
4	6.16	5.98	5.95	5.81	5.70	5.49	5.45	5.72
5	6.16	5.98	5.95	5.81	5.70	5.49	5.45	5.72
6	6.17	5.99	5.96	5.82	5.71	5.50	5.46	5.73
7	6.18	5.99	5.96	5.82	5.72	5.50	5.46	5.73
8	6.18	6.00	5.97	5.83	5.72	5.51	5.47	5.74
9	6.19	6.01	5.98	5.83	5.73	5.51	5.47	5.75
10	6.20	6.01	5.98	5.84	5.74	5.52	5.48	5.75
11	6.20	6.02	5.99	5.85	5.74	5.52	5.48	5.76
12	6.21	6.03	6.00	5.85	5.75	5.53	5.48	5.77
13	6.22	6.04	6.01	5.86	5.75	5.53	5.48	5.77
14	6.23	6.04	6.01	5.87	5.76	5.53	5.48	5.77
15	6.23	6.04	6.02	5.88	5.77	5.53	5.48	5.78
16	6.23	6.04	6.02	5.89	5.79	5.54	5.49	5.79
17	6.22	6.04	6.02	5.89	5.81	5.55	5.50	5.80
18	6.20	6.02	6.01	5.89	5.81	5.57	5.52	5.80
19	6.17	5.99	6.00	5.87	5.81	5.58	5.53	5.79
20	6.13	5.95	5.97	5.83	5.79	5.59	5.54	5.78
21	6.08	5.87	5.93	5.78	5.76	5.57	5.52	5.74
22	6.02	5.82	5.87	5.72	5.72	5.53	5.48	5.69
23	5.95	5.74	5.79	5.65	5.66	5.48	5.43	5.63
24	5.87	5.64	5.71	5.56	5.59	5.43	5.37	5.56
25	5.78	5.53	5.61	5.48	5.50	5.38	5.32	5.49
26	5.68	5.41	5.50	5.38	5.41	5.28	5.23	5.39
27	5.53	5.29	5.39	5.27	5.29	5.14	5.08	5.26
28	5.37	5.17	5.28	5.17	5.16	4.97	4.90	5.12
29	5.18	5.04	5.14	5.03	5.02	4.80	4.71	4.96
30	4.99	4.88	4.96	4.88	4.89	4.66	4.57	4.81
31	4.79	4.67	4.73	4.70	4.76	4.54	4.45	4.66
32	4.58	4.46	4.50	4.50	4.58	4.38	4.31	4.47
33	4.36	4.24	4.28	4.28	4.37	4.20	4.15	4.27
34	4.14	4.02	4.07	4.05	4.14	3.99	3.95	4.05
35	3.93	3.80	3.86	3.83	3.89	3.77	3.74	3.83
36	3.72	3.59	3.64	3.60	3.64	3.53	3.51	3.60
37	3.51	3.39	3.42	3.38	3.40	3.29	3.27	3.37
38	3.29	3.18	3.20	3.15	3.16	3.06	3.04	3.14
39	3.07	2.97	2.98	2.94	2.93	2.84	2.82	2.92
40	2.82	2.74	2.75	2.71	2.71	2.64	2.61	2.70
41	2.57	2.51	2.52	2.49	2.50	2.45	2.42	2.49
42	2.31	2.28	2.30	2.28	2.30	2.26	2.22	2.28
43	2.07	2.07	2.09	2.07	2.10	2.08	2.03	2.08
44	1.88	1.86	1.89	1.87	1.90	1.89	1.86	1.88
45	1.73	1.67	1.70	1.68	1.71	1.70	1.72	1.70
46	1.56	1.49	1.51	1.50	1.53	1.52	1.55	1.52
47	1.39	1.32	1.34	1.33	1.36	1.34	1.38	1.35
48	1.23	1.16	1.18	1.17	1.21	1.19	1.21	1.19
49	1.08	1.02	1.04	1.03	1.08	1.06	1.07	1.06
50	.95	.89	.91	.91	.96	.95	.95	.94
51	.83	.78	.80	.80	.86	.86	.86	.84
52	.72	.68	.70	.71	.77	.78	.78	.75
53	.64	.60	.61	.62	.69	.70	.69	.66
54	.56	.52	.53	.54	.60	.61	.61	.58
55	.49	.46	.47	.47	.52	.52	.52	.50
56	.43	.40	.41	.41	.45	.44	.44	.43
57	.36	.34	.34	.34	.38	.37	.37	.36
58	.30	.29	.29	.29	.31	.31	.31	.30
59	.25	.24	.24	.23	.25	.25	.25	.25
60	.20	.20	.19	.19	.21	.21	.21	.20

TABLE XIII

MEASURED RADIANCE PROFILES FOR 315 cm<sup>-1</sup> TO 475 cm<sup>-1</sup>

Tangent height, km	Radiance, W/m <sup>2</sup> -sr									
0.0	10.35	11.50	11.53	12.06	11.51	11.39	11.17	11.06	11.14	11.00
1.0	10.50	11.25	11.49	11.99	11.47	11.29	11.01	11.01	10.89	10.83
2.0	10.51	10.84	11.34	11.86	11.39	11.12	10.79	10.90	10.64	10.63
3.0	10.24	10.36	11.17	11.66	11.30	10.89	10.55	10.72	10.37	10.35
4.0	9.79	9.82	10.95	11.43	11.12	10.63	10.31	10.48	10.04	9.98
5.0	9.06	9.16	10.82	11.20	10.82	10.33	10.06	10.16	9.63	9.56
6.0	8.05	8.34	10.62	10.88	10.49	9.93	9.69	9.76	9.16	9.09
7.0	7.07	7.46	10.32	10.46	10.13	9.31	9.17	9.27	8.64	8.54
8.0	6.71	6.56	9.90	9.99	9.61	8.44	8.59	8.69	8.01	7.85
9.0	6.83	5.78	9.35	9.49	9.02	7.46	7.97	7.99	7.27	6.92
10.0	6.81	5.15	8.68	8.87	8.43	6.46	7.24	7.16	6.46	5.81
11.0	6.63	4.59	7.74	8.14	7.63	5.40	6.39	6.20	5.60	4.68
12.0	6.00	3.97	6.70	7.24	6.47	4.25	5.33	5.22	4.78	3.66
13.0	5.13	3.20	5.56	6.18	5.11	3.17	4.30	4.33	3.97	2.88
14.0	4.16	2.51	4.42	4.99	3.71	2.35	3.40	3.51	3.22	2.38
15.0	3.20	2.02	3.31	3.85	2.58	1.81	2.65	2.81	2.62	2.09
16.0	2.36	1.67	2.40	2.89	2.02	1.46	2.04	2.29	2.21	1.83
17.0	1.59	1.38	1.77	2.24	1.75	1.27	1.59	2.00	1.87	1.64
18.0	1.34	1.21	1.37	1.98	1.62	1.10	1.28	1.82	1.55	1.50
19.0	1.11	1.09	1.06	1.90	1.55	1.02	1.08	1.67	1.28	1.30
20.0	.81	1.03	.86	1.82	1.43	.99	.96	1.49	1.08	1.06
21.0	.88	.94	.77	1.67	1.26	.93	.86	1.28	.99	.91
22.0	.86	.73	.70	1.47	1.11	.90	.75	1.11	.90	.85
23.0	.57	.59	.62	1.28	.95	.89	.67	1.02	.77	.77
24.0	.40	.55	.61	1.14	.76	.83	.61	.95	.69	.68
25.0	.29	.54	.74	1.04	.57	.65	.52	.83	.67	.62
26.0	.16	.52	.71	.88	.52	.48	.39	.67	.64	.60
27.0	.30	.47	.57	.66	.53	.48	.23	.53	.53	.58
28.0	.44	.31	.43	.52	.56	.56	.12	.41	.44	.51
29.0	.46	.23	.32	.47	.54	.55	.10	.27	.41	.41
30.0	.20	.33	.39	.51	.57	.45	.20	.17	.38	.31
31.0		.33	.46	.51	.49	.42	.33	.14	.32	.17
32.0		.27	.44	.51	.32	.42		.13	.27	.08
33.0		.21	.41	.51	.25	.37		.07	.26	.06
34.0		.09	.27	.47	.28	.30		-.02	.28	.00
35.0		-.04		.47	.28	.26		-.04	.25	-.16
LAT.	10.4	10.9	12.0	12.8	13.2	13.4	15.0	16.7	17.9	18.9
LONG.	70.9	62.1	61.4	58.5	59.4	61.2	55.4	53.0	52.4	51.0
Detector	1	1	1	1	1	1	1	1	1	1

TABLE XIII.- Continued

MEASURED RADIANCE PROFILES FOR 315 cm<sup>-1</sup> TO 475 cm<sup>-1</sup>

Tangent height, km	Radiance, W/m <sup>2</sup> -sr									
0.0	11.14	10.87	11.18	10.96	10.77	11.04	10.89	11.18	11.23	10.19
1.0	10.98	10.69	10.96	10.85	10.59	10.86	10.74	11.04	11.17	10.11
2.0	10.77	10.48	10.68	10.67	10.37	10.62	10.51	10.85	11.09	9.96
3.0	10.56	10.24	10.41	10.43	10.11	10.36	10.21	10.63	10.93	9.67
4.0	10.34	9.95	10.09	10.12	9.78	10.06	9.86	10.40	10.74	9.33
5.0	10.06	9.57	9.70	9.75	9.37	9.71	9.51	10.12	10.52	8.99
6.0	9.70	9.07	9.23	9.30	8.88	9.27	9.12	9.77	10.23	8.65
7.0	9.24	8.48	8.68	8.78	8.36	8.78	8.64	9.36	9.85	8.27
8.0	8.68	7.84	8.05	8.21	7.76	8.23	8.03	8.85	9.38	7.79
9.0	7.98	7.12	7.27	7.58	7.08	7.61	7.33	8.20	8.81	7.22
10.0	7.16	6.31	6.42	6.82	6.29	6.91	6.55	7.40	8.16	6.53
11.0	6.23	5.45	5.52	5.93	5.40	6.09	5.69	6.48	7.35	5.70
12.0	5.29	4.57	4.64	5.05	4.56	5.27	4.72	5.47	6.39	4.73
13.0	4.40	3.73	3.83	4.20	3.80	4.42	3.79	4.43	5.39	3.79
14.0	3.56	3.03	3.12	3.48	3.18	3.63	3.06	3.47	4.38	3.03
15.0	2.81	2.45	2.54	2.92	2.67	2.92	2.52	2.69	3.44	2.41
16.0	2.21	1.98	2.05	2.50	2.23	2.30	2.12	1.98	2.72	1.96
17.0	1.80	1.62	1.80	2.18	1.82	1.77	1.83	1.37	2.25	1.66
18.0	1.56	1.34	1.60	1.91	1.47	1.39	1.59	1.05	1.96	1.44
19.0	1.42	1.15	1.47	1.66	1.29	1.15	1.39	1.01	1.79	1.27
20.0	1.33	1.02	1.34	1.41	1.27	1.02	1.20	1.03	1.60	1.17
21.0	1.25	.91	1.22	1.23	1.22	.94	1.07	1.07	1.43	1.10
22.0	1.18	.82	1.10	1.14	1.01	.87	.98	1.12	1.30	1.00
23.0	1.10	.73	.98	1.10	.73	.80	.89	1.10	1.21	.84
24.0	.99	.63	.81	1.07	.43	.75	.79	.97	1.06	.65
25.0	.85	.53	.65	1.00	.26	.71	.75	.81	.90	.46
26.0	.69	.46	.53	.92	.23	.69	.69	.71	.78	.34
27.0	.55	.42	.49	.82	.28	.64	.61	.64	.72	.32
28.0	.45	.38	.49	.75	.36	.55	.52	.56	.72	.33
29.0	.45	.33	.48	.70	.44	.44	.45	.44	.72	.29
30.0	.47	.28	.45	.64	.46	.33	.42	.33	.70	.21
31.0	.46	.25	.41	.59	.43	.26	.36	.30	.66	.09
32.0	.41	.25	.37	.53	.36	.24	.29	.28	.57	.02
33.0	.32	.24	.35	.45	.22	.24	.17	.25	.48	.02
34.0	.17	.19	.34	.35	.12	.21	.14	.23	.42	.05
35.0	.03	.16	.34	.29	.08	.12	.11	.23	.37	.11
LAT.	19.8	21.3	22.4	23.2	24.3	25.2	25.4	26.8	28.5	29.6
LONG.	50.8	49.2	49.6	48.0	47.5	47.2	46.8	47.2	46.7	45.8
Detector	1	1	1	1	1	1	1	1	1	1

TABLE XIII. - Continued

MEASURED RADIANCE PROFILES FOR 315 cm<sup>-1</sup> TO 475 cm<sup>-1</sup>

Tangent height, km	Radiance, W/m <sup>2</sup> -sr									
0.0	9.84	9.91	9.56	9.78	8.67	9.43	7.30	7.10	6.66	7.18
1.0	9.87	9.80	9.37	9.76	8.71	9.46	7.47	7.24	6.51	6.81
2.0	9.87	9.67	9.14	9.69	8.75	9.38	7.56	7.36	6.36	6.56
3.0	9.78	9.52	8.90	9.54	8.74	9.18	7.60	7.41	6.17	6.39
4.0	9.61	9.35	8.62	9.30	8.68	8.90	7.58	7.39	5.93	6.22
5.0	9.31	9.14	8.35	9.00	8.56	8.63	7.54	7.30	5.63	5.99
6.0	8.98	8.87	8.03	8.61	8.35	8.41	7.44	7.17	5.32	5.69
7.0	8.62	8.53	7.65	8.16	8.07	8.20	7.28	6.99	5.06	5.43
8.0	8.19	8.10	7.20	7.68	7.68	7.95	7.04	6.77	4.83	5.23
9.0	7.71	7.59	6.68	7.16	7.15	7.53	6.77	6.52	4.62	5.02
10.0	7.09	7.04	6.07	6.60	6.47	6.92	6.48	6.25	4.34	4.80
11.0	6.41	6.43	5.41	5.96	5.72	6.15	6.04	5.89	4.04	4.53
12.0	5.69	5.69	4.76	5.26	4.92	5.31	5.50	5.45	3.68	4.19
13.0	4.94	4.80	4.13	4.48	4.07	4.47	4.84	4.92	3.27	3.77
14.0	4.12	3.86	3.53	3.66	3.25	3.68	4.13	4.29	2.83	3.28
15.0	3.27	2.99	2.97	2.94	2.52	2.95	3.45	3.61	2.40	2.71
16.0	2.49	2.30	2.42	2.31	1.96	2.38	2.86	2.96	2.04	2.19
17.0	1.92	1.84	1.98	1.86	1.60	1.95	2.37	2.43	1.83	1.78
18.0	1.56	1.63	1.67	1.56	1.37	1.66	1.98	2.14	1.65	1.51
19.0	1.31	1.55	1.40	1.35	1.23	1.50	1.71	1.96	1.51	1.38
20.0	1.14	1.45	1.19	1.19	1.12	1.38	1.50	1.81	1.39	1.29
21.0	1.00	1.28	1.04	1.04	1.03	1.21	1.33	1.65	1.28	1.20
22.0	.90	1.11	.95	.88	.96	1.00	1.19	1.48	1.18	1.08
23.0	.85	.97	.89	.72	.90	.82	1.06	1.35	1.08	.97
24.0	.81	.87	.81	.60	.80	.75	.89	1.26	.96	.90
25.0	.77	.80	.69	.55	.66	.73	.71	1.20	.86	.85
26.0	.70	.73	.52	.52	.56	.73	.55	1.15	.78	.79
27.0	.62	.65	.35	.51	.52	.66	.46	1.08	.71	.71
28.0	.53	.60	.23	.48	.47	.59	.44	1.00	.70	.59
29.0	.47	.58	.16	.43	.38	.55	.45	.92	.72	.47
30.0	.41	.59	.12	.38	.26	.56	.47	.82	.74	.38
31.0	.36	.58	.07	.32	.14	.58	.49	.72	.71	.33
32.0	.33	.53	.02	.25	.04	.55	.48	.63	.60	.33
33.0	.21	.48	-.04	.17	-.02	.48	.43	.54	.47	.35
34.0	.25	.45	-.10	.11	-.08	.43	.34	.50	.35	.33
35.0	.17	.40	-.13	.08	-.09	.41	.23	.48	.25	.27
LAT.	30.8	31.3	32.5	33.7	33.9	35.2	37.6	38.0	40.3	40.5
LONG.	44.9	44.9	45.0	45.6	44.5	49.2	44.3	44.0	44.3	45.3
Detector	1	1	1	1	1	1	1	1	1	1

TABLE XIII. - Continued

MEASURED RADIANCE PROFILES FOR 315 cm<sup>-1</sup> TO 475 cm<sup>-1</sup>

Tangent height, km	Radiance, W/m <sup>2</sup> -sr									
0.0	9.95	10.30	8.69	10.31	9.19	8.50	9.30	9.78	8.38	8.56
1.0	9.65	10.12	8.28	10.18	9.21	8.46	9.09	9.73	8.55	8.53
2.0	9.24	9.92	7.88	10.00	9.16	8.40	8.90	9.59	8.67	8.49
3.0	8.73	9.73	7.57	9.78	9.09	8.35	8.65	9.34	8.67	8.45
4.0	8.22	9.52	7.29	9.52	9.01	8.25	8.38	9.04	8.50	8.46
5.0	7.74	9.30	7.00	9.19	8.86	8.08	8.16	8.74	8.22	8.45
6.0	7.31	9.02	6.72	8.80	8.54	7.76	7.88	8.34	7.85	8.36
7.0	6.94	8.68	6.47	8.35	7.97	7.27	7.39	7.79	7.46	8.10
8.0	6.55	8.27	6.23	7.81	7.16	6.69	6.73	7.12	7.07	7.67
9.0	6.11	7.72	5.99	7.19	6.20	6.10	5.87	6.38	6.58	7.11
10.0	5.65	7.02	5.61	6.47	5.25	5.43	4.93	5.56	5.90	6.42
11.0	5.16	6.15	5.04	5.68	4.38	4.72	4.00	4.71	5.04	5.61
12.0	4.64	5.24	4.36	4.89	3.68	4.02	3.31	3.90	4.22	4.73
13.0	4.10	4.39	3.68	4.19	3.17	3.47	2.80	3.30	3.51	3.92
14.0	3.54	3.64	3.06	3.56	2.77	3.08	2.49	2.91	2.94	3.25
15.0	2.96	3.04	2.59	3.04	2.43	2.78	2.24	2.67	2.46	2.80
16.0	2.51	2.59	2.21	2.61	2.11	2.43	1.96	2.47	2.10	2.51
17.0	2.16	2.29	1.94	2.27	1.83	2.00	1.66	2.25	1.89	2.32
18.0	1.89	2.09	1.69	2.01	1.60	1.60	1.41	2.00	1.74	2.16
19.0	1.69	1.91	1.45	1.81	1.43	1.33	1.24	1.74	1.51	2.00
20.0	1.52	1.70	1.27	1.63	1.31	1.15	1.15	1.52	1.23	1.83
21.0	1.35	1.48	1.16	1.45	1.21	1.02	1.12	1.37	.95	1.62
22.0	1.25	1.27	1.05	1.25	1.10	.90	1.08	1.27	.77	1.33
23.0	1.18	1.10	.88	1.03	.97	.79	.98	1.15	.70	1.11
24.0	1.11	.95	.66	.83	.85	.66	.83	.99	.64	1.00
25.0	1.03	.88	.47	.73	.76	.52	.71	.89	.61	.97
26.0	.94	.84	.41	.69	.71	.42	.63	.94	.57	.95
27.0	.82	.77	.45	.69	.62	.36	.57	1.01	.51	.88
28.0	.72	.62	.51	.69	.53	.35	.48	.93	.46	.75
29.0	.65	.43		.67	.48	.36	.32	.71	.46	.64
30.0	.59	.26		.59	.51	.36	.19	.59	.46	.56
31.0	.53	.16		.47	.56	.34	.12	.59	.40	.50
32.0	.46	.10		.37	.53	.31	.11	.56	.24	.40
33.0	.40	.09		.28	.43	.28	.07	.47	.05	.30
34.0	.35	.13		.23	.33	.27	.04	.38	-.04	.26
35.0	.31	.22		.22	.26	.27	.03	.29	-.03	.25
LAT.	42.7	45.4	46.4	46.9	48.0	49.0	50.6	51.0	51.6	51.6
LONG.	44.9	46.2	58.3	47.0	49.4	55.8	52.1	56.7	60.5	64.3
Detector	1	1	1	1	1	1	1	1	1	1

TABLE XIII.- Continued

MEASURED RADIANCE PROFILES FOR 315 cm<sup>-1</sup> TO 475 cm<sup>-1</sup>

Tangent height, km	Radiance, W/m <sup>2</sup> -sr									
0.0	9.07	9.17	9.90	9.48	10.82	8.54	8.19	8.48	9.40	9.50
1.0	8.99	9.01	9.75	9.29	10.51	8.76	8.42	8.20	9.29	9.28
2.0	8.93	8.79	9.65	9.09	10.13	8.93	8.68	8.15	9.16	8.94
3.0	8.88	8.55	9.46	8.90	9.73	9.03	8.93	8.23	8.94	8.62
4.0	8.78	8.30	9.26	8.73	9.25	8.96	9.01	8.15	8.65	8.36
5.0	8.57	8.04	9.04	8.54	8.72	8.76	8.79	7.93	8.26	8.16
6.0	8.19	7.81	8.72	8.27	8.25	8.48	8.41	7.69	7.84	7.92
7.0	7.73	7.53	8.21	7.86	7.78	8.04	7.94	7.34	7.38	7.54
8.0	7.23	7.17	7.51	7.34	7.19	7.42	7.31	6.77	6.87	7.07
9.0	6.59	6.73	6.68	6.65	6.42	6.63	6.55	5.94	6.23	6.56
10.0	5.81	6.17	5.70	5.82	5.55	5.76	5.62	5.00	5.50	5.78
11.0	4.96	5.53	4.73	4.93	4.62	4.78	4.53	4.19	4.69	4.80
12.0	4.12	4.85	3.85	4.12	3.82	3.83	3.59	3.53	3.91	3.98
13.0	3.39	4.13	3.18	3.47	3.18	3.10	3.07	3.08	3.26	3.48
14.0	2.84	3.52	2.64	2.94	2.73	2.63	2.74	2.77	2.80	3.25
15.0	2.49	3.02	2.29	2.58	2.40	2.29	2.49	2.55	2.41	2.99
16.0	2.18	2.63	2.06	2.30	2.19	2.02	2.21	2.42	2.16	2.54
17.0	1.92	2.33	1.92	2.11	2.04	1.81	1.96	2.26	2.02	2.13
18.0	1.70	2.08	1.78	1.90	1.92	1.60	1.71	1.97	1.88	1.88
19.0	1.54	1.88	1.63	1.70	1.80	1.39	1.48	1.68	1.73	1.79
20.0	1.36	1.69	1.48	1.50	1.67	1.26	1.29	1.52	1.60	1.70
21.0	1.16	1.50	1.30	1.30	1.53	1.14	1.13	1.36	1.51	1.59
22.0	.99	1.37	1.14	1.13	1.36	.99	1.00	1.21	1.41	1.43
23.0	.84	1.28	1.03	.99	1.22	.80	.96	1.11	1.23	1.25
24.0	.67	1.21	.96	.90	1.11	.63	.98	1.00	1.04	1.09
25.0	.55	1.12	.85	.87	.98	.52	.97	.89	.92	1.00
26.0	.56	1.00	.72	.85	.81	.48	.88	.76	.82	.96
27.0	.63	.87	.58	.78	.68	.45	.70	.69	.71	.95
28.0	.67	.75	.47	.67	.62	.42	.56	.61	.61	.86
29.0	.65	.64	.40	.50	.62	.39	.47	.45	.53	.71
30.0	.56	.54	.33	.32	.57	.41	.40	.29	.47	.57
31.0	.48	.46	.27	.18	.43	.36	.34	.20	.38	.47
32.0	.40	.37	.25	.09	.22	.25	.27	.18	.26	.39
33.0	.31	.30	.20	.04	.09	.12	.20	.26	.15	.35
34.0	.24	.25	.11	.04	.08	.03	.16	.31	.09	.30
35.0	.22	.23	.01	.09	.08	.01	.12	.24	.04	.28
LAT.	51.7	52.8	53.7	53.7	53.7	54.1	54.3	56.6	56.8	57.2
LONG.	55.7	54.2	54.7	55.1	69.9	61.3	84.1	63.3	67.8	67.6
Detector	1	1	1	1	1	1	1	1	1	1

TABLE XIII.- Continued

MEASURED RADIANCE PROFILES FOR 315 cm<sup>-1</sup> TO 475 cm<sup>-1</sup>

Tangent height, km	Radiance, W/m <sup>2</sup> -sr									
0.0	11.66	11.92	11.60	11.61	11.82	11.32	11.14	11.24	10.99	11.12
1.0	11.52	11.82	11.50	11.39	11.50	11.26	11.05	11.03	10.82	10.97
2.0	11.36	11.71	11.35	11.16	11.25	11.06	10.91	10.77	10.65	10.78
3.0	11.16	11.56	11.21	10.90	11.10	10.83	10.71	10.50	10.39	10.53
4.0	10.91	11.37	11.06	10.57	10.88	10.63	10.44	10.23	10.03	10.16
5.0	10.57	11.12	10.78	10.16	10.53	10.38	10.09	9.95	9.59	9.71
6.0	10.07	10.84	10.42	9.65	10.09	10.00	9.66	9.64	9.06	9.20
7.0	9.48	10.49	10.09	9.03	9.53	9.52	9.11	9.22	8.40	8.54
8.0	8.75	10.04	9.75	8.35	8.85	8.95	8.45	8.67	7.61	7.66
9.0	8.14	9.36	9.35	7.69	7.99	8.16	7.71	7.97	6.65	6.69
10.0	7.29	8.47	8.68	6.94	6.99	7.18	6.86	7.11	5.61	5.63
11.0	6.07	7.41	7.83	6.04	5.95	6.10	5.92	6.16	4.57	4.62
12.0	4.98	6.30	6.95	5.04	4.95	4.99	4.96	5.15	3.70	3.78
13.0	4.01	5.19	6.02	4.14	4.11	3.91	4.11	4.17	2.99	3.16
14.0	3.11	4.19	4.89	3.32	3.48	2.94	3.40	3.36	2.43	2.66
15.0	2.28	3.30	3.77	2.67	2.92	2.25	2.82	2.70	2.03	2.20
16.0	1.79	2.59	2.86	2.19	2.51	1.86	2.33	2.20	1.71	1.76
17.0	1.53	2.09	2.21	1.90	2.23	1.71	1.96	1.79	1.47	1.48
18.0	1.34	1.72	1.83	1.75	2.05	1.64	1.74	1.49	1.27	1.33
19.0	1.32	1.41	1.65	1.66	1.89	1.47	1.63	1.31	1.10	1.23
20.0	1.31	1.25	1.55	1.52	1.73	1.24	1.55	1.19	.96	1.09
21.0	1.22	1.19	1.40	1.33	1.54	1.03	1.38	1.05	.80	.97
22.0	1.16	1.18	1.22	1.15	1.37	.85	1.18	.93	.66	.93
23.0	.93	1.08	1.16	1.01	1.27	.80	1.04	.84	.56	.85
24.0	.69	.90	1.04	.95	1.15	.78	.96	.77	.49	.71
25.0	.60	.78	.78	.88	1.03	.70	.90	.72	.39	.64
26.0	.53	.69	.57	.76	.90	.59	.82	.69	.28	.63
27.0	.53	.59	.58	.63	.80	.44	.69	.64	.20	.51
28.0	.38	.53	.66	.57	.77	.33	.50	.55	.20	.41
29.0	.29	.51	.62	.56	.81	.21	.32	.46	.25	.37
30.0	.44	.42	.51	.55	.85	.11	.24	.41	.23	.30
31.0	.35	.30	.43	.47	.85	.14	.24	.35	.11	.27
32.0	.17	.36	.29	.40	.77	.25	.25	.29	-.01	.29
33.0	.05	.48	.13	.35	.64	.17	.24	.24	-.11	.28
34.0	.03	.48	.13	.30	.55	.13	.26	.17	-.14	.19
35.0	.04	.36	.13	.25	.50	.16	.28	.08	-.11	.14
LAT.	10.4	10.9	12.1	12.8	13.4	13.5	15.3	17.2	18.5	19.9
LONG.	67.8	59.8	59.0	56.7	59.1	57.0	54.2	51.7	51.0	49.5
Detector	2	2	2	2	2	2	2	2	2	2

TABLE XIII.- Continued

MEASURED RADIANCE PROFILES FOR 315 cm<sup>-1</sup> TO 475 cm<sup>-1</sup>

Tangent height, km	Radiance, W/m <sup>2</sup> -sr									
0.0	11.29	11.10	10.95	10.84	10.91	11.01	10.73	10.64	10.24	9.71
1.0	11.18	10.86	10.81	10.66	10.78	10.85	10.63	10.52	10.38	9.77
2.0	11.05	10.60	10.70	10.43	10.61	10.65	10.52	10.35	10.45	9.78
3.0	10.89	10.31	10.58	10.18	10.39	10.38	10.36	10.17	10.37	9.76
4.0	10.66	9.98	10.41	9.90	10.13	10.04	10.15	9.96	10.18	9.68
5.0	10.35	9.60	10.17	9.55	9.82	9.65	9.87	9.71	9.86	9.53
6.0	9.96	9.19	9.84	9.14	9.48	9.13	9.50	9.39	9.46	9.24
7.0	9.55	8.69	9.42	8.67	9.06	8.52	9.02	8.98	8.93	8.82
8.0	9.09	8.07	8.90	8.13	8.56	7.80	8.44	8.42	8.30	8.30
9.0	8.52	7.30	8.29	7.50	8.01	6.97	7.75	7.69	7.59	7.67
10.0	7.75	6.41	7.57	6.77	7.38	5.99	6.99	6.77	6.79	6.98
11.0	6.76	5.54	6.73	6.00	6.69	4.99	6.12	5.81	5.87	6.25
12.0	5.76	4.64	5.88	5.18	5.89	4.08	5.16	4.82	4.97	5.44
13.0	4.77	3.83	4.99	4.29	5.09	3.31	4.24	3.89	4.18	4.63
14.0	3.98	3.13	4.20	3.50	4.34	2.70	3.38	3.10	3.47	3.82
15.0	3.35	2.54	3.42	2.88	3.67	2.22	2.72	2.45	2.89	3.05
16.0	2.84	2.10	2.72	2.44	3.08	1.88	2.24	2.02	2.46	2.42
17.0	2.45	1.80	2.16	2.11	2.59	1.64	1.94	1.81	2.16	2.00
18.0	2.12	1.65	1.78	1.86	2.15	1.46	1.73	1.69	1.93	1.76
19.0	1.80	1.57	1.53	1.64	1.81	1.31	1.55	1.60	1.73	1.61
20.0	1.49	1.52	1.34	1.43	1.56	1.20	1.37	1.50	1.62	1.48
21.0	1.25	1.41	1.22	1.26	1.38	1.10	1.23	1.37	1.55	1.35
22.0	1.10	1.25	1.13	1.14	1.24	1.00	1.15	1.23	1.46	1.21
23.0	.99	1.07	1.07	1.03	1.10	.91	1.06	1.03	1.30	1.07
24.0	.90	.89	.98	.90	.96	.87	.94	.81	1.15	.93
25.0	.81	.77	.88	.73	.82	.84	.82	.61	1.02	.81
26.0	.70	.72	.77	.60	.71	.80	.75	.49	.90	.76
27.0	.60	.68	.62	.51	.62	.71	.68	.40	.79	.74
28.0	.51	.62	.44	.47	.54	.60	.64	.37	.66	.69
29.0	.48	.52	.27	.43	.45	.51	.64	.37	.52	.63
30.0	.50	.45	.18	.38	.34	.46	.60	.37	.43	.62
31.0	.52	.43	.20	.31	.25	.41	.50	.29	.41	.65
32.0	.55	.45	.24	.23	.20	.32	.43	.15	.38	.62
33.0	.56	.48	.25	.17	.19	.24	.43	.01	.35	.55
34.0	.52	.48	.21	.13	.22	.27	.48	-.08	.35	.47
35.0	.45	.44	.18	.11	.23	.37	.52	-.10	.36	.41
LAT.	20.4	21.7	22.3	23.7	24.9	25.0	26.3	26.8	28.6	30.3
LONG.	49.6	48.4	48.6	47.2	46.5	46.7	46.1	46.4	46.0	45.4
Detector	2	2	2	2	2	2	2	2	2	2

TABLE XIII.- Continued

MEASURED RADIANCE PROFILES FOR 315 cm<sup>-1</sup> TO 475 cm<sup>-1</sup>

Tangent height, km	Radiance, W/m <sup>2</sup> -sr									
0.0	9.36	9.66	9.67	9.02	8.72	9.73	6.26	6.37	9.02	10.23
1.0	9.16	9.58	9.63	9.12	8.53	9.70	6.09	6.20	8.59	9.91
2.0	8.97	9.53	9.56	9.25	8.36	9.58	5.96	6.04	8.12	9.56
3.0	8.77	9.45	9.45	9.34	8.19	9.38	5.87	5.90	7.68	9.15
4.0	8.53	9.30	9.31	9.26	8.04	9.09	5.76	5.78	7.23	8.65
5.0	8.25	9.05	9.12	8.99	7.88	8.74	5.62	5.66	6.75	8.08
6.0	7.90	8.70	8.87	8.63	7.72	8.38	5.46	5.56	6.29	7.43
7.0	7.50	8.30	8.57	8.25	7.50	8.04	5.31	5.46	5.92	6.74
8.0	7.04	7.87	8.16	7.86	7.26	7.72	5.18	5.36	5.65	6.06
9.0	6.51	7.44	7.69	7.39	6.99	7.41	5.08	5.26	5.44	5.37
10.0	5.96	6.96	7.12	6.81	6.68	7.07	4.97	5.17	5.20	4.71
11.0	5.36	6.36	6.45	6.10	6.30	6.60	4.78	5.01	4.89	4.13
12.0	4.68	5.60	5.71	5.28	5.80	5.93	4.47	4.76	4.49	3.60
13.0	3.99	4.77	4.90	4.39	5.19	5.13	4.05	4.39	3.98	3.13
14.0	3.34	4.02	4.09	3.56	4.52	4.20	3.53	3.89	3.45	2.72
15.0	2.80	3.38	3.30	2.89	3.82	3.33	3.03	3.34	2.95	2.35
16.0	2.39	2.86	2.61	2.43	3.14	2.62	2.60	2.81	2.49	2.05
17.0	2.07	2.45	2.08	2.11	2.60	2.10	2.25	2.40	2.12	1.82
18.0	1.82	2.12	1.73	1.89	2.15	1.79	1.98	2.12	1.83	1.65
19.0	1.62	1.87	1.49	1.73	1.77	1.64	1.76	1.94	1.63	1.51
20.0	1.48	1.68	1.32	1.60	1.46	1.54	1.58	1.80	1.46	1.34
21.0	1.34	1.50	1.17	1.47	1.24	1.43	1.42	1.64	1.34	1.16
22.0	1.17	1.35	1.00	1.33	1.08	1.34	1.26	1.45	1.24	1.00
23.0	1.02	1.20	.86	1.20	.95	1.25	1.12	1.28	1.12	.85
24.0	.92	1.05	.76	1.11	.84	1.15	1.01	1.12	.93	.74
25.0	.88	.93	.68	1.04	.74	1.07	.90	.98	.77	.67
26.0	.84	.79	.63	.99	.66	.96	.81	.85	.71	.64
27.0	.77	.68	.58	.91	.61	.80	.71	.75	.70	.60
28.0	.65	.58	.53	.80	.57	.67	.61	.69	.72	.52
29.0	.52	.49	.48	.69	.51	.56	.52	.66	.70	.42
30.0	.41	.41	.43	.59	.43	.48	.43	.60	.61	.33
31.0	.31	.35	.38	.53	.34	.42	.40	.51	.47	.29
32.0	.22	.32	.30	.48	.25	.37	.43	.40	.32	.28
33.0	.14	.26	.21	.45	.19	.33	.47	.33	.23	.29
34.0	.10	.19	.13	.42	.14	.32	.45	.32	.20	.31
35.0	.08	.12	.07	.36	.09	.37	.38	.36	.21	.30
LAT.	30.7	32.1	33.2	34.0	34.3	36.1	37.6	38.9	40.5	41.4
LONG.	44.6	44.5	44.9	44.3	45.6	49.5	44.4	44.1	44.6	45.9
Detector	2	2	2	2	2	2	2	2	2	2

TABLE XIII.- Continued

MEASURED RADIANCE PROFILES FOR 315 cm<sup>-1</sup> TO 475 cm<sup>-1</sup>

Tangent height, km	Radiance, W/m <sup>2</sup> -sr									
0.0	5.98	10.64	9.47	10.15	9.78	8.44	9.16	9.16	9.78	8.90
1.0	9.79	10.52	9.23	10.06	9.51	8.34	9.02	9.08	9.63	8.83
2.0	5.57	10.34	9.01	9.90	9.17	8.20	8.90	8.92	9.31	8.77
3.0	5.34	10.08	8.86	9.67	8.77	8.08	8.80	8.76	8.92	8.69
4.0	5.12	9.77	8.81	9.37	8.38	8.00	8.66	8.65	8.63	8.56
5.0	8.91	9.38	8.73	9.01	7.97	7.96	8.45	8.52	8.43	8.32
6.0	8.68	8.90	8.56	8.60	7.54	7.87	8.27	8.29	8.11	8.03
7.0	8.44	8.38	8.21	8.09	7.06	7.62	8.10	8.03	7.62	7.67
8.0	8.14	7.72	7.70	7.47	6.45	7.26	7.84	7.65	6.95	7.20
9.0	7.75	6.91	7.00	6.74	5.61	6.77	7.45	7.13	6.13	6.45
10.0	7.24	5.99	6.21	5.94	4.67	6.19	6.81	6.36	5.07	5.56
11.0	6.55	5.04	5.33	5.11	3.89	5.48	5.96	5.42	4.10	4.68
12.0	5.76	4.20	4.43	4.31	3.36	4.72	5.01	4.45	3.49	3.98
13.0	4.94	3.54	3.53	3.60	3.03	3.95	4.10	3.55	3.11	3.41
14.0	4.13	3.03	2.83	3.07	2.75	3.31	3.41	2.90	2.81	2.99
15.0	3.39	2.66	2.37	2.71	2.47	2.86	2.92	2.53	2.51	2.65
16.0	2.81	2.35	2.06	2.40	2.21	2.54	2.55	2.24	2.30	2.31
17.0	2.42	2.12	1.85	2.12	2.00	2.29	2.24	2.00	2.10	2.06
18.0	2.16	1.93	1.70	1.85	1.88	2.05	2.01	1.84	1.88	1.91
19.0	1.96	1.77	1.56	1.62	1.76	1.79	1.80	1.69	1.64	1.76
20.0	1.79	1.63	1.37	1.43	1.59	1.57	1.55	1.48	1.45	1.58
21.0	1.64	1.48	1.14	1.28	1.36	1.35	1.32	1.27	1.23	1.41
22.0	1.54	1.34	1.01	1.17	1.11	1.18	1.16	1.15	1.02	1.24
23.0	1.43	1.23	.98	1.06	.90	1.02	1.05	1.11	.90	1.09
24.0	1.31	1.13	.94	.94	.79	.87	.95	1.02	.78	.98
25.0	1.18	1.02	.88	.81	.70	.70	.84	.91	.68	.91
26.0	1.03	.92	.80	.69	.61	.57	.73	.76	.60	.87
27.0	.89	.82	.67	.62	.53	.48	.65	.68	.53	.75
28.0	.77	.74	.56	.60	.47	.43	.63	.66	.47	.57
29.0	.67	.71	.49	.60	.40	.36	.62	.64	.38	.37
30.0	.59	.69	.45	.58	.34	.27	.58	.60	.25	.26
31.0	.51	.68	.35	.53	.31	.22	.48	.54	.18	.23
32.0	.43	.61	.23	.46	.27	.23	.40	.46	.19	.24
33.0	.37	.55	.16	.38	.21	.23	.38	.38	.24	.26
34.0	.31	.49	.13	.31	.12	.23	.44	.33	.25	.32
35.0	.25	.48		.25	.07	.19	.51	.25	.22	.39
LAT.	43.6	45.9	46.7	47.2	49.3	49.6	51.8	52.0	52.1	52.2
LONG.	45.5	47.2	59.5	48.0	51.3	57.6	59.3	67.0	55.2	63.2
Detector	2	2	2	2	2	2	2	2	2	2

TABLE XIII.- Continued

MEASURED RADIANCE PROFILES FOR 315 cm<sup>-1</sup> TO 475 cm<sup>-1</sup>

Tangent height, km	Radiance, W/m <sup>2</sup> -sr									
0.0	9.03	10.14	9.63	10.95	10.08	9.56	9.11	10.40	10.68	11.00
1.0	9.06	9.69	9.41	10.99	10.00	9.53	8.94	10.36	10.46	10.81
2.0	9.18	9.46	9.18	10.85	9.86	9.48	8.71	10.24	10.17	10.62
3.0	9.25	9.21	8.94	10.64	9.66	9.36	8.47	9.98	9.73	10.43
4.0	9.21	8.83	8.69	10.56	9.39	9.16	8.20	9.66	9.34	10.09
5.0	9.14	8.48	8.45	10.37	9.05	8.82	8.11	9.26	8.95	9.66
6.0	8.97	8.31	8.17	9.89	8.67	8.39	8.16	8.73	8.46	9.06
7.0	8.56	8.66	7.86	9.29	8.26	7.80	8.12	8.10	8.03	8.25
8.0	7.96	8.70	7.49	8.70	7.74	7.05	7.65	7.36	7.55	7.43
9.0	7.18	8.11	7.05	7.91	7.11	6.12	6.92	6.61	6.78	6.48
10.0	6.27	6.82	6.53	6.91	6.34	5.22	6.09	5.77	5.77	5.50
11.0	5.28	5.24	5.87	5.75	5.53	4.45	5.05	4.79	4.86	4.55
12.0	4.33	3.77	5.10	4.63	4.78	3.87	3.99	3.87	3.99	3.78
13.0	3.52	2.98	4.37	3.78	4.06	3.43	3.28	3.19	3.36	3.23
14.0	2.98	2.57	3.74	3.16	3.39	3.09	2.86	2.73	3.08	2.86
15.0	2.66	2.21	3.22	2.76	2.82	2.75	2.54	2.43	2.89	2.56
16.0	2.47	1.98	2.81	2.48	2.42	2.39	2.24	2.23	2.73	2.32
17.0	2.27	1.69	2.50	2.20	2.09	2.07	2.02	2.04	2.52	2.16
18.0	2.05	1.60	2.27	1.97	1.79	1.84	1.85	1.87	2.18	2.06
19.0	1.85	1.43	2.02	1.76	1.55	1.65	1.66	1.76	1.90	1.94
20.0	1.63	1.25	1.78	1.63	1.42	1.47	1.41	1.68	1.72	1.82
21.0	1.36	1.17	1.55	1.50	1.35	1.29	1.16	1.55	1.45	1.61
22.0	1.12	1.01	1.34	1.36	1.28	1.15	.98	1.40	1.17	1.30
23.0	.98	.91	1.18	1.21	1.15	1.03	.87	1.27	.97	1.08
24.0	.93	.81	1.05	1.02	.99	.90	.72	1.15	.85	.97
25.0	.89	.72	.93	.86	.82	.76	.50	.98	.81	.82
26.0	.80	.66	.83	.71	.66	.61	.33	.81	.78	.65
27.0	.64	.47	.72	.57	.52	.50	.19	.67	.75	.51
28.0	.47	.32	.63	.47	.40	.47	.10	.57	.71	.42
29.0	.34	.33	.56	.39	.33	.50	.09	.52	.65	.49
30.0	.27	.32	.49	.33	.26	.50	.15	.50	.64	.62
31.0	.33	.17	.42	.36	.22	.47	.19	.48	.63	.63
32.0	.36	.09	.37	.46	.21	.42	.11	.44	.56	.54
33.0	.30	.05	.34	.53	.16	.38	.04	.35	.52	.49
34.0	.18	.05	.35	.46	.11	.34	.05	.24	.60	.43
35.0	.11	.13	.38	.30	.08	.28	.06	.18	.57	.32
LAT.	52.5	53.0	53.6	53.8	54.2	54.4	54.7	57.1	57.3	57.4
LONG.	58.8	89.1	56.3	73.7	57.6	57.6	65.4	72.0	68.6	72.7
Detector	2	2	2	2	2	2	2	2	2	2

TABLE XIII.- Continued

MEASURED RADIANCE PROFILES FOR 315 cm<sup>-1</sup> TO 475 cm<sup>-1</sup>

Tangent height, km	Radiance, W/m <sup>2</sup> -sr									
0.0	11.69	11.44	11.32	11.58	11.50	11.34	11.26	11.50	11.18	11.69
1.0	11.65	11.39	11.28	11.42	11.38	11.24	11.05	11.31	11.04	11.57
2.0	11.63	11.31	11.24	11.23	11.24	11.08	10.82	11.10	10.90	11.43
3.0	11.52	11.19	11.16	10.99	10.98	10.91	10.58	10.95	10.73	11.21
4.0	11.44	11.00	11.00	10.70	10.61	10.74	10.34	10.78	10.51	10.91
5.0	11.27	10.82	10.78	10.38	10.15	10.49	10.09	10.55	10.21	10.59
6.0	10.90	10.63	10.54	10.06	9.61	10.15	9.82	10.23	9.86	10.25
7.0	10.41	10.40	10.25	9.73	8.94	9.69	9.47	9.79	9.45	9.78
8.0	9.81	10.08	9.83	9.28	8.09	9.05	8.97	9.25	8.90	9.02
9.0	9.09	9.64	9.29	8.65	7.07	8.26	8.27	8.57	8.14	8.04
10.0	7.93	9.08	8.65	7.76	5.99	7.33	7.37	7.75	7.22	6.96
11.0	6.49	8.36	7.86	6.65	4.90	6.37	6.39	6.78	6.23	5.85
12.0	5.20	7.39	6.78	5.48	3.88	5.26	5.44	5.80	5.19	4.73
13.0	4.12	6.26	5.56	4.37	3.13	4.13	4.54	4.86	4.25	3.75
14.0	3.23	5.09	4.41	3.44	2.60	3.22	3.72	4.05	3.36	2.99
15.0	2.55	3.93	3.41	2.70	2.21	2.50	3.00	3.32	2.66	2.49
16.0	2.05	2.89	2.68	2.13	1.81	2.02	2.45	2.72	2.14	2.17
17.0	1.80	2.11	2.16	1.73	1.49	1.72	2.11	2.30	1.77	1.93
18.0	1.68	1.65	1.81	1.53	1.34	1.54	1.86	2.03	1.52	1.73
19.0	1.54	1.44	1.58	1.42	1.28	1.44	1.61	1.80	1.35	1.57
20.0	1.53	1.30	1.44	1.36	1.22	1.36	1.35	1.54	1.24	1.48
21.0	1.46	1.14	1.30	1.31	1.14	1.28	1.15	1.31	1.16	1.42
22.0	1.28	.98	1.13	1.20	1.04	1.08	1.02	1.17	1.09	1.35
23.0	1.14	.87	.99	1.05	.95	.86	.93	1.08	.97	1.23
24.0	1.01	.83	.85	.93	.88	.82	.85	1.01	.81	1.11
25.0	.87	.81	.68	.83	.82	.86	.79	.98	.66	1.05
26.0	.80	.73	.53	.73	.77	.74	.73	.94	.55	1.02
27.0	.66	.64	.52	.62	.68	.54	.67	.90	.50	.94
28.0	.57	.58	.58	.52	.56	.38	.61	.84	.49	.86
29.0	.45	.58	.60	.48	.43	.24	.53	.78	.49	.76
30.0	.34	.58	.51	.45	.35	.17	.40	.77	.45	.66
31.0	.17	.60	.31	.34	.38	.17	.27	.74	.42	.56
32.0	.20	.57	.12	.18	.46	.16	.21	.60	.44	.52
33.0	.47	.51	.09	.07	.44	.16	.15	.45	.45	.51
34.0	.33	.40	.09	.08	.36	.14	.08	.37	.44	.53
35.0	.16	.22	-.05	.14	.26	.03	.06	.35	.37	.48
LAT.	10.5	10.9	12.2	12.8	13.5	13.5	15.5	17.6	18.8	20.4
LONG.	66.0	59.0	57.9	55.8	58.1	55.9	53.5	51.0	50.3	48.9
Detector	3	3	3	3	3	3	3	3	3	3

TABLE XIII.- Continued

MEASURED RADIANCE PROFILES FOR 315 cm<sup>-1</sup> TO 475 cm<sup>-1</sup>

Tangent height, km	Radiance, W/m <sup>2</sup> -sr									
0.0	11.50	11.21	10.92	10.97	10.93	11.13	11.26	10.78	10.03	10.34
1.0	11.36	11.07	10.81	10.79	10.79	10.91	11.16	10.59	9.78	10.08
2.0	11.24	10.88	10.69	10.60	10.64	10.64	11.00	10.37	9.63	9.81
3.0	11.07	10.66	10.54	10.39	10.42	10.37	10.77	10.13	9.59	9.62
4.0	10.85	10.40	10.34	10.14	10.14	10.18	10.48	9.89	9.62	9.49
5.0	10.57	10.11	10.04	9.86	9.78	9.99	10.14	9.66	9.59	9.32
6.0	10.25	9.80	9.60	9.53	9.38	9.69	9.73	9.43	9.41	9.03
7.0	9.87	9.40	9.07	9.12	8.94	9.19	9.20	9.16	9.16	8.65
8.0	9.38	8.86	8.47	8.64	8.46	8.53	8.56	8.79	8.85	8.19
9.0	8.77	8.17	7.85	8.03	7.86	7.77	7.87	8.27	8.44	7.62
10.0	8.00	7.36	7.16	7.27	7.14	6.90	7.07	7.55	7.87	6.96
11.0	7.09	6.47	6.34	6.39	6.27	5.92	6.13	6.64	7.15	6.16
12.0	6.12	5.53	5.50	5.47	5.37	4.97	5.11	5.62	6.26	5.30
13.0	5.15	4.69	4.65	4.58	4.52	4.05	4.23	4.57	5.30	4.46
14.0	4.26	3.92	3.92	3.81	3.79	3.32	3.51	3.68	4.37	3.70
15.0	3.54	3.22	3.33	3.19	3.17	2.77	3.00	2.95	3.49	3.04
16.0	2.93	2.58	2.86	2.68	2.68	2.37	2.57	2.44	2.77	2.54
17.0	2.40	2.04	2.48	2.23	2.30	2.07	2.25	2.06	2.26	2.19
18.0	1.95	1.65	2.14	1.87	2.02	1.83	2.00	1.85	1.97	1.99
19.0	1.65	1.39	1.85	1.60	1.82	1.64	1.82	1.70	1.81	1.83
20.0	1.47	1.25	1.64	1.40	1.67	1.46	1.71	1.53	1.69	1.70
21.0	1.32	1.16	1.48	1.26	1.54	1.27	1.63	1.41	1.56	1.57
22.0	1.16	1.06	1.36	1.12	1.41	1.08	1.55	1.32	1.41	1.43
23.0	1.00	.96	1.21	.98	1.27	.90	1.43	1.22	1.21	1.27
24.0	.84	.84	1.06	.84	1.15	.80	1.27	1.05	1.04	1.09
25.0	.67	.72	.93	.68	1.03	.75	1.09	.85	.94	.92
26.0	.53	.65	.87	.55	.90	.72	.89	.76	.87	.74
27.0	.47	.63	.80	.47	.78	.67	.74	.76	.84	.57
28.0	.45	.62	.69	.44	.64	.60	.61	.74	.83	.46
29.0	.43	.56	.58	.45	.56	.52	.53	.67	.83	.39
30.0	.40	.47	.49	.46	.51	.47	.48	.56	.79	.37
31.0	.37	.37	.41	.44	.47	.48	.46	.47	.74	.33
32.0	.34	.31	.36	.42	.42	.52	.43	.40	.63	.29
33.0	.30	.29	.32	.40	.36	.54	.37	.31	.47	.28
34.0	.26	.30	.32	.36	.29	.53	.36	.25	.37	.29
35.0	.24	.32	.34	.31	.25	.52	.36	.22	.33	.29
LAT.	20.7	22.0	22.2	24.0	24.7	25.4	26.7	26.9	28.7	30.7
LONG.	49.1	47.9	48.1	46.8	46.2	46.4	45.8	46.0	45.7	44.5
Detector	3	3	3	3	3	3	3	3	3	3

TABLE XIII. - Continued

MEASURED RADIANCE PROFILES FOR 315 cm<sup>-1</sup> TO 475 cm<sup>-1</sup>

Tangent height, km	Radiance, W/m <sup>2</sup> -sr									
0.0	9.93	9.93	8.44	9.37	9.84	9.66	6.85	6.98	9.22	10.56
1.0	9.72	9.80	8.41	9.12	9.72	9.45	6.70	6.85	8.83	10.43
2.0	9.53	9.66	8.42	8.88	9.58	9.34	6.60	6.75	8.40	10.28
3.0	9.40	9.51	8.43	8.70	9.40	9.32	6.45	6.64	7.95	10.08
4.0	9.30	9.36	8.39	8.54	9.21	9.32	6.26	6.49	7.54	9.87
5.0	9.18	9.19	8.33	8.36	9.00	9.24	6.03	6.33	7.19	9.63
6.0	9.01	9.00	8.28	8.11	8.76	9.08	5.80	6.15	6.87	9.29
7.0	8.76	8.79	8.25	7.80	8.49	8.82	5.59	5.95	6.51	8.83
8.0	8.45	8.54	8.17	7.43	8.17	8.46	5.38	5.75	6.09	8.23
9.0	8.02	8.16	7.98	7.00	7.76	7.97	5.17	5.57	5.62	7.48
10.0	7.50	7.62	7.61	6.49	7.25	7.38	4.92	5.38	5.08	6.71
11.0	6.87	6.97	7.11	5.88	6.62	6.73	4.60	5.14	4.57	6.00
12.0	6.09	6.19	6.53	5.17	5.84	6.03	4.16	4.82	4.08	5.28
13.0	5.19	5.39	5.89	4.42	5.04	5.32	3.65	4.42	3.58	4.57
14.0	4.23	4.58	5.20	3.69	4.28	4.57	3.11	3.95	3.10	3.81
15.0	3.36	3.81	4.43	3.05	3.59	3.84	2.61	3.49	2.67	3.10
16.0	2.68	3.17	3.65	2.57	3.01	3.15	2.20	3.01	2.34	2.54
17.0	2.19	2.68	2.98	2.22	2.54	2.56	1.86	2.59	2.13	2.15
18.0	1.89	2.34	2.46	2.00	2.16	2.13	1.59	2.26	1.98	1.89
19.0	1.65	2.07	2.08	1.82	1.86	1.84	1.36	2.02	1.84	1.71
20.0	1.49	1.83	1.81	1.65	1.59	1.65	1.21	1.85	1.67	1.55
21.0	1.38	1.66	1.57	1.47	1.40	1.52	1.11	1.72	1.48	1.42
22.0	1.27	1.52	1.38	1.25	1.28	1.41	.99	1.56	1.30	1.34
23.0	1.14	1.41	1.18	1.08	1.17	1.27	.91	1.40	1.12	1.28
24.0	1.01	1.29	1.01	.92	1.05	1.10	.84	1.27	.98	1.27
25.0	.93	1.15	.85	.75	.94	.97	.78	1.18	.87	1.28
26.0	.87	1.00	.76	.61	.84	.87	.71	1.07	.78	1.26
27.0	.79	.87	.71	.49	.79	.77	.59	.95	.69	1.18
28.0	.67	.77	.69	.43	.75	.68	.48	.84	.60	1.04
29.0	.54	.72	.63	.41	.71	.61	.35	.77	.52	.89
30.0	.44	.69	.55	.39	.66	.58	.26	.74	.45	.73
31.0	.39	.62	.44	.36	.64	.58	.20	.74	.38	.61
32.0	.39	.52	.36	.35	.61	.62	.17	.75	.33	.52
33.0	.42	.44	.32	.31	.56	.64	.11	.69	.27	.46
34.0	.41	.40	.34	.21	.46	.63	.01	.62	.19	.40
35.0	.36	.37	.37	.11	.35	.54	-.09	.56	.14	.34
LAT.	30.8	32.5	33.6	34.1	34.6	36.6	37.8	39.4	40.5	41.8
LONG.	45.3	44.4	44.9	44.2	45.7	49.7	44.5	44.3	44.9	46.2
Detector	3	3	3	3	3	3	3	3	3	3

TABLE XIII.- Continued

MEASURED RADIANCE PROFILES FOR 315 cm<sup>-1</sup> TO 475 cm<sup>-1</sup>

Tangent height, km	Radiance, W/m <sup>2</sup> -sr									
0.0	10.25	10.74	9.50	10.38	7.99	9.69	10.61	10.81	9.06	9.06
1.0	10.22	10.68	9.27	10.32	8.00	9.43	10.77	10.74	8.92	9.08
2.0	10.14	10.59	9.08	10.20	8.06	9.24	10.89	10.63	8.81	9.08
3.0	10.01	10.45	8.91	10.02	8.12	9.05	11.00	10.49	8.66	9.06
4.0	9.83	10.23	8.78	9.73	8.16	8.77	10.80	10.27	8.43	8.96
5.0	9.57	9.94	8.67	9.36	8.16	8.32	10.46	9.95	8.22	8.78
6.0	9.24	9.58	8.51	8.92	8.14	7.80	10.14	9.57	8.04	8.55
7.0	8.87	9.11	8.17	8.41	8.04	7.20	9.63	9.17	7.76	8.23
8.0	8.43	8.56	7.72	7.82	7.78	6.53	8.77	8.68	7.32	7.77
9.0	7.91	7.84	7.20	7.15	7.36	5.75	7.67	7.96	6.72	7.09
10.0	7.28	7.00	6.56	6.44	6.80	4.95	6.38	7.03	5.99	6.16
11.0	6.51	6.07	5.73	5.76	6.10	4.13	5.44	5.97	5.14	5.12
12.0	5.66	5.04	4.82	5.03	5.31	3.44	4.47	4.90	4.23	4.10
13.0	4.81	4.03	3.90	4.31	4.44	2.95	3.50	3.95	3.46	3.37
14.0	4.06	3.21	3.15	3.67	3.67	2.62	2.82	3.30	2.90	2.90
15.0	3.44	2.69	2.76	3.14	3.04	2.35	2.50	2.87	2.52	2.54
16.0	2.89	2.34	2.39	2.75	2.60	2.12	2.31	2.52	2.25	2.21
17.0	2.46	2.13	2.10	2.48	2.34	1.97	2.07	2.22	2.07	1.96
18.0	2.14	2.00	1.77	2.24	2.20	1.83	1.83	2.02	1.93	1.81
19.0	1.89	1.90	1.45	2.00	2.07	1.67	1.67	1.88	1.80	1.70
20.0	1.75	1.77	1.34	1.78	1.84	1.55	1.42	1.72	1.62	1.52
21.0	1.64	1.58	1.28	1.61	1.56	1.46	1.31	1.52	1.46	1.33
22.0	1.52	1.32	1.16	1.46	1.30	1.34	1.15	1.29	1.31	1.16
23.0	1.39	1.05	1.00	1.31	1.13	1.19	.81	1.11	1.16	1.06
24.0	1.24	.84	.88	1.13	1.05	1.02	.77	1.03	1.01	1.03
25.0	1.11	.74	.82	.94	.96	.89	.86	.96	.88	.95
26.0	.99	.73	.79	.81	.83	.77	.80	.85	.79	.84
27.0	.91	.76	.75	.72	.71	.62	.73	.75	.69	.74
28.0	.85	.77	.66	.66	.61	.51	.61	.65	.52	.59
29.0	.82	.74	.54	.62	.54	.48	.45	.52	.34	.44
30.0	.82	.67	.40	.57	.46	.48	.37	.43	.22	.35
31.0	.81	.62	.22	.48	.40	.41	.40	.37	.19	.31
32.0	.78	.55	.10	.39	.35	.28	.44	.34	.22	.26
33.0	.74	.43	.07	.32	.33	.16	.26	.31	.27	.19
34.0	.65	.34	.16	.27	.30	.15	.20	.30	.25	.11
35.0	.52	.27	.25	.25	.28	.19	.21	.29	.18	.03
LAT.	44.1	46.3	47.0	47.4	50.0	50.0	52.1	52.2	52.2	52.5
LONG.	45.9	47.8	60.2	48.7	58.6	52.4	91.6	68.6	60.7	64.8
Detector	3	3	3	3	3	3	3	3	3	3

TABLE XIII.- Continued

MEASURED RADIANCE PROFILES FOR 315 cm<sup>-1</sup> TO 475 cm<sup>-1</sup>

Tangent height, km	Radiance, W/m <sup>2</sup> -sr									
0.0	9.27	10.29	9.86	10.39	9.85	9.34	9.11	11.02	10.89	10.83
1.0	9.11	10.36	10.30	10.31	9.60	9.18	8.62	10.86	10.87	10.73
2.0	9.17	10.29	10.22	10.15	9.37	9.04	8.37	10.64	10.83	10.55
3.0	9.32	10.01	10.12	9.93	9.22	8.90	8.39	10.39	10.73	10.42
4.0	9.43	9.74	10.24	9.64	9.15	8.74	8.52	10.06	10.51	10.20
5.0	9.54	9.57	10.18	9.29	9.06	8.61	8.62	9.72	10.25	9.89
6.0	9.43	9.32	9.74	8.89	8.88	8.50	8.67	9.27	10.02	9.58
7.0	9.03	8.79	9.03	8.40	8.59	8.25	8.76	8.69	9.73	9.02
8.0	8.46	8.05	8.20	7.82	8.19	7.73	8.67	7.96	9.23	8.32
9.0	7.79	7.12	7.31	7.19	7.68	6.97	8.21	7.03	8.45	7.49
10.0	6.99	6.01	6.45	6.49	6.58	6.09	7.44	6.01	7.38	6.63
11.0	6.00	4.91	5.63	5.77	6.06	5.11	6.53	5.04	6.05	5.65
12.0	4.93	3.93	4.74	4.96	4.98	4.14	5.44	4.26	4.74	4.59
13.0	4.03	3.28	4.04	4.23	4.09	3.47	4.35	3.66	3.71	3.73
14.0	3.41	2.82	3.57	3.60	3.48	3.09	3.60	3.20	3.03	3.12
15.0	2.96	2.40	3.18	3.09	3.06	2.82	3.12	2.82	2.58	2.75
16.0	2.65	2.07	2.84	2.71	2.73	2.58	2.72	2.47	2.32	2.49
17.0	2.42	1.93	2.52	2.44	2.42	2.34	2.33	2.20	2.11	2.31
18.0	2.21	1.87	2.23	2.22	2.15	2.19	2.02	1.99	1.93	2.12
19.0	2.03	1.67	2.02	2.02	1.97	2.06	1.85	1.79	1.76	1.86
20.0	1.88	1.45	1.93	1.80	1.83	1.93	1.73	1.58	1.51	1.71
21.0	1.73	1.36	1.76	1.60	1.69	1.80	1.55	1.37	1.29	1.35
22.0	1.53	1.24	1.49	1.44	1.54	1.64	1.37	1.21	1.20	1.03
23.0	1.32	1.04	1.24	1.30	1.37	1.49	1.32	1.14	1.09	1.02
24.0	1.06	.86	1.11	1.14	1.23	1.38	1.34	1.03	.90	.95
25.0	.80	.69	1.07	.97	1.10	1.24	1.21	.87	.79	.79
26.0	.67	.60	1.04	.81	1.02	1.09	1.07	.70	.81	.71
27.0	.65	.60	.93	.69	.93	.93	.99	.59	.79	.76
28.0	.62	.56	.73	.61	.82	.84	.84	.56	.73	.79
29.0	.54	.47	.55	.56	.73	.80	.74	.56	.75	.69
30.0	.47	.36	.41	.50	.67	.71	.69	.52	.77	.61
31.0	.44	.30	.36	.44	.61	.56	.62	.44	.72	.54
32.0	.37	.20	.31	.39	.55	.45	.47	.35	.66	.40
33.0	.32	.16	.27	.34	.47	.43	.38	.26	.55	.31
34.0	.31	.16	.22	.28	.39	.38	.35	.21	.48	.29
35.0	.30	.15	.17	.23	.29	.29	.23	.20	.48	.26
LAT.	52.9	52.9	53.8	54.0	54.5	54.8	54.9	57.1	57.4	57.4
LONG.	60.6	57.0	75.7	57.4	59.1	59.2	67.7	74.3	75.4	71.6
Detector	3	3	3	3	3	3	3	3	3	3

TABLE XIII.- Continued

MEASURED RADIANCE PROFILES FOR 315 cm<sup>-1</sup> TO 475 cm<sup>-1</sup>

Tangent height, km	Radiance, W/m <sup>2</sup> -sr									
0.0	12.16	12.18	12.40	11.75	12.01	11.73	11.77	12.55	12.47	12.32
1.0	12.21	12.16	12.27	11.66	11.89	11.62	11.65	12.41	12.31	12.23
2.0	12.19	12.14	12.15	11.53	11.81	11.52	11.50	12.23	12.12	12.06
3.0	12.10	12.11	11.98	11.39	11.72	11.36	11.35	12.03	11.94	11.84
4.0	11.87	11.93	11.76	11.17	11.55	11.13	11.16	11.80	11.70	11.58
5.0	11.59	11.61	11.51	10.85	11.22	10.82	10.91	11.53	11.33	11.20
6.0	11.24	11.15	11.17	10.49	10.82	10.48	10.52	11.18	10.82	10.69
7.0	10.83	10.96	10.68	10.03	10.38	10.04	10.04	10.72	10.20	10.05
8.0	10.37	9.83	10.08	9.46	9.78	9.45	9.43	10.13	9.52	9.23
9.0	9.78	9.00	9.36	8.70	9.04	8.61	8.70	9.37	8.75	8.25
10.0	9.01	8.04	8.52	7.80	8.12	7.61	7.77	8.46	7.88	7.15
11.0	8.11	6.96	7.57	6.76	7.01	6.48	6.75	7.41	6.96	6.01
12.0	7.14	5.86	6.55	5.63	5.74	5.26	5.70	6.28	5.92	4.92
13.0	5.98	4.90	5.60	4.55	4.50	4.12	4.68	5.24	4.99	3.99
14.0	4.74	3.99	4.68	3.66	3.40	3.27	3.88	4.35	4.15	3.30
15.0	3.61	3.21	3.81	2.94	2.62	2.64	3.25	3.65	3.45	2.81
16.0	2.68	2.60	3.13	2.35	2.16	2.20	2.76	3.02	2.94	2.49
17.0	2.05	2.18	2.66	1.88	1.94	1.89	2.33	2.57	2.55	2.29
18.0	1.62	1.94	2.35	1.58	1.77	1.69	1.99	2.23	2.26	2.10
19.0	1.29	1.87	2.07	1.39	1.62	1.58	1.69	2.07	1.99	1.86
20.0	1.09	1.89	1.81	1.29	1.38	1.53	1.43	2.00	1.75	1.67
21.0	1.00	1.81	1.64	1.23	1.13	1.39	1.26	1.96	1.57	1.56
22.0	.93	1.62	1.53	1.14	1.02	1.20	1.13	1.86	1.48	1.43
23.0	.81	1.38	1.44	1.02	1.05	1.05	1.06	1.68	1.46	1.31
24.0	.76	1.16	1.29	.88	1.04	.96	1.03	1.50	1.40	1.22
25.0	.85	1.02	1.10	.75	.88	.84	1.01	1.35	1.26	1.11
26.0	.79	.91	1.03	.63	.76	.69	.93	1.24	1.08	.96
27.0	.68	.81	1.05	.58	.77	.53	.79	1.10	.94	.74
28.0	.56	.74	1.05	.52	.79	.42	.65	1.02	.87	.55
29.0	.45	.65	.98	.40	.70	.38	.55	.99	.83	.48
30.0	.27	.56	.85	.30	.47	.43	.52	.97	.78	.54
31.0	.12	.46	.74	.28	.23	.49	.50	.89	.74	.62
32.0	.04	.41	.66	.32	.17	.47	.48	.75	.71	.62
33.0	.01	.36	.62	.34	.28	.36	.45	.64	.63	.60
34.0	.13	.34	.57	.28	.38	.17	.41	.58	.50	.57
35.0	.16	.31	.48	.15	.35	.10	.32	.55	.40	.51
LAT.	10.5	11.0	12.2	12.8	13.5	13.6	15.7	17.9	19.1	20.8
LONG.	64.4	57.8	56.8	55.0	57.1	54.9	52.8	50.4	49.7	48.2
Detector	4	4	4	4	4	4	4	4	4	4

TABLE XIII. - Continued

MEASURED RADIANCE PROFILES FOR 315 cm<sup>-1</sup> TO 475 cm<sup>-1</sup>

Tangent height, km	Radiance, W/m <sup>2</sup> -sr									
0.0	12.08	11.84	11.69	12.21	11.79	11.68	10.92	11.41	10.67	9.49
1.0	11.94	11.62	11.50	12.08	11.57	11.60	10.97	11.25	10.45	9.51
2.0	11.80	11.32	11.32	11.92	11.34	11.51	10.95	11.15	10.17	9.60
3.0	11.66	10.97	11.12	11.72	11.10	11.37	10.87	11.04	9.92	9.67
4.0	11.49	10.58	10.90	11.44	10.82	11.15	10.68	10.92	9.72	9.64
5.0	11.25	10.14	10.63	11.09	10.47	10.83	10.38	10.74	9.56	9.52
6.0	10.97	9.68	10.26	10.70	10.02	10.40	9.94	10.44	9.40	9.33
7.0	10.63	9.19	9.80	10.24	9.47	9.90	9.46	10.06	9.19	9.10
8.0	10.21	8.60	9.28	9.67	8.85	9.28	8.97	9.51	8.80	8.84
9.0	9.69	7.89	8.70	9.00	8.15	8.60	8.40	8.82	8.30	8.50
10.0	9.02	7.02	8.05	8.23	7.33	7.79	7.68	7.96	7.77	8.04
11.0	8.20	6.07	7.28	7.38	6.39	6.90	6.81	6.96	7.19	7.37
12.0	7.24	5.09	6.35	6.43	5.38	5.98	5.86	5.93	6.54	6.54
13.0	6.17	4.12	5.41	5.43	4.40	5.08	4.92	4.92	5.72	5.63
14.0	5.10	3.27	4.56	4.50	3.63	4.25	4.04	4.03	4.80	4.70
15.0	4.08	2.64	3.83	3.76	3.01	3.50	3.27	3.28	3.91	3.88
16.0	3.33	2.25	3.22	3.19	2.57	2.89	2.73	2.76	3.17	3.10
17.0	2.79	2.03	2.73	2.77	2.28	2.42	2.38	2.37	2.60	2.51
18.0	2.39	1.86	2.38	2.47	2.07	2.05	2.09	2.12	2.20	2.13
19.0	2.05	1.69	2.09	2.20	1.88	1.78	1.83	1.94	1.96	1.87
20.0	1.76	1.50	1.84	2.02	1.70	1.59	1.67	1.81	1.79	1.68
21.0	1.49	1.31	1.62	1.86	1.56	1.47	1.58	1.67	1.64	1.52
22.0	1.27	1.18	1.43	1.71	1.41	1.34	1.47	1.53	1.45	1.35
23.0	1.12	1.13	1.24	1.55	1.27	1.18	1.30	1.35	1.28	1.18
24.0	1.07	1.07	1.04	1.39	1.15	1.03	1.08	1.18	1.11	1.07
25.0	1.08	.98	.86	1.23	1.06	.92	.83	1.03	.95	1.01
26.0	1.07	.88	.68	1.08	1.04	.85	.63	.91	.82	.94
27.0	1.01	.77	.53	.94	1.04	.80	.51	.89	.73	.84
28.0	.90	.63	.44	.82	1.01	.75	.48	.86	.63	.72
29.0	.75	.43	.42	.74	.96	.70	.49	.75	.55	.63
30.0	.60	.25	.47	.67	.90	.66	.52	.62	.53	.58
31.0	.51	.18	.51	.62	.83	.64	.53	.55	.53	.58
32.0	.46	.18	.51	.59	.77	.63	.48	.52	.50	.54
33.0	.41	.18	.46	.56	.71	.64	.36	.50	.47	.46
34.0	.36	.15	.39	.50	.67	.65	.23	.46	.46	.36
35.0	.33	.14	.29	.44	.60	.62	.17	.45	.43	.33
LAT.	21.0	22.1	22.2	24.3	24.6	25.9	27.0	27.3	28.8	30.7
LONG.	48.5	47.7	47.5	46.4	45.9	46.1	45.7	45.5	45.4	44.4
Detector	4	4	4	4	4	4	4	4	4	4

TABLE XIII.- Continued

MEASURED RADIANCE PROFILES FOR 315 cm<sup>-1</sup> TO 475 cm<sup>-1</sup>

Tangent height, km	Radiance, W/m <sup>2</sup> -sr									
0.0	10.91	10.53	10.51	8.14	9.43	10.72	9.45	8.47	10.40	10.53
1.0	10.77	10.49	10.35	8.25	9.52	10.43	8.84	8.44	10.23	10.50
2.0	10.54	10.45	10.22	8.25	9.61	10.08	8.28	7.97	9.98	10.42
3.0	10.24	10.39	10.13	8.20	9.67	9.69	7.83	7.57	9.64	10.32
4.0	9.90	10.29	10.02	8.13	9.62	9.31	7.48	7.31	9.29	10.22
5.0	9.51	10.14	9.87	8.03	9.42	9.03	7.26	7.15	8.96	10.11
6.0	9.11	9.95	9.65	7.86	9.10	8.90	7.06	7.00	8.63	9.93
7.0	8.74	9.67	9.38	7.62	8.74	8.89	6.85	6.80	8.20	9.63
8.0	8.25	9.26	9.07	7.31	8.36	8.84	6.58	6.57	7.65	9.18
9.0	7.86	8.72	8.71	6.95	7.96	8.60	6.22	6.31	6.97	8.62
10.0	7.23	8.09	8.29	6.53	7.51	8.16	5.81	5.98	6.15	7.98
11.0	6.47	7.38	7.74	6.02	6.97	7.55	5.39	5.59	5.23	7.26
12.0	5.64	6.58	7.03	5.37	6.32	6.77	4.94	5.14	4.37	6.50
13.0	4.79	5.75	6.24	4.62	5.54	5.79	4.50	4.63	3.65	5.64
14.0	4.02	4.90	5.39	3.84	4.72	4.70	3.98	4.08	3.08	4.72
15.0	3.38	4.12	4.52	3.18	3.96	3.72	3.42	3.48	2.68	3.89
16.0	2.85	3.43	3.78	2.71	3.28	3.02	2.89	2.92	2.41	3.23
17.0	2.47	2.93	3.16	2.39	2.74	2.56	2.45	2.51	2.16	2.78
18.0	2.24	2.57	2.66	2.19	2.33	2.20	2.14	2.17	1.98	2.44
19.0	2.09	2.31	2.30	2.08	2.02	1.91	1.89	1.93	1.85	2.14
20.0	1.94	2.08	2.04	1.99	1.82	1.67	1.71	1.74	1.73	1.88
21.0	1.72	1.86	1.84	1.88	1.68	1.53	1.60	1.56	1.60	1.64
22.0	1.47	1.63	1.67	1.74	1.52	1.36	1.48	1.39	1.45	1.42
23.0	1.24	1.43	1.49	1.55	1.36	1.15	1.40	1.22	1.29	1.24
24.0	1.08	1.27	1.34	1.33	1.19	.94	1.32	1.05	1.13	1.10
25.0	1.01	1.15	1.23	1.14	1.02	.84	1.23	.91	.95	1.00
26.0	.97	1.04	1.13	1.03	.86	.81	1.15	.79	.82	.89
27.0	.92	.97	.95	.98	.75	.79	1.01	.71	.71	.77
28.0	.83	.97	.81	.91	.71	.76	.84	.67	.64	.69
29.0	.73	1.00	.66	.79	.71	.70	.66	.62	.62	.66
30.0	.63	1.05	.54	.67	.69	.55	.55	.56	.60	.63
31.0	.56	1.09	.50	.59	.64	.32	.53	.48	.54	.55
32.0	.52	1.07	.52	.51	.60	.12	.54	.40	.46	.43
33.0	.51	.99	.53	.49	.53	.06	.55	.31	.36	.33
34.0	.51	.88	.50	.49	.42	.09	.52	.24	.27	.27
35.0	.50	.74	.46	.51	.31	.11	.46	.20	.21	.26
LAT.	31.2	32.9	33.9	34.3	35.1	37.1	38.1	39.9	40.8	42.4
LONG.	45.2	44.3	44.9	44.2	45.7	49.9	44.7	44.4	45.2	46.6
Detector	4	4	4	4	4	4	4	4	4	4

TABLE XIII. - Continued

MEASURED RADIANCE PROFILES FOR 315 cm<sup>-1</sup> TO 475 cm<sup>-1</sup>

Tangent height, km	Radiance, W/m <sup>2</sup> -sr									
0.0	11.05	11.16	10.21	10.42	8.66	10.51		11.85	9.61	11.25
1.0	11.06	11.07	10.08	10.27	8.61	10.44	11.90	11.75	9.59	10.98
2.0	11.04	10.96	9.97	10.12	8.60	10.17	11.67	11.69	9.45	10.71
3.0	10.94	10.80	9.86	9.95	8.63	9.80	11.52	11.56	9.21	10.49
4.0	10.75	10.58	9.73	9.72	8.66	9.41	11.47	11.29	8.91	10.32
5.0	10.51	10.20	9.56	9.42	8.66	9.02	11.31	10.88	8.66	10.07
6.0	10.17	9.72	9.40	9.04	8.62	8.58	11.25	10.42	8.48	9.77
7.0	9.72	9.12	9.18	8.58	8.51	8.05	10.81	9.86	8.23	9.38
8.0	9.12	8.42	8.87	8.01	8.29	7.44	10.06	9.24	7.85	8.74
9.0	8.46	7.54	8.41	7.29	7.90	6.73	9.67	8.50	7.25	7.87
10.0	7.75	6.52	7.75	6.50	7.26	5.89	9.04	7.67	6.39	6.80
11.0	6.69	5.49	6.96	5.69	6.46	5.00	7.35	6.66	5.31	5.70
12.0	6.13	4.66	5.99	4.92	5.58	4.19	5.45	5.46	4.34	4.80
13.0	5.25	4.02	4.88	4.26	4.77	3.63	4.09	4.44	3.66	4.11
14.0	4.42	3.52	3.92	3.74	4.10	3.30	3.62	3.70	3.19	3.58
15.0	3.75	3.17	3.22	3.35	3.55	3.01	3.34	3.20	2.83	3.12
16.0	3.24	2.91	2.74	3.00	3.12	2.73	3.11	2.87	2.50	2.67
17.0	2.87	2.66	2.45	2.67	2.74	2.47	2.82	2.60	2.20	2.30
18.0	2.57	2.35	2.32	2.39	2.47	2.23	2.52	2.35	1.98	2.07
19.0	2.33	2.00	2.20	2.16	2.29	1.97	2.35	2.15	1.81	1.93
20.0	2.17	1.70	2.00	1.94	2.08	1.75	2.24	1.93	1.65	1.79
21.0	2.04	1.48	1.75	1.72	1.81	1.60	2.07	1.70	1.48	1.64
22.0	1.88	1.32	1.50	1.49	1.58	1.48	1.91	1.44	1.30	1.41
23.0	1.67	1.22	1.26	1.29	1.42	1.37	1.69	1.25	1.17	1.17
24.0	1.44	1.14	1.00	1.13	1.35	1.24	1.53	1.11	1.07	1.03
25.0	1.20	1.08	.81	1.00	1.27	1.11	1.33	1.00	.88	.95
26.0	1.00	1.04	.75	.91	1.12	.99	1.05	.86	.62	.86
27.0	.85	.95	.68	.82	.96	.90	.93	.69	.43	.69
28.0	.78	.81	.55	.73	.82	.84	.92	.58	.38	.52
29.0	.74	.66	.42	.62	.73	.78	.87	.55	.37	.46
30.0	.73	.50	.34	.52	.64	.69	.73	.55	.36	.44
31.0	.67	.40	.32	.45	.53	.57	.50	.48	.33	.43
32.0	.58	.38	.33	.39	.45	.49	.45	.43	.34	.37
33.0	.46	.39	.34	.34	.40	.46	.46	.36	.34	.34
34.0	.37	.42	.33	.29	.32	.46	.37	.29	.32	.34
35.0	.32	.39	.30	.24	.23	.46	.25	.31	.28	.34
LAT.	44.5	46.6	47.3	47.6	50.3	50.6	51.1	52.3	52.6	52.8
LONG.	46.3	48.5	61.1	49.3	59.7	53.7	93.7	70.2	62.3	66.6
Detector	4	4	4	4	4	4	4	4	4	4

TABLE XIII.- Concluded

MEASURED RADIANCE PROFILES FOR 315 cm<sup>-1</sup> TO 475 cm<sup>-1</sup>

Tangent height, km	Radiance, W/m <sup>2</sup> -sr									
0.0	9.30	8.21	10.46	10.78	10.37	11.33	10.00	10.38	10.98	11.28
1.0	9.03	8.49	10.40	10.59	10.13	11.00	9.72	10.32	10.97	11.27
2.0	8.88	8.90	10.36	10.44	9.95	10.77	9.43	10.20	10.75	11.39
3.0	8.80	9.44	10.20	10.31	9.78	10.43	9.21	10.04	10.65	11.48
4.0	8.82	9.73	9.82	10.15	9.61	9.99	9.20	9.86	10.61	11.35
5.0	8.85	9.70	9.40	9.88	9.42	9.69	9.38	9.55	10.72	11.18
6.0	8.80	9.49	9.03	9.47	9.23	9.45	9.56	9.16	10.70	11.00
7.0	8.69	9.45	8.61	8.95	9.10	9.16	9.48	8.58	10.22	10.67
8.0	8.48	9.47	7.95	8.34	8.89	8.84	9.07	7.80	9.64	10.10
9.0	8.05	8.92	7.01	7.62	8.46	8.29	8.46	6.85	8.90	9.22
10.0	7.18	7.93	5.84	6.82	7.74	7.37	7.68	5.81	7.94	8.09
11.0	6.09	6.65	4.85	5.95	6.81	6.14	6.77	4.75	6.85	6.88
12.0	5.07	5.31	4.15	5.08	5.89	5.05	5.78	3.75	5.57	5.62
13.0	4.22	4.09	3.64	4.38	4.98	4.23	4.84	2.97	4.65	4.46
14.0	3.57	3.27	3.35	3.82	4.22	3.68	4.01	2.48	4.12	3.65
15.0	3.11	2.85	3.12	3.38	3.64	3.31	3.35	2.14	3.72	3.13
16.0	2.77	2.56	2.80	3.01	3.20	3.02	2.84	1.77	3.32	2.83
17.0	2.55	2.33	2.47	2.73	2.84	2.80	2.53	1.43	2.96	2.73
18.0	2.42	2.06	2.18	2.52	2.49	2.60	2.30	1.27	2.58	2.61
19.0	2.30	1.93	1.93	2.34	2.22	2.35	1.98	1.22	2.32	2.32
20.0	2.04	1.97	1.72	2.16	2.06	2.06	1.67	1.17	2.03	1.99
21.0	1.67	1.82	1.48	2.00	2.00	1.80	1.48	1.04	1.68	1.73
22.0	1.37	1.66	1.24	1.82	1.90	1.52	1.31	.76	1.49	1.54
23.0	1.21	1.53	1.15	1.63	1.74	1.24	1.13	.50	1.42	1.46
24.0	1.13	1.33	1.10	1.45	1.55	1.03	.95	.42	1.29	1.34
25.0	.99	1.19	.96	1.28	1.38	1.00	.90	.44	1.06	1.16
26.0	.83	1.12	.89	1.12	1.25	.91	.88	.34	.89	.99
27.0	.71	1.00	.81	.96	1.16	.74	.76	.20	.84	.72
28.0	.60	.81	.66	.82	1.05	.65	.57	.12	.74	.59
29.0	.57	.62	.48	.72	.94	.60	.43	.05	.56	.58
30.0	.59	.50	.42	.68	.90	.53	.39	-.01	.44	.55
31.0	.59	.51	.41	.68	.88	.45	.41	-.03	.42	.58
32.0	.49	.53	.43	.65	.80	.47	.39	-.01	.44	.57
33.0	.35	.48	.46	.58	.66	.46	.29	.02	.55	.44
34.0	.26	.41	.45	.46	.54	.41	.17	.00	.57	.29
35.0	.29	.31	.42	.34	.48	.42	.11	-.04	.45	.27
LAT.	53.2	53.6	53.6	54.3	54.7	55.1	55.1	57.1	57.2	57.5
LONG.	62.6	77.9	59.1	58.7	60.6	70.2	61.0	76.7	78.4	74.9
Detector	4	4	4	4	4	4	4	4	4	4

TABLE XIV

AVERAGE MEASURED RADIANCE PROFILES FOR 315 cm<sup>-1</sup> TO 475 cm<sup>-1</sup>

Tangent height, km	Radiance, W/m <sup>2</sup> -sr									
0.0	11.46	11.76	11.71	11.75	11.68	11.47	11.33	11.59	11.44	11.53
1.0	11.47	11.66	11.63	11.62	11.52	11.40	11.19	11.44	11.27	11.40
2.0	11.42	11.50	11.52	11.45	11.36	11.26	11.01	11.25	11.08	11.22
3.0	11.26	11.31	11.38	11.23	11.17	11.10	10.80	11.05	10.86	10.98
4.0	11.00	11.03	11.20	10.97	10.92	10.91	10.56	10.82	10.57	10.66
5.0	10.62	10.68	10.97	10.65	10.56	10.63	10.29	10.55	10.19	10.27
6.0	10.06	10.24	10.69	10.27	10.11	10.28	9.92	10.20	9.72	9.80
7.0	9.45	9.73	10.33	9.81	9.54	9.85	9.45	9.75	9.17	9.23
8.0	8.91	9.12	9.90	9.27	8.79	9.26	8.86	9.18	8.51	8.44
9.0	8.46	8.45	9.34	8.63	7.89	8.51	8.16	8.47	7.70	7.48
10.0	7.76	7.68	8.63	7.84	6.89	7.64	7.31	7.62	6.79	6.39
11.0	6.83	6.83	7.75	6.90	5.81	6.64	6.36	6.64	5.84	5.29
12.0	5.83	5.88	6.75	5.85	4.70	5.49	5.36	5.61	4.90	4.27
13.0	4.81	4.89	5.69	4.81	3.73	4.32	4.41	4.65	4.05	3.44
14.0	3.81	3.94	4.60	3.85	2.96	3.28	3.60	3.82	3.29	2.83
15.0	2.91	3.12	3.58	3.04	2.39	2.50	2.93	3.12	2.69	2.40
16.0	2.22	2.44	2.77	2.39	1.99	2.03	2.40	2.56	2.25	2.06
17.0	1.74	1.94	2.20	1.94	1.73	1.77	2.00	2.17	1.92	1.84
18.0	1.50	1.63	1.84	1.71	1.56	1.62	1.72	1.89	1.65	1.66
19.0	1.31	1.45	1.59	1.59	1.45	1.51	1.50	1.71	1.43	1.49
20.0	1.19	1.37	1.41	1.50	1.33	1.39	1.32	1.56	1.26	1.33
21.0	1.14	1.27	1.28	1.38	1.19	1.24	1.16	1.40	1.13	1.22
22.0	1.06	1.13	1.15	1.24	1.08	1.06	1.02	1.27	1.03	1.14
23.0	.87	.98	1.05	1.09	1.04	.91	.93	1.16	.94	1.04
24.0	.71	.86	.95	.98	.98	.83	.86	1.06	.85	.93
25.0	.65	.79	.82	.88	.84	.74	.81	.97	.74	.86
26.0	.57	.71	.71	.75	.73	.63	.71	.89	.64	.80
27.0	.54	.62	.68	.62	.68	.51	.59	.79	.55	.69
28.0	.49	.54	.68	.53	.67	.42	.47	.71	.50	.58
29.0	.42	.49	.63	.48	.62	.34	.38	.62	.49	.51
30.0	.31	.47	.57	.45	.53	.32	.34	.58	.46	.45
31.0		.42	.48	.40	.47	.32	.33	.53	.40	.40
32.0		.40	.38	.35	.46	.30		.44	.35	.38
33.0		.39	.31	.32	.43	.24		.35	.31	.36
34.0		.33	.27	.28	.40	.18		.27	.27	.33
35.0		.21		.25	.34	.14		.24	.23	.24
LAT.	10.5	10.9	12.2	12.8	13.5	13.5	15.5	17.4	18.6	20.0
LONG.	66.8	59.8	58.6	56.5	58.9	56.8	53.7	51.5	50.9	49.4

TABLE XIV.- Continued

AVERAGE MEASURED RADIANCE PROFILES FOR 315 cm<sup>-1</sup> TO 475 cm<sup>-1</sup>

Tangent height, km	Radiance, W/m <sup>2</sup> -sr									
0.0	11.50	11.22	11.22	11.25	11.17	11.15	11.07	10.88	10.54	10.18
1.0	11.37	11.03	11.05	11.09	11.00	10.99	10.94	10.78	10.44	10.09
2.0	11.22	10.82	10.85	10.91	10.80	10.79	10.79	10.63	10.33	9.95
3.0	11.04	10.58	10.63	10.68	10.57	10.56	10.60	10.45	10.20	9.77
4.0	10.84	10.31	10.36	10.40	10.28	10.29	10.35	10.23	10.06	9.55
5.0	10.56	9.98	10.01	10.06	9.94	9.96	10.06	9.97	9.88	9.30
6.0	10.22	9.58	9.59	9.66	9.54	9.53	9.70	9.63	9.63	9.00
7.0	9.82	9.09	9.09	9.20	9.06	8.99	9.23	9.24	9.29	8.65
8.0	9.34	8.51	8.50	8.66	8.52	8.35	8.63	8.76	8.83	8.22
9.0	8.74	7.82	7.82	8.03	7.91	7.60	7.94	8.14	8.29	7.69
10.0	7.98	7.03	7.04	7.27	7.19	6.74	7.14	7.35	7.65	7.06
11.0	7.07	6.18	6.17	6.43	6.36	5.81	6.23	6.44	6.89	6.32
12.0	6.11	5.27	5.28	5.53	5.48	4.90	5.23	5.44	6.04	5.48
13.0	5.12	4.41	4.40	4.62	4.61	4.06	4.30	4.45	5.15	4.60
14.0	4.22	3.66	3.62	3.83	3.85	3.36	3.50	3.57	4.25	3.78
15.0	3.45	3.01	2.98	3.19	3.19	2.79	2.88	2.84	3.44	3.05
16.0	2.83	2.47	2.48	2.70	2.66	2.34	2.42	2.29	2.78	2.48
17.0	2.36	2.05	2.12	2.32	2.23	1.99	2.10	1.91	2.32	2.08
18.0	2.01	1.76	1.84	2.03	1.91	1.70	1.86	1.67	2.02	1.83
19.0	1.73	1.55	1.63	1.77	1.66	1.51	1.67	1.53	1.82	1.66
20.0	1.51	1.41	1.45	1.57	1.49	1.38	1.52	1.43	1.67	1.52
21.0	1.33	1.28	1.31	1.40	1.35	1.27	1.40	1.35	1.54	1.39
22.0	1.18	1.14	1.19	1.28	1.23	1.10	1.30	1.28	1.40	1.23
23.0	1.05	1.00	1.10	1.16	1.11	.93	1.18	1.16	1.25	1.07
24.0	.95	.85	.98	1.05	1.00	.78	1.05	.98	1.09	.92
25.0	.85	.72	.86	.91	.91	.69	.92	.78	.95	.80
26.0	.75	.63	.76	.79	.84	.65	.81	.65	.84	.73
27.0	.66	.57	.67	.68	.77	.62	.73	.58	.77	.69
28.0	.58	.51	.56	.62	.69	.58	.66	.54	.71	.63
29.0	.53	.46	.44	.58	.60	.54	.59	.49	.66	.55
30.0	.49	.42	.34	.54	.52	.51	.53	.44	.62	.48
31.0	.47	.39	.30	.49	.45	.49	.47	.39	.58	.42
32.0	.44	.38	.29	.44	.41	.46	.42	.33	.52	.39
33.0	.40	.37	.27	.39	.38	.41	.37	.24	.44	.37
34.0	.33	.34	.25	.34	.35	.39	.36	.16	.40	.36
35.0	.26	.30	.25	.28	.30	.40	.36	.13	.37	.35
LAT.	20.5	21.8	22.3	23.8	24.8	25.1	26.4	26.9	28.6	30.5
LONG.	49.5	48.2	48.5	47.1	46.5	46.7	46.0	46.3	45.9	45.4

TABLE XIV.- Continued

AVERAGE MEASURED RADIANCE PROFILES FOR 315 cm<sup>-1</sup> TO 475 cm<sup>-1</sup>

Tangent height, km	Radiance, W/m <sup>2</sup> -sr									
0.0	9.76	10.01	9.55	8.80	9.44	9.88	7.47	7.23	8.82	9.62
1.0	9.66	9.92	9.44	8.80	9.38	9.76	7.27	7.18	8.54	9.41
2.0	9.56	9.83	9.33	8.78	9.31	9.60	7.10	7.03	8.21	9.21
3.0	9.46	9.72	9.23	8.74	9.20	9.39	6.94	6.88	7.86	8.99
4.0	9.32	9.57	9.09	8.65	9.04	9.15	6.77	6.74	7.50	8.74
5.0	9.10	9.38	8.91	8.48	8.83	8.91	6.61	6.61	7.13	8.45
6.0	8.81	9.13	8.70	8.24	8.55	8.69	6.44	6.47	6.78	8.09
7.0	8.47	8.82	8.46	7.94	8.22	8.49	6.26	6.30	6.42	7.66
8.0	8.06	8.44	8.15	7.57	7.86	8.24	6.05	6.11	6.06	7.17
9.0	7.58	7.98	7.76	7.12	7.47	7.88	5.81	5.91	5.66	6.62
10.0	7.01	7.43	7.27	6.57	7.01	7.38	5.54	5.69	5.19	6.05
11.0	6.32	6.79	6.68	5.93	6.46	6.76	5.20	5.41	4.68	5.48
12.0	5.55	6.01	6.01	5.18	5.80	6.01	4.77	5.04	4.15	4.89
13.0	4.75	5.18	5.29	4.37	5.06	5.18	4.26	4.59	3.62	4.28
14.0	3.97	4.34	4.55	3.58	4.29	4.29	3.69	4.05	3.11	3.63
15.0	3.25	3.57	3.80	2.91	3.58	3.46	3.13	3.48	2.68	3.01
16.0	2.63	2.94	3.12	2.42	2.93	2.79	2.64	2.93	2.32	2.50
17.0	2.17	2.48	2.55	2.08	2.44	2.29	2.23	2.48	2.06	2.13
18.0	1.87	2.17	2.13	1.86	2.05	1.94	1.92	2.17	1.86	1.88
19.0	1.66	1.95	1.82	1.71	1.75	1.72	1.68	1.96	1.71	1.68
20.0	1.50	1.76	1.59	1.59	1.52	1.56	1.50	1.80	1.56	1.51
21.0	1.36	1.57	1.40	1.46	1.34	1.42	1.36	1.64	1.42	1.35
22.0	1.21	1.40	1.25	1.32	1.19	1.28	1.23	1.47	1.29	1.21
23.0	1.08	1.25	1.11	1.18	1.05	1.12	1.12	1.31	1.15	1.09
24.0	.97	1.12	.98	1.04	.92	.98	1.01	1.18	1.00	1.00
25.0	.89	1.01	.86	.90	.81	.91	.91	1.07	.86	.95
26.0	.81	.89	.76	.80	.72	.84	.80	.97	.77	.89
27.0	.70	.79	.66	.72	.66	.76	.69	.87	.71	.81
28.0	.59	.73	.57	.65	.63	.67	.59	.80	.66	.71
29.0	.50	.70	.48	.56	.59	.60	.49	.74	.64	.61
30.0	.44	.68	.41	.48	.54	.54	.43	.68	.60	.52
31.0	.39	.66	.35	.40	.48	.48	.40	.61	.53	.44
32.0	.35	.61	.30	.34	.43	.42	.41	.54	.43	.39
33.0	.30	.54	.26	.30	.36	.38	.39	.47	.33	.36
34.0	.25	.48	.22	.26	.28	.37	.33	.42	.25	.33
35.0	.22	.41	.19	.22	.21	.36	.24	.40	.20	.29
LAT.	30.8	32.2	33.3	34.1	34.4	36.2	37.7	39.1	40.6	41.4
LONG.	44.6	44.5	44.5	44.3	45.7	49.6	44.5	44.2	44.7	46.0

TABLE XIV.- Continued

AVERAGE MEASURED RADIANCE PROFILES FOR 315 cm<sup>-1</sup> TO 475 cm<sup>-1</sup>

Tangent height, km	Radiance, W/m <sup>2</sup> -sr									
0.0	10.31	10.71	9.47	10.32	9.79	8.40	9.40	10.09	9.96	9.40
1.0	10.18	10.60	9.22	10.21	9.65	8.35	9.31	10.02	9.87	9.36
2.0	10.00	10.45	8.99	10.06	9.43	8.32	9.19	9.93	9.72	9.31
3.0	9.75	10.27	8.80	9.85	9.18	8.30	9.00	9.82	9.44	9.23
4.0	9.48	10.02	8.65	9.59	8.89	8.27	8.76	9.67	9.14	9.09
5.0	9.18	9.71	8.50	9.25	8.54	8.21	8.52	9.45	8.89	8.85
6.0	8.85	9.31	8.30	8.84	8.12	8.10	8.28	9.16	8.59	8.55
7.0	8.49	8.83	8.01	8.36	7.57	7.86	7.97	8.79	8.10	8.18
8.0	8.06	8.24	7.63	7.78	6.89	7.51	7.53	8.31	7.42	7.69
9.0	7.56	7.50	7.15	7.09	6.07	7.03	6.95	7.67	6.53	7.00
10.0	6.58	6.63	6.53	6.34	5.19	6.42	6.19	6.87	5.46	6.11
11.0	6.30	5.69	5.77	5.56	4.35	5.69	5.28	5.91	4.46	5.13
12.0	5.55	4.79	4.90	4.79	3.67	4.91	4.37	4.88	3.72	4.27
13.0	4.78	4.00	4.00	4.09	3.20	4.16	3.63	3.97	3.21	3.60
14.0	4.04	3.35	3.25	3.51	2.86	3.54	3.10	3.29	2.87	3.10
15.0	3.38	2.89	2.73	3.06	2.56	3.06	2.73	2.85	2.57	2.69
16.0	2.87	2.55	2.35	2.69	2.29	2.67	2.44	2.53	2.29	2.32
17.0	2.48	2.30	2.09	2.39	2.07	2.34	2.19	2.28	2.04	2.05
18.0	2.19	2.09	1.87	2.12	1.88	2.08	1.98	2.09	1.84	1.88
19.0	1.57	1.90	1.68	1.90	1.71	1.87	1.79	1.93	1.62	1.73
20.0	1.81	1.70	1.49	1.69	1.55	1.66	1.59	1.74	1.44	1.53
21.0	1.67	1.50	1.33	1.51	1.41	1.44	1.41	1.53	1.30	1.33
22.0	1.55	1.31	1.18	1.34	1.26	1.24	1.26	1.30	1.14	1.15
23.0	1.42	1.15	1.03	1.17	1.11	1.09	1.13	1.15	1.02	1.01
24.0	1.27	1.02	.87	1.01	.98	.98	1.01	1.04	.89	.92
25.0	1.13	.93	.74	.87	.86	.87	.87	.96	.77	.86
26.0	.59	.88	.69	.77	.77	.74	.77	.86	.68	.78
27.0	.87	.82	.64	.71	.67	.63	.69	.75	.63	.67
28.0	.78	.74	.57	.67	.59	.55	.61	.66	.54	.54
29.0	.72	.64		.63	.54	.50	.51	.59	.41	.43
30.0	.68	.53		.56	.50	.43	.44	.53	.31	.38
31.0	.63	.47		.48	.46	.37	.40	.47	.25	.34
32.0	.56	.41		.40	.39	.33	.38	.41	.24	.27
33.0	.49	.37		.33	.31	.31	.36	.34	.23	.21
34.0	.42	.35		.28	.26	.28	.35	.29	.22	.18
35.0	.35	.34		.24	.25	.24	.31	.28	.20	.18
LAT.	43.6	46.1	47.1	47.3	49.5	49.7	51.9	52.1	52.3	52.3
LONG.	45.6	47.4	60.2	48.3	51.7	57.9	59.7	67.5	55.9	64.0

TABLE XIV.- Concluded

AVERAGE MEASURED RADIANCE PROFILES FOR 315 cm<sup>-1</sup> TO 475 cm<sup>-1</sup>

Tangent height, km	Radiance, W/m <sup>2</sup> -sr									
0.0	9.17		9.99	9.96	9.95	9.70	9.52	10.30	10.32	10.59
1.0	9.04	10.19	9.83	10.07	9.75	9.55	9.33	10.21	10.17	10.49
2.0	9.04	10.17	9.64	10.02	9.57	9.40	9.20	10.06	10.06	10.28
3.0	9.06	10.17	9.43	9.98	9.39	9.23	9.08	9.84	9.97	10.11
4.0	9.06	10.03	9.20	9.95	9.22	9.09	8.92	9.56	9.76	9.89
5.0	9.03	9.76	8.92	9.74	9.02	8.97	8.79	9.20	9.49	9.70
6.0	8.85	9.53	8.58	9.34	8.76	8.79	8.69	8.75	9.18	9.43
7.0	8.50	9.26	8.18	8.89	8.46	8.44	8.52	8.19	8.77	8.94
8.0	8.03	8.71	7.71	8.39	8.04	7.84	8.14	7.50	8.19	8.34
9.0	7.40	8.00	7.15	7.64	7.48	7.06	7.51	6.68	7.36	7.60
10.0	6.56	6.96	6.50	6.71	6.72	6.17	6.67	5.77	6.37	6.65
11.0	5.58	5.64	5.78	5.66	5.83	5.26	5.63	4.82	5.40	5.56
12.0	4.61	4.32	5.00	4.63	4.95	4.41	4.58	3.95	4.43	4.52
13.0	3.79	3.41	4.28	3.77	4.15	3.73	3.74	3.27	3.66	3.77
14.0	3.20	2.94	3.67	3.18	3.51	3.21	3.19	2.80	3.15	3.32
15.0	2.81	2.64	3.18	2.80	3.02	2.80	2.82	2.45	2.83	2.96
16.0	2.52	2.40	2.79	2.52	2.66	2.47	2.50	2.16	2.62	2.62
17.0	2.29	2.14	2.50	2.27	2.36	2.22	2.24	1.92	2.46	2.34
18.0	2.10	1.91	2.27	2.05	2.08	2.03	2.02	1.75	2.22	2.11
19.0	1.93	1.73	2.06	1.88	1.86	1.83	1.81	1.63	1.94	1.95
20.0	1.73	1.55	1.86	1.80	1.70	1.64	1.62	1.51	1.74	1.76
21.0	1.48	1.42	1.66	1.65	1.58	1.47	1.41	1.37	1.47	1.54
22.0	1.25	1.27	1.49	1.47	1.46	1.31	1.21	1.20	1.24	1.35
23.0	1.09	1.09	1.35	1.30	1.31	1.17	1.06	1.03	1.14	1.21
24.0	.95	1.02	1.21	1.14	1.17	1.05	.93	.91	1.03	1.06
25.0	.81	.97	1.08	1.03	1.04	.94	.81	.80	.91	.92
26.0	.71	.85	.94	.92	.94	.82	.70	.67	.81	.83
27.0	.66	.71	.81	.79	.85	.69	.59	.54	.73	.77
28.0	.59	.60	.70	.66	.73	.59	.50	.46	.67	.69
29.0	.53	.53	.62	.54	.62	.53	.46	.42	.59	.63
30.0	.47	.46	.55	.45	.54	.48	.44	.37	.52	.60
31.0	.46	.36	.50	.41	.47	.43	.41	.32	.49	.56
32.0	.40	.31	.45	.38	.41	.38	.33	.26	.43	.51
33.0	.32	.24	.39	.34	.33	.32	.25	.20	.38	.48
34.0	.25	.19	.34	.29	.27	.25	.21	.14	.37	.44
35.0	.23	.18	.30	.22	.24	.17	.18	.10	.34	.38
LAT.	52.6	52.7	53.7	53.7	54.3	54.5	54.7	57.0	57.2	57.3
LONG.	59.4	89.4	56.6	74.3	58.1	58.1	66.1	72.7	69.6	73.5

TABLE XV

MEASURED AND ANALYTICAL PROFILES FOR 315 cm<sup>-1</sup> TO 475 cm<sup>-1</sup>

NEAR LATITUDES 17° N AND 53° N

Tangent height, km	Measured radiance, W/m <sup>2</sup> -sr, near -		Analytical radiance, W/m <sup>2</sup> -sr, near -	
	17° N	53° N	17° N	53° N
0	11.57	9.65		
1	11.44	9.53		
2	11.28	9.40		
3	11.08	9.25		
4	10.84	9.08		
5	10.52	8.89		
6	10.14	8.62		
7	9.66	8.26		
8	9.06	7.75		
9	8.33	7.08		
10	6.67	6.26		
11	6.49	5.33		5.31
12	5.46	4.48		4.48
13	4.47	3.77	4.47	3.70
14	3.59	3.24	3.59	3.24
15	2.86	2.83	2.86	2.80
16	2.33	2.50	2.32	2.47
17	1.95	2.24	1.94	2.26
18	1.70	2.03	1.67	2.06
19	1.52	1.83	1.52	1.83
20	1.38	1.64	1.38	1.66
21	1.25	1.46	1.25	1.47
22	1.11	1.29	1.11	1.29
23	1.00	1.15	1.00	1.15
24	.91	1.03	.92	1.03
25	.81	.91	.81	.89
26	.71	.81	.71	.81
27	.62	.71	.61	.71
28	.55	.61	.54	.61
29	.49	.52	.49	.53
30	.45	.45	.45	.45
31	.42	.41	.41	.42
32	.38	.36	.37	.36
33	.34	.31	.34	.31
34	.29	.27	.29	.28
35	.24	.23	.23	.23

TABLE XVI

## WATER-VAPOR DISTRIBUTION NEAR LATITUDES 17° N AND 53° N

Altitude, km	Mixing ratio, g/kg, near —		Relative humidity, percent, near —	
	17° N	53° N	17° N	53° N
11		0.0126		30.76
12		.0083		6.05
13	0.0214	.0060	41.72	4.61
14	.0172	.0055	68.85	4.08
15	.0127	.0045	107.23	2.61
16	.0089	.0040	82.05	1.82
17	.0064	.0045	40.86	1.60
18	.0050	.0050	12.66	1.44
19	.0050	.0050	11.34	1.20
20	.0051	.0058	4.58	1.09
21	.0054	.0060	3.11	.95
22	.0051	.0058	1.74	.70
23	.0056	.0062	1.47	.76
24	.0068	.0068	1.40	.61
25	.0066	.0066	.64	.48
26	.0064	.0080	.36	.47
27	.0062	.0085	.25	.43
28	.0066	.0081	.26	.31
29	.0076	.0076	.29	.18
30	.0086	.0072	.34	.06
31	.0103	.0096	.22	.07
32	.0119	.0099	.14	.05
33	.0153	.0110	.07	.05
34	.0161	.0144	.04	.04
35	.0170	.0155	.03	.03

TABLE XVII

## TEMPERATURE AND WIND DATA DERIVED FROM WALLOPS ISLAND

MRN LAUNCH AT 0706 GMT, AUGUST 16, 1966

Altitude, km	Temperature, °K	Altitude, km	-N+S wind velocity, m/sec	-E+W wind velocity, m/sec
57.0	255.0	57	-14	-44
55.5	258.4	55	-12	-41
53.4	258.4	53	-4	-33
50.6	266.6	51	1	-32
48.0	267.2	48	-10	-33
46.6	270.0	47	-13	-31
45.1	265.0	45	-11	-37
44.2	263.3	44	-8	-33
42.7	255.9	43	-1	-24
40.5	258.4	41	5	-20
37.2	241.6	37	-1	-18
36.0	240.5	36	-2	-12
35.2	242.4	35	-1	-11
33.8	239.4	34	4	-12
32.7	239.9	32	3	-18
28.6	226.0	29	-3	-16
24.0	222.2	24	2	-10
20.9	220.0	21	-1	-7
20.0	216.2	20	-3	-5

TABLE XVIII

## TEMPERATURE AND WIND DATA DERIVED FROM EGLIN AIR FORCE BASE

MRN LAUNCH AT 0750 GMT, AUGUST 16, 1966

Altitude, km	Temperature, °K	Altitude, km	-N+S wind velocity, m/sec	-E+W wind velocity, m/sec
54	261.1	54	-11	-40
52	266.1	52	-15	-33
50	271.7	50	-8	-20
48	272.0	48	-6	-34
46	267.5	46	-4	-26
44	265.4	44	-6	-35
42	262.0	42	-5	-28
40	252.9	40	14	-24
38	245.0	38	0	-29
36	238.8	36	-15	-28
34	233.7	34	7	-11
32	255.3	32	1	-10
30	233.1	30	-2	-24
28	230.5	28	2	-26
26	224.7	26	9	-13
24	218.5	24	1	-24

TABLE XIX

## TEMPERATURE AND WIND DATA DERIVED FROM FORT CHURCHILL

MRN LAUNCH AT 0730 GMT, AUGUST 16, 1966

Altitude, km	Temperature, °K	Altitude, km	-N+S wind velocity, m/sec	-E+W wind velocity, m/sec
54.8	268.2	54.8	-15	-24
52.0	266.6	52.4	-8	-15
50.0	271.8	50.3	1	-6
48.0	270.6	47.6	2	-15
45.6	275.1	44.5	-9	-16
43.6	267.1	42.0	-6	-12
42.1	266.4	39.8	-2	-4
40.0	258.5	38.0	3	-3
37.7	252.1	34.9	0	-3
35.8	248.2	33.6	1	-6
33.5	239.8	32.4	-1	-2
32.5	240.6	30.4	1	-4
30.1	234.7	28.6	0	-3
28.3	231.8	25.1	0	2
25.0	227.4	22.4	2	2
22.9	225.5	20.9	-1	4
20.6	223.5			

TABLE XX

TEMPERATURE DATA DERIVED FROM  
WHITE SANDS MISSILE RANGE  
MRN LAUNCH AT 0730 GMT,  
AUGUST 16, 1966

Altitude, km	Temperature, °K
54.0	261.0
52.0	262.3
50.0	263.9
48.0	265.7
46.0	263.1
44.0	256.6
42.0	260.2
40.0	257.9
38.0	248.2
36.0	241.0
34.0	235.2
32.0	235.2
30.0	231.6
28.0	225.7
26.0	225.8
24.0	222.3
22.0	218.8
20.0	214.4

TABLE XXI

## MODEL ATMOSPHERES DERIVED FROM METEOROLOGICAL DATA

Altitude, km	Cell 1 (58° N 68° W)		Cell 2 (53° N 60° W)		Cell 3 (47° N 57° W)		Cell 4 (43° N 45° W)	
	Temperature, °K	Pressure, mb	Temperature, °K	Pressure, mb	Temperature, °K	Pressure, mb	Temperature, °K	Pressure, mb
0	288.0	1010.000	288.0	1010.000	286.0	1012.000	294.0	1025.000
2	277.0	800.511	277.4	800.575	280.1	807.089	284.3	811.321
4	263.2	626.923	264.2	625.462	268.4	634.169	278.2	637.879
6	250.9	477.778	251.3	477.778	257.3	485.542	260.8	489.881
8	234.7	362.245	237.1	364.762	243.3	371.429	246.5	375.253
10	221.7	267.500	221.7	268.487	230.0	277.642	231.3	281.707
12	224.9	196.296	223.8	196.543	217.1	203.652	213.9	207.343
14	224.0	145.370	221.2	145.000	218.0	149.000	213.1	148.810
16	224.0	111.025	222.7	106.884	218.0	110.075	216.5	105.932
18	224.3	79.783	224.0	79.690	219.6	80.161	219.5	81.053
20	225.0	59.065	225.0	59.039	223.1	56.319	222.0	59.115
22	225.6	43.153	225.9	42.702	224.6	43.495	222.6	43.420
24	227.6	31.922	226.0	31.787	225.8	32.132	223.0	31.998
26	232.0	23.590	227.0	23.475	227.2	23.761	225.2	23.583
28	233.6	17.715	228.3	17.491	230.6	17.690	228.1	17.676
30	235.0	13.200	235.0	12.950	237.0	13.170	232.7	13.151
32	237.8	9.910	237.0	9.720	237.0	9.900	238.0	9.740
34	240.6	7.470	240.0	7.320	240.0	7.450	241.0	7.340
36	245.6	5.650	244.0	5.530	245.0	5.640	246.0	5.560
38	252.8	4.310	251.0	4.210	251.0	4.290	250.0	4.240
40	260.0	3.310	258.0	3.230	257.0	3.290	256.0	3.240
42	262.8	2.556	261.0	2.490	260.0	2.535	260.0	2.498
44	256.6	1.971	264.0	1.920	263.0	1.959	263.0	1.930
46	267.0	1.523	265.0	1.491	265.0	1.517	265.0	1.495
48	266.0	1.183	264.0	1.156	265.0	1.177	264.0	1.159
50	265.0	.918	263.0	.895	262.0	.911	262.0	.897
52	261.4	.710	259.0	.691	260.0	.704	261.0	.694
54	258.8	.548	256.0	.532	257.0	.543	260.0	.536
56	257.5	.442	254.7	.431	255.0	.439	257.0	.433
58	256.3	.336	253.3	.331	253.0	.334	254.0	.331
60	255.0	.230	252.0	.230	251.0	.230	251.0	.228
62	246.2	.180	244.4	.180	243.8	.179	243.0	.178
64	237.4	.130	236.8	.130	236.6	.128	235.0	.128
66	229.0	.095	229.0	.095	229.0	.093	227.6	.093
68	221.0	.074	221.0	.074	221.0	.073	220.8	.073
70	213.0	.053	213.0	.053	213.0	.053	214.0	.053

TABLE XXI.- Concluded

## MODEL ATMOSPHERES DERIVED FROM METEOROLOGICAL DATA

Altitude, km	Cell 5 (35° N 48° W)		Cell 6 (21° N 55° W)		Cell 7 (17° N 60° W)	
	Temperature, °K	Pressure, mb	Temperature, °K	Pressure, mb	Temperature, °K	Pressure, mb
0	299.0	1023.000	301.0	1016.000	301.0	1016.000
2	284.1	785.377	287.8	808.129	287.8	808.129
4	274.8	639.370	275.2	637.736	275.2	637.736
6	264.5	495.294	259.7	492.669	259.7	492.669
8	250.5	380.612	252.7	379.412	252.7	379.412
10	235.3	287.600	237.1	286.800	237.1	286.800
12	218.2	213.194	220.9	213.014	220.9	213.014
14	204.0	155.000	209.0	154.749	209.0	154.749
16	207.5	112.398	201.0	110.853	201.0	110.853
18	213.0	81.087	205.0	78.659	205.0	78.659
20	217.1	59.074	212.6	57.080	212.6	57.080
22	220.5	43.253	217.5	41.525	217.5	41.525
24	222.7	31.744	219.0	30.412	219.0	30.422
26	225.6	23.350	227.0	22.585	227.0	22.585
28	227.7	17.360	227.7	16.833	227.7	16.839
30	230.0	12.830	227.0	12.390	225.0	12.380
32	239.0	9.620	235.0	9.250	233.0	9.220
34	244.0	7.270	242.0	6.970	241.0	6.930
36	248.0	5.520	247.0	5.290	247.0	5.260
38	251.0	4.220	250.0	4.030	250.0	4.010
40	254.0	3.230	253.0	3.080	253.0	3.070
42	259.0	2.481	259.0	2.370	259.0	2.358
44	264.0	1.917	266.0	1.834	260.0	1.825
46	265.0	1.487	268.0	1.426	270.0	1.420
48	264.0	1.153	265.0	1.108	269.0	1.107
50	262.0	.893	262.0	.859	262.0	.859
52	265.0	.692	267.0	.666	268.0	.667
54	268.0	.538	273.0	.520	273.0	.520
56	264.0	.434	267.0	.422	266.3	.425
58	260.0	.329	261.0	.323	259.7	.330
60	256.0	.225	255.0	.225	253.0	.235
62	248.4	.181	247.8	.181	246.2	.189
64	240.8	.136	240.6	.136	239.4	.143
66	233.4	.102	233.2	.102	232.6	.108
68	226.2	.077	225.6	.077	225.8	.083
70	219.0	.053	218.0	.053	219.0	.058

TABLE XXII

RADIANCE DEVIATIONS FROM 1962 U.S. STANDARD ATMOSPHERE  
FOR MRN AND MAP ANALYSIS

Tangent height, km	Unperturbed radiance, W/m <sup>2</sup> -sr	MRN error, W/m <sup>2</sup> -sr	Map analysis error ( $\pm 2^\circ$ K), W/m <sup>2</sup> -sr	Error bounds, W/m <sup>2</sup> -sr
10	5.43	0.12	$\pm 0.09$	+0.15 -.09
20	5.34	.13	$\pm .10$	+0.17 -.10
30	4.24	.18	$\pm .17$	+0.25 -.17
40	2.46	.17	$\pm .09$	+0.19 -.09
50	.96	.10	$\pm .03$	+0.11 -.03
60	.24	.04	$\pm .01$	+0.04 -.01

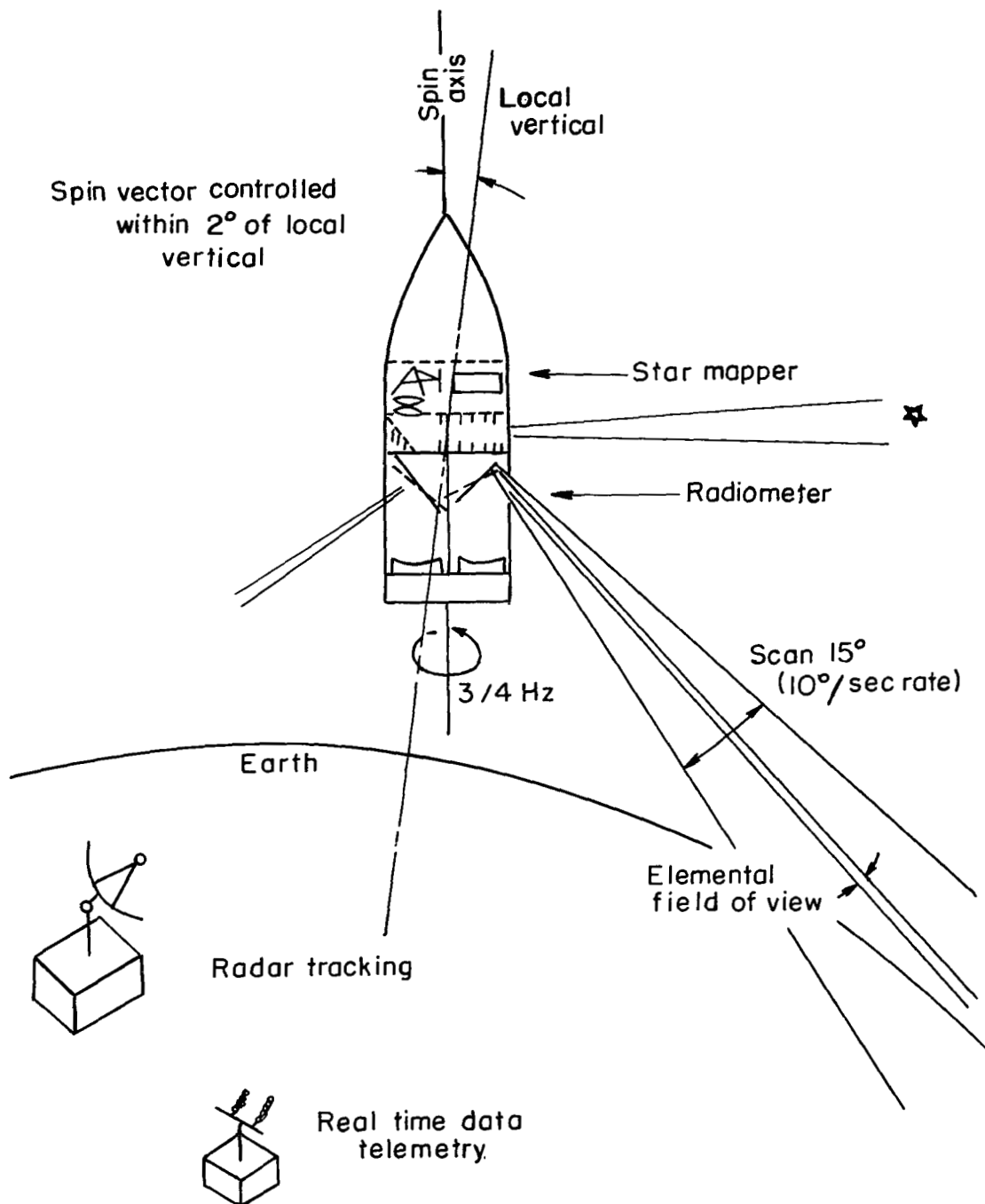


Figure 1.- Operational schematic of flight experiment.

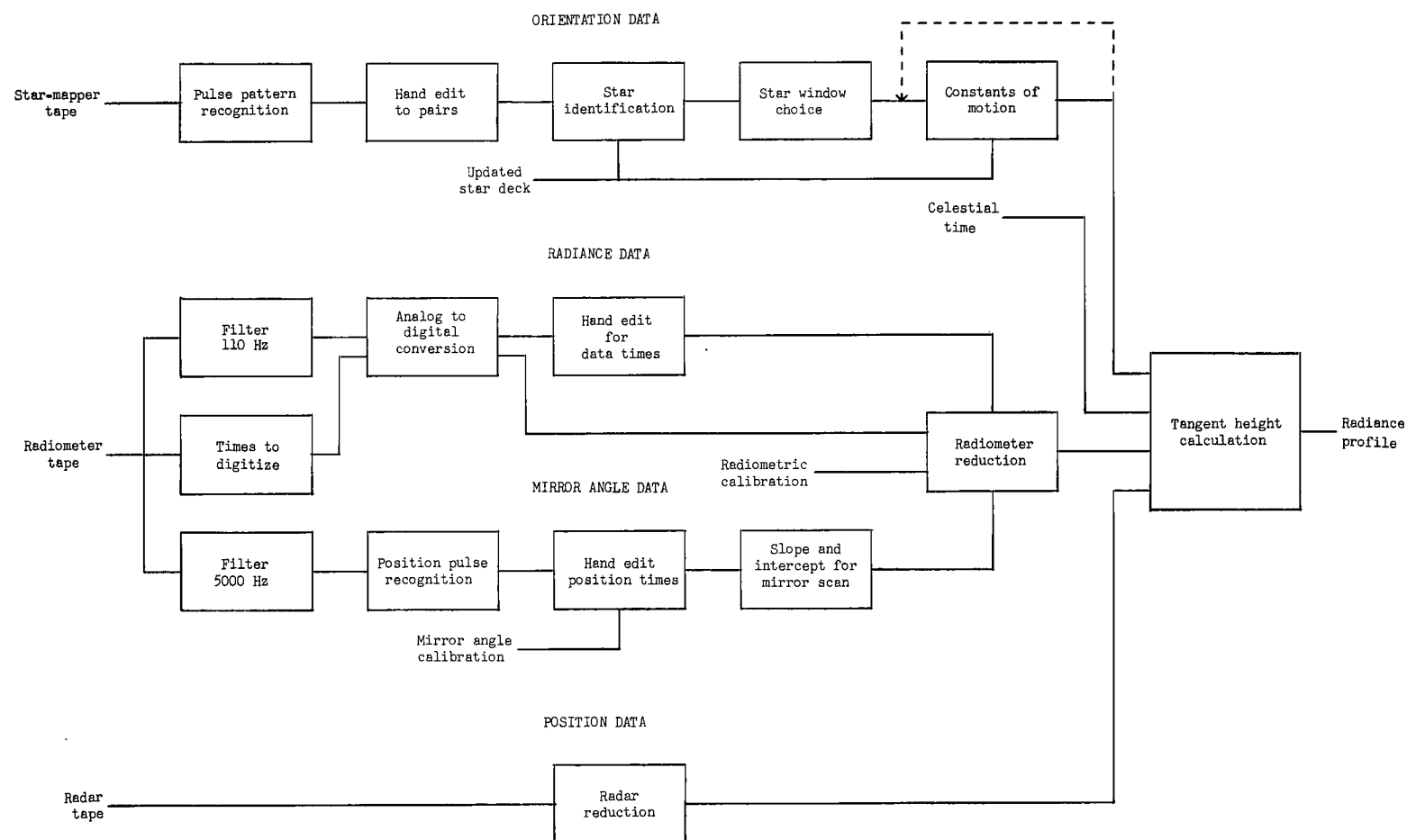


Figure 2.- Block diagram of reduction of Star mapper, dual radiometer, and radar data.

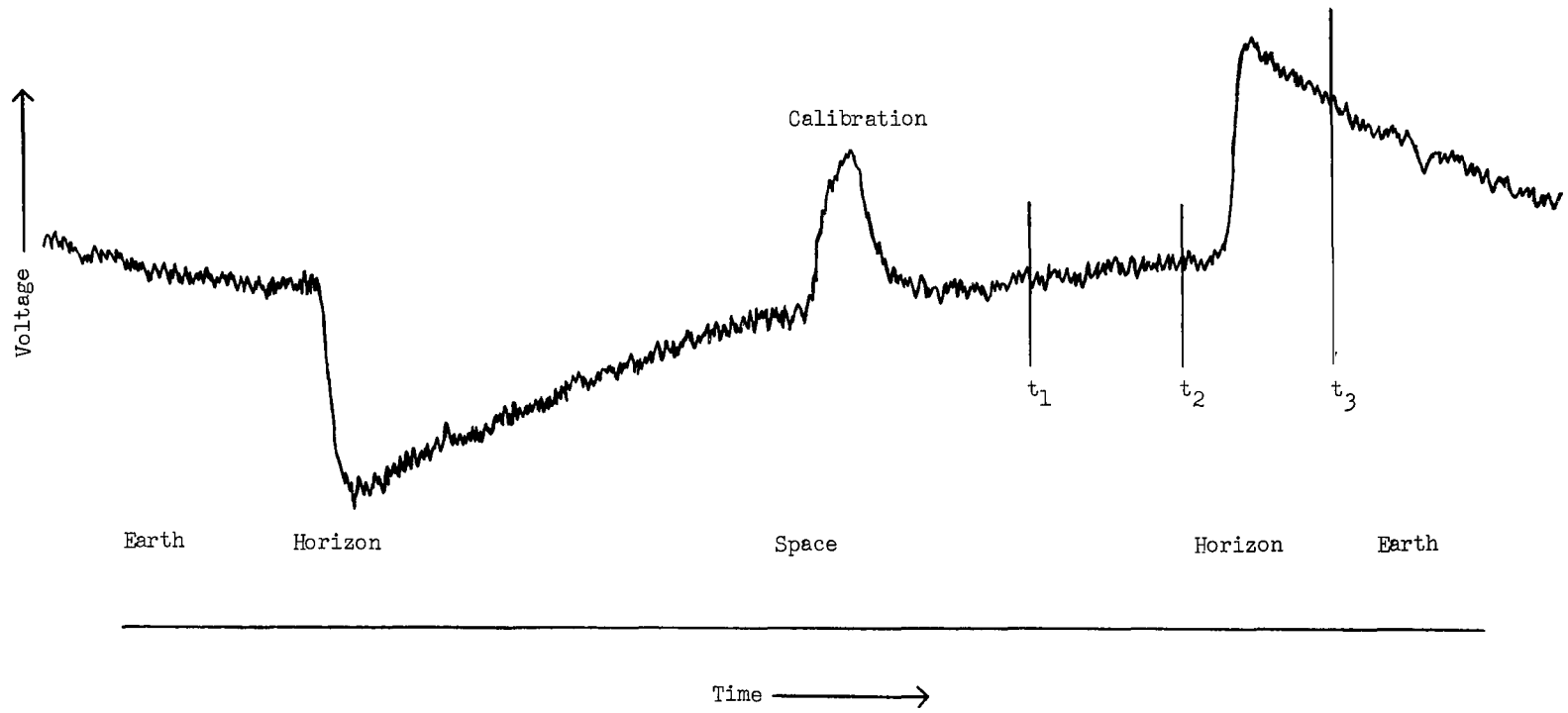
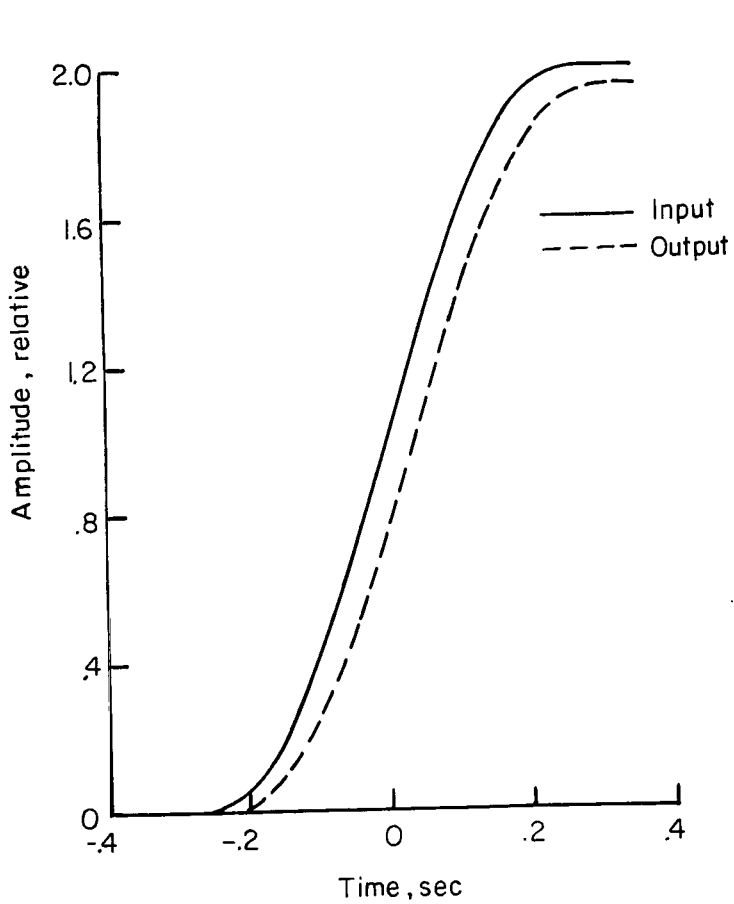
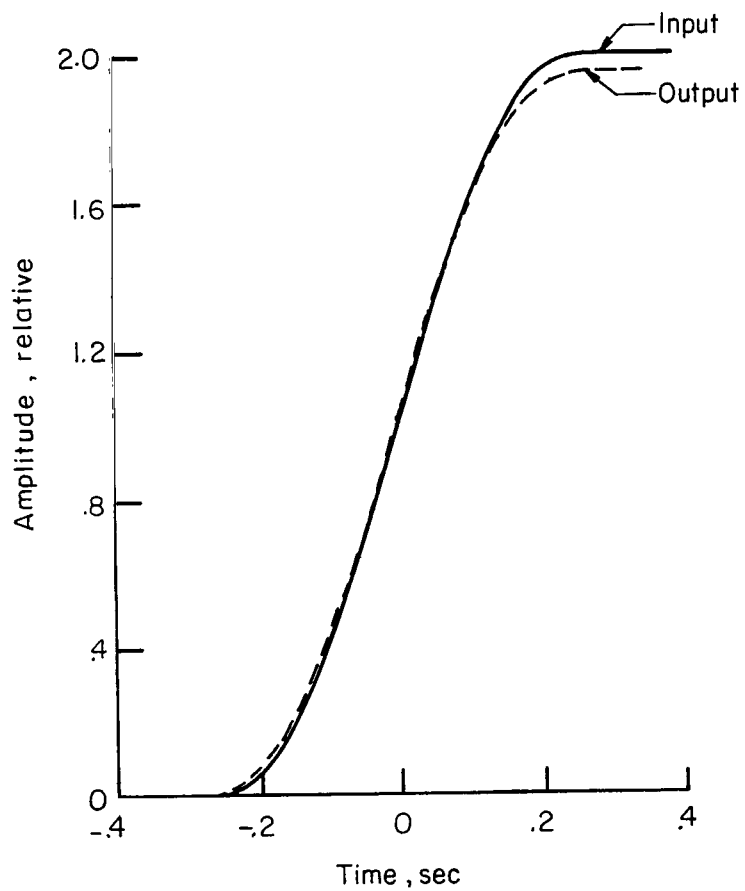


Figure 3.- Typical time history of radiometer output.

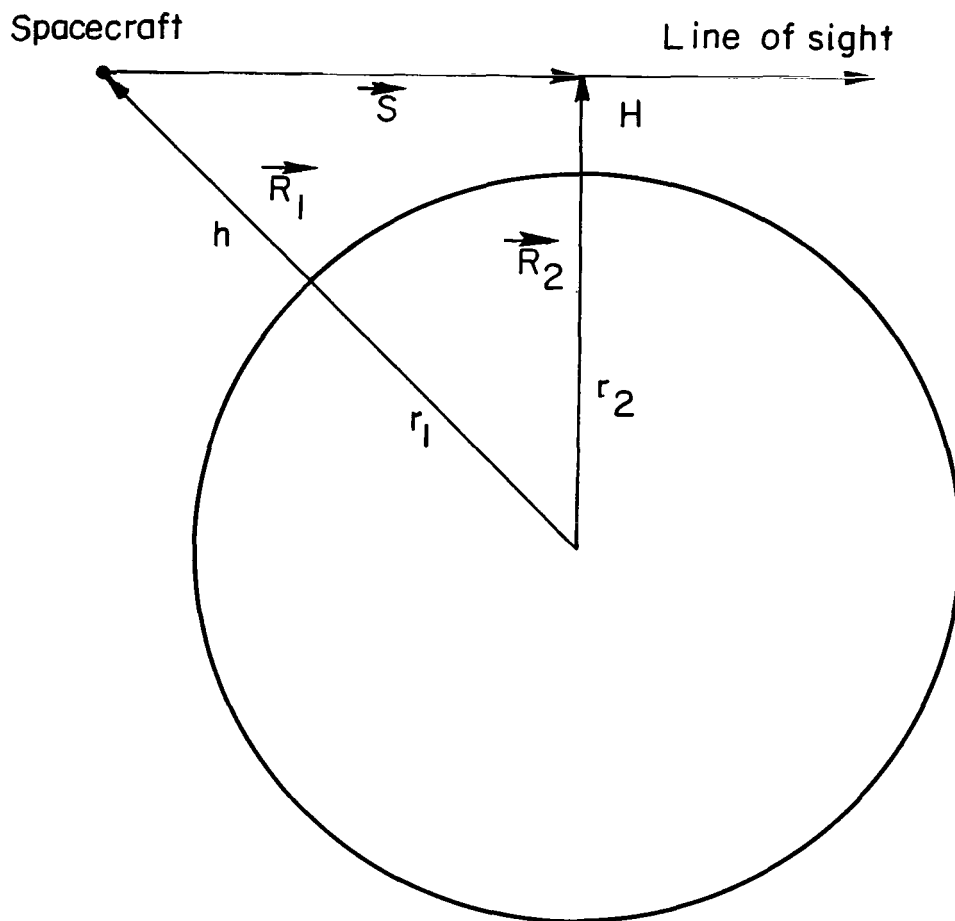


(a) Input and output in real time.



(b) Output with delay in time.

Figure 4.- Effect of time delay on radiometer response.



$$H = |\vec{R}_2| - r_2$$

Figure 5.- Definition of tangent height.

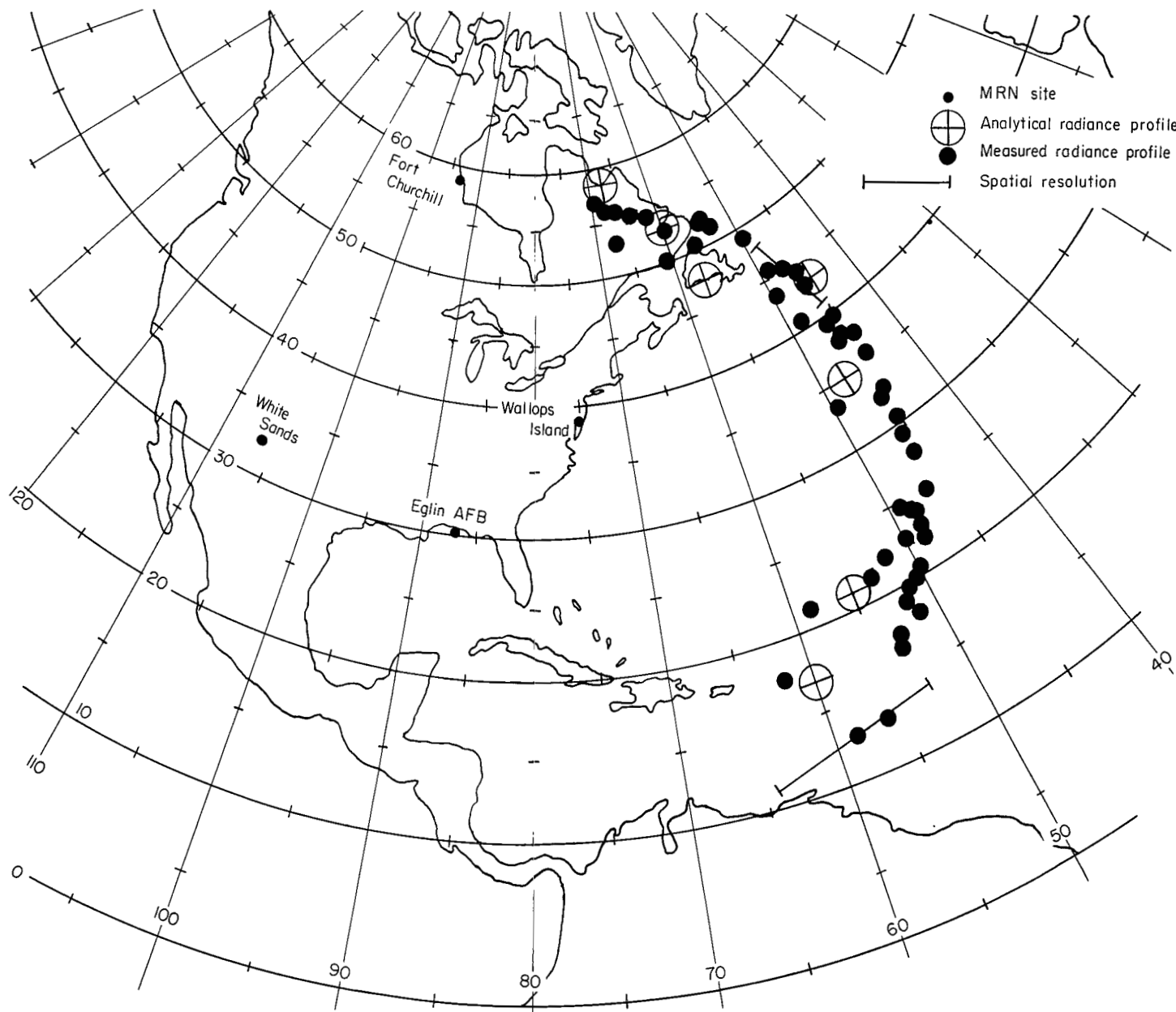


Figure 6.- Geographic location of analytical and measured horizon radiance profiles for  $615\text{ cm}^{-1}$  to  $715\text{ cm}^{-1}$  ( $\text{CO}_2$ ).

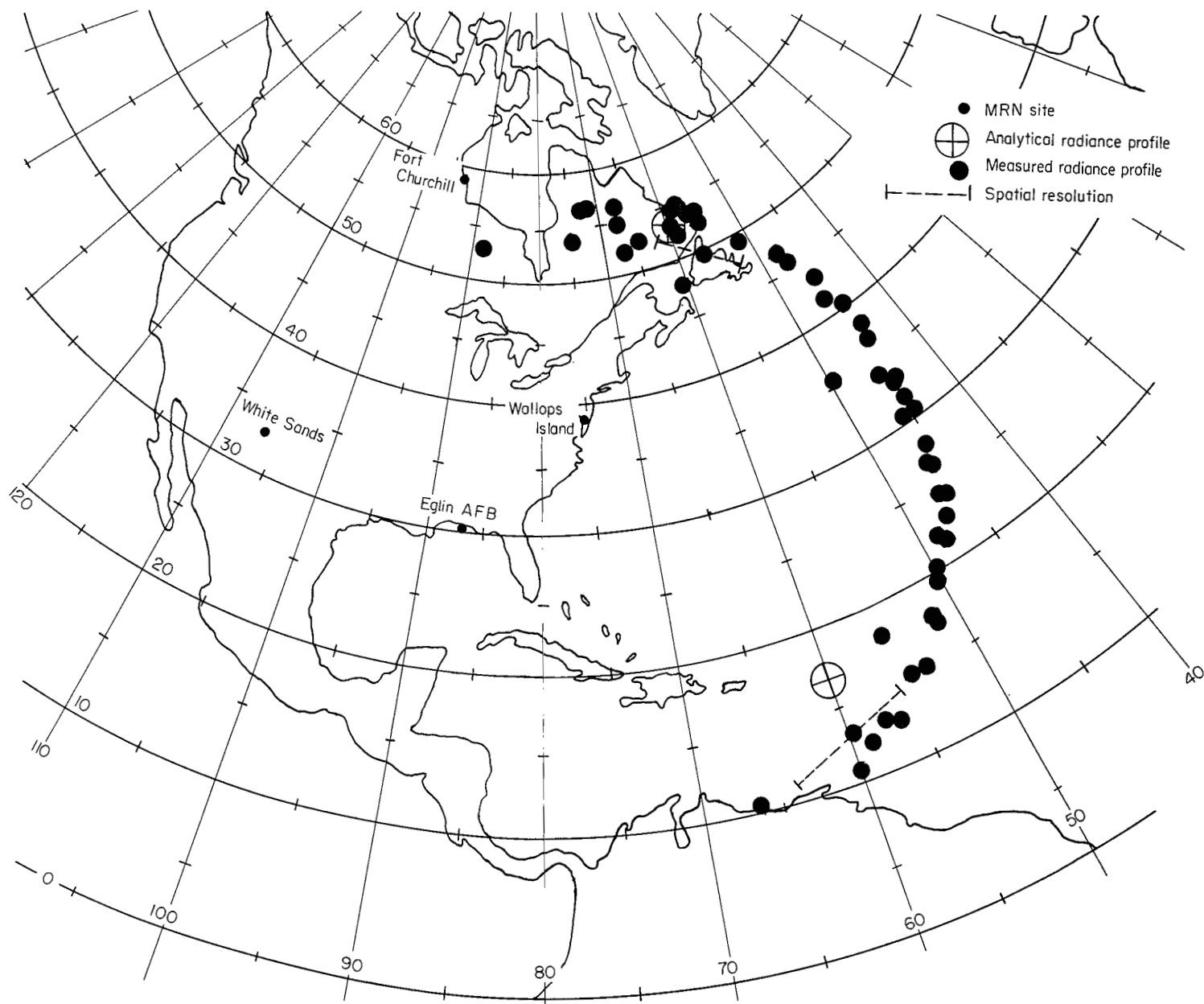


Figure 7.- Geographic location of measured horizon radiance profiles for  $315\text{ cm}^{-1}$  to  $475\text{ cm}^{-1}$  ( $\text{H}_2\text{O}$ ).

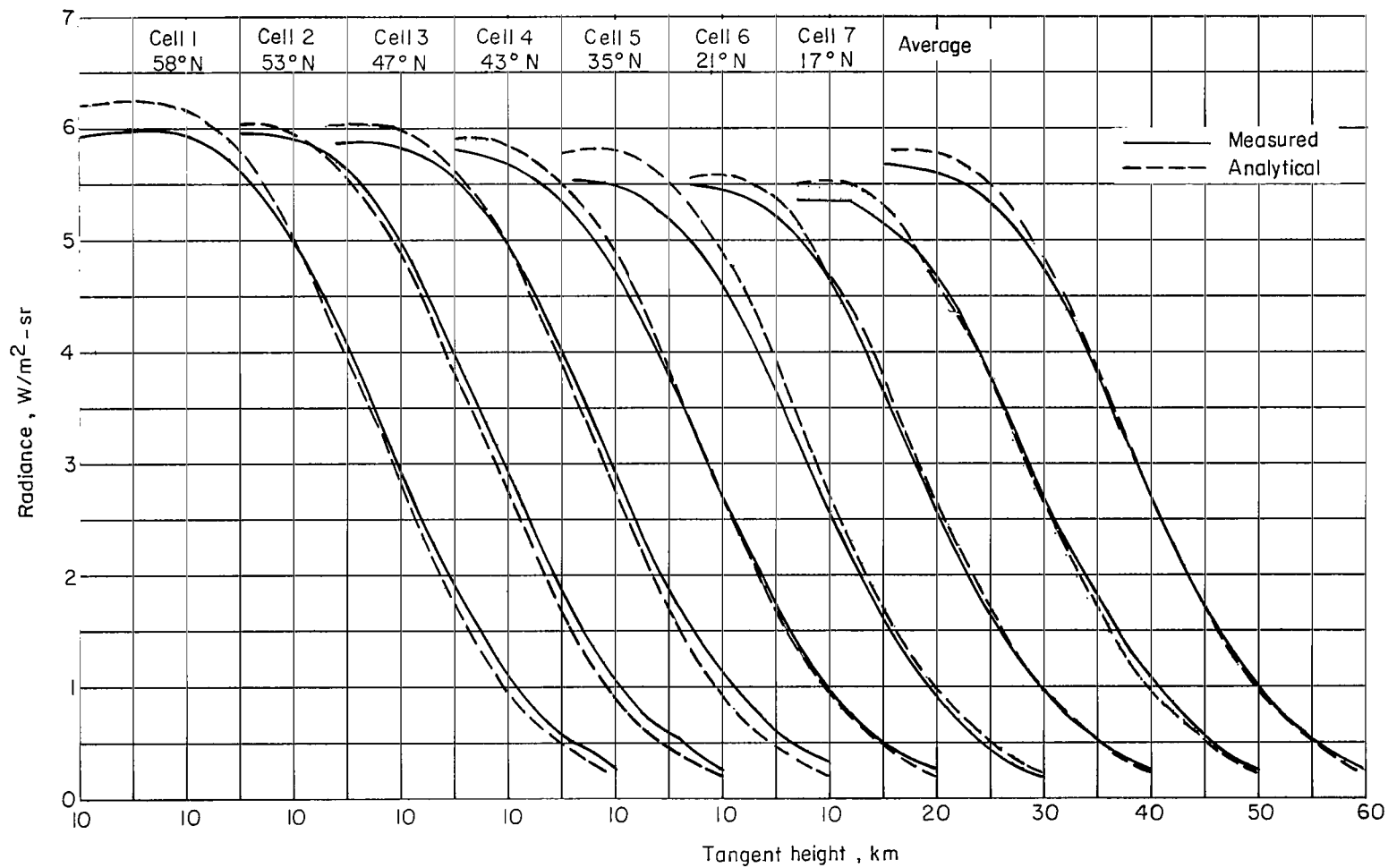


Figure 8.- Measured and analytical radiance profiles in 615 cm<sup>-1</sup> to 715 cm<sup>-1</sup> spectral band.

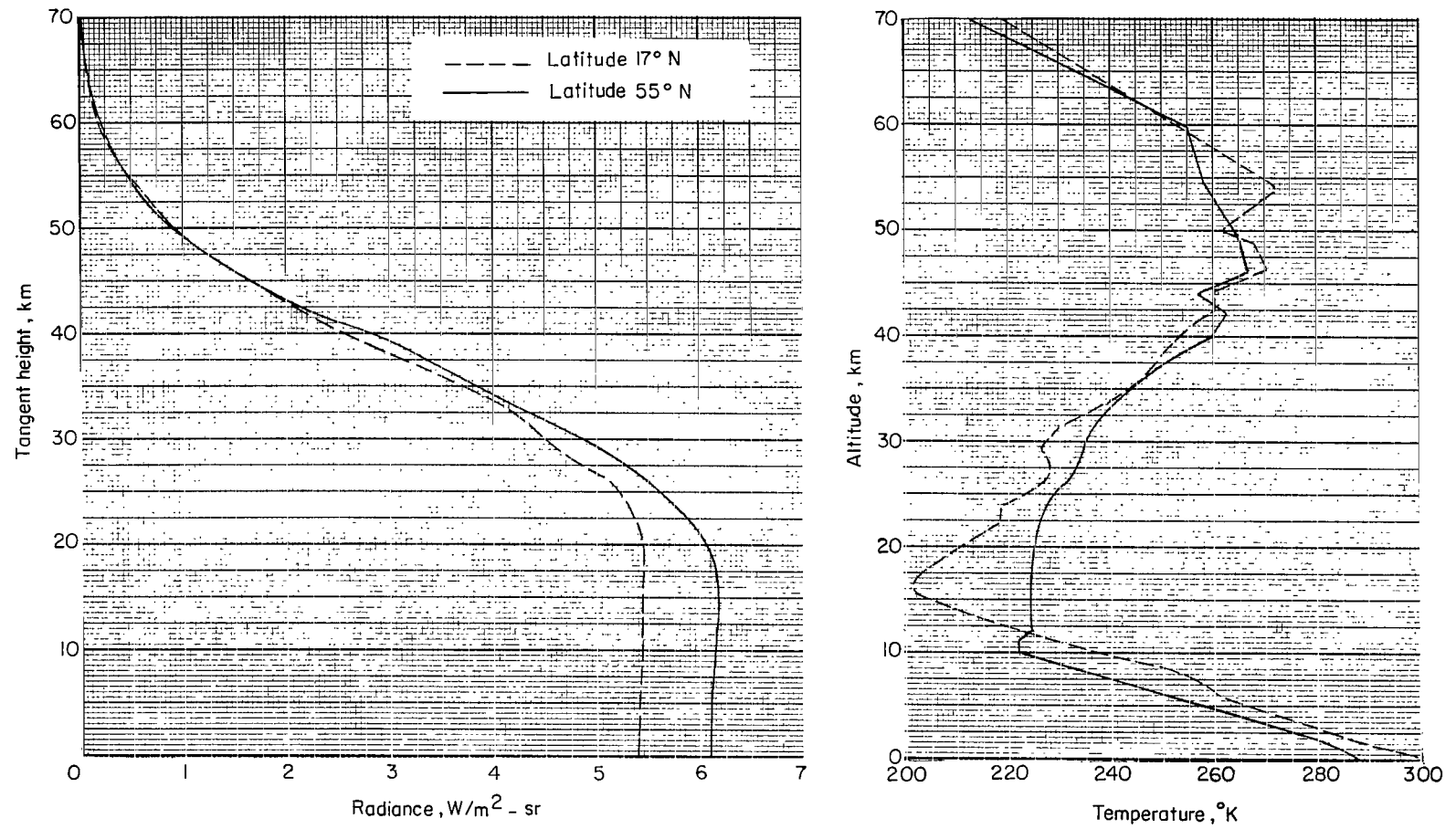


Figure 9.- Analytical radiance profiles in  $615\text{ cm}^{-1}$  to  $715\text{ cm}^{-1}$  spectral band and temperature profiles for extremes in latitude.

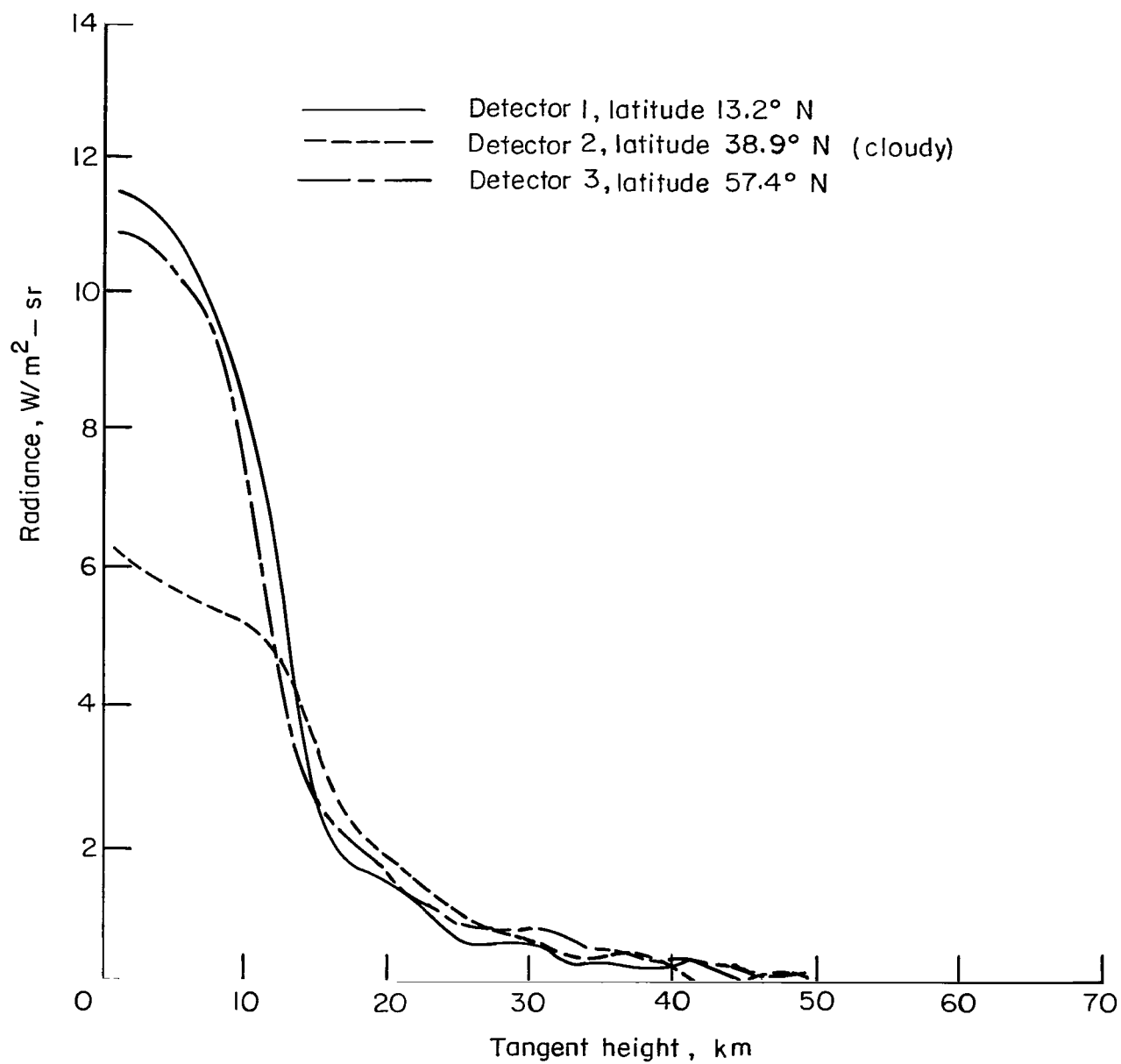


Figure 10.- Measured radiance profiles in 315  $\text{cm}^{-1}$  to 475  $\text{cm}^{-1}$  spectral band.

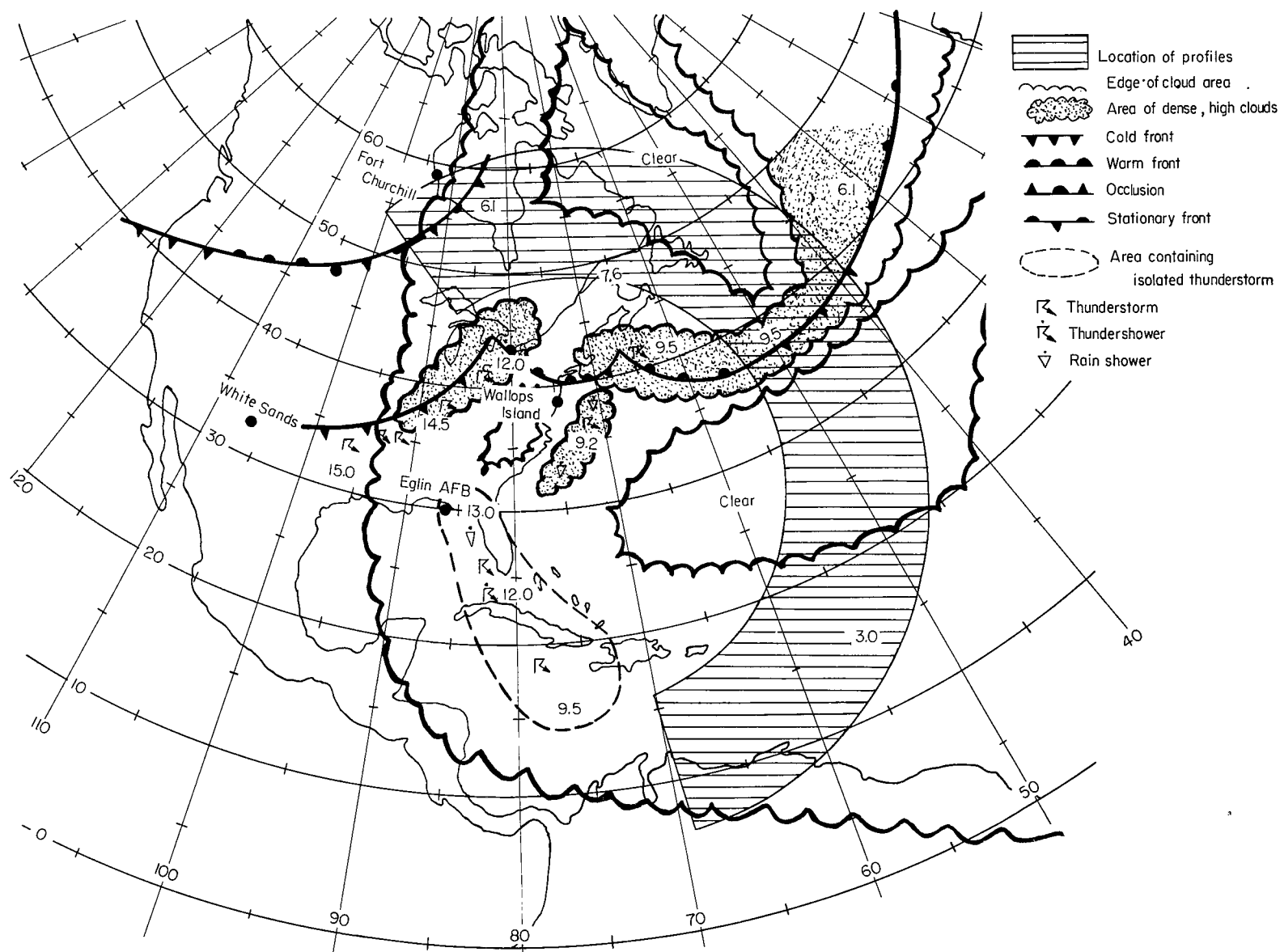


Figure 11.- Nephanalysis and significant weather for Scanner mission of August 16, 1966. Heights of highest clouds in km are indicated by numbers.

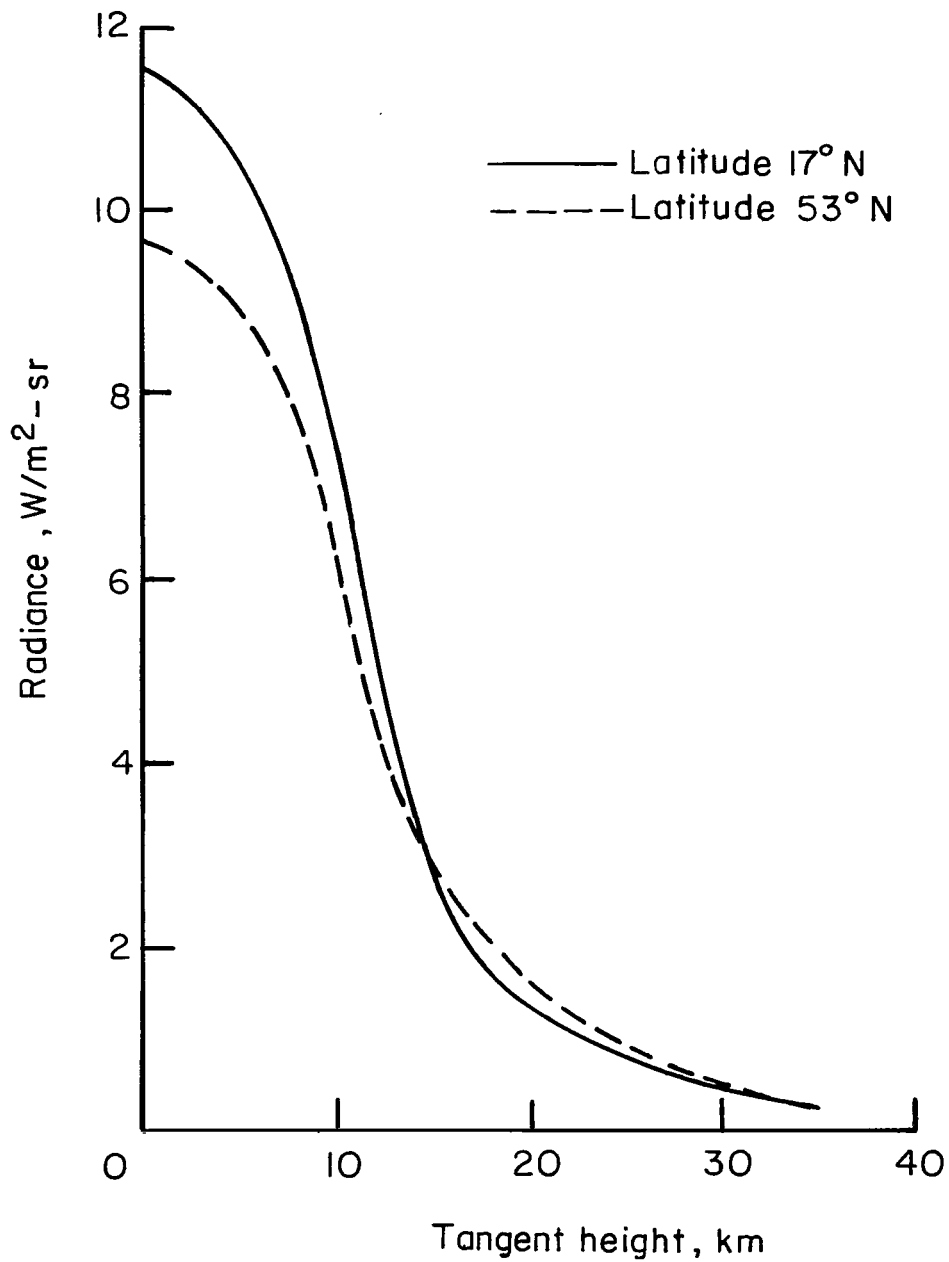


Figure 12.- Averages of several measured radiance profiles in 315 cm<sup>-1</sup> to 475 cm<sup>-1</sup> spectral band.

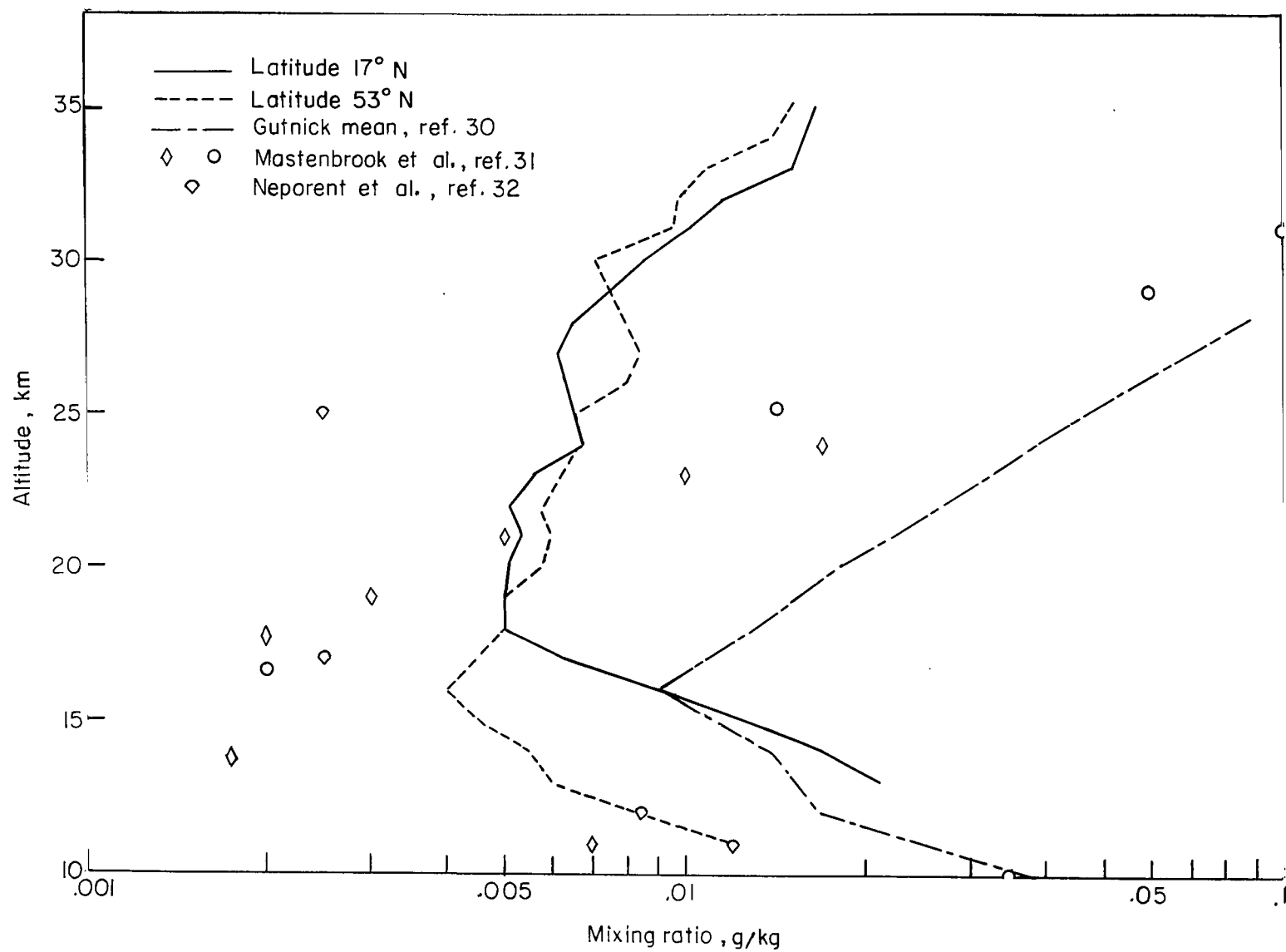
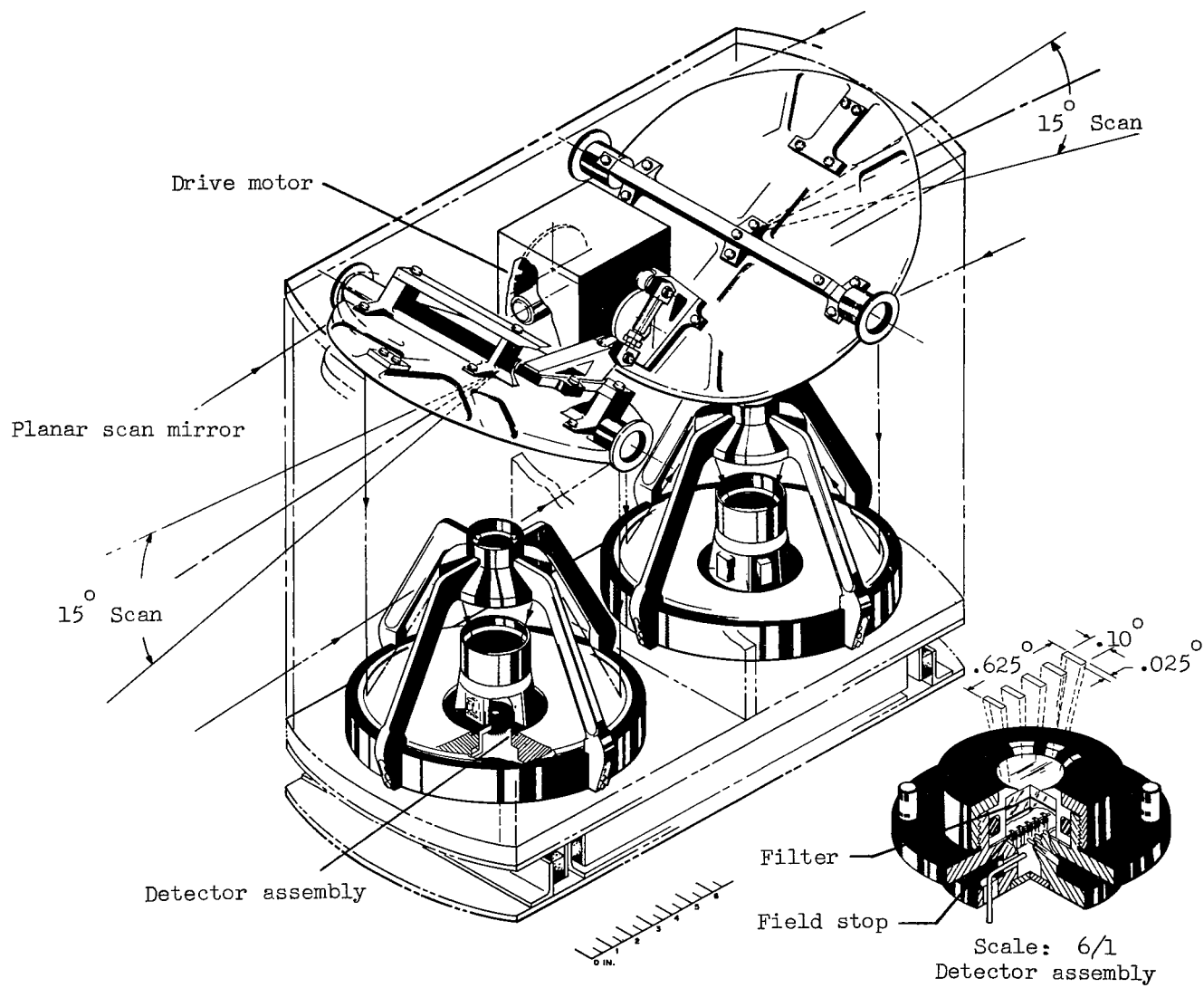
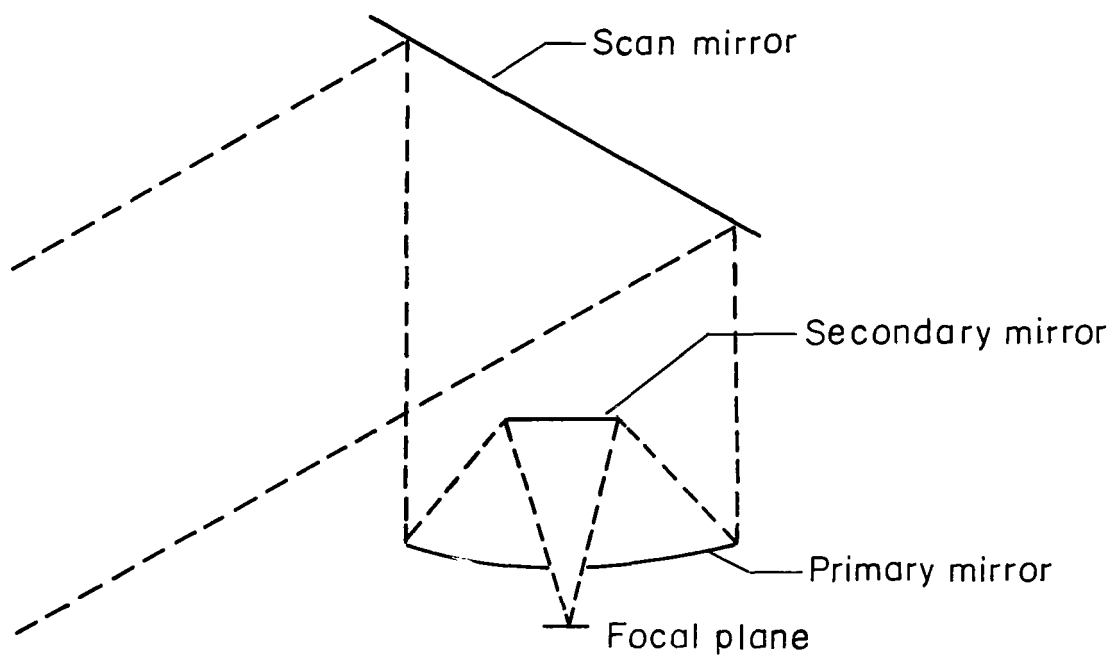


Figure 13.- Water-vapor mixing ratios deduced from Scanner data and from other studies research.



(a) Dual radiometer assembly.

Figure 14.- Dual radiometer.



(b) Optical schematic.

Figure 14.- Concluded.

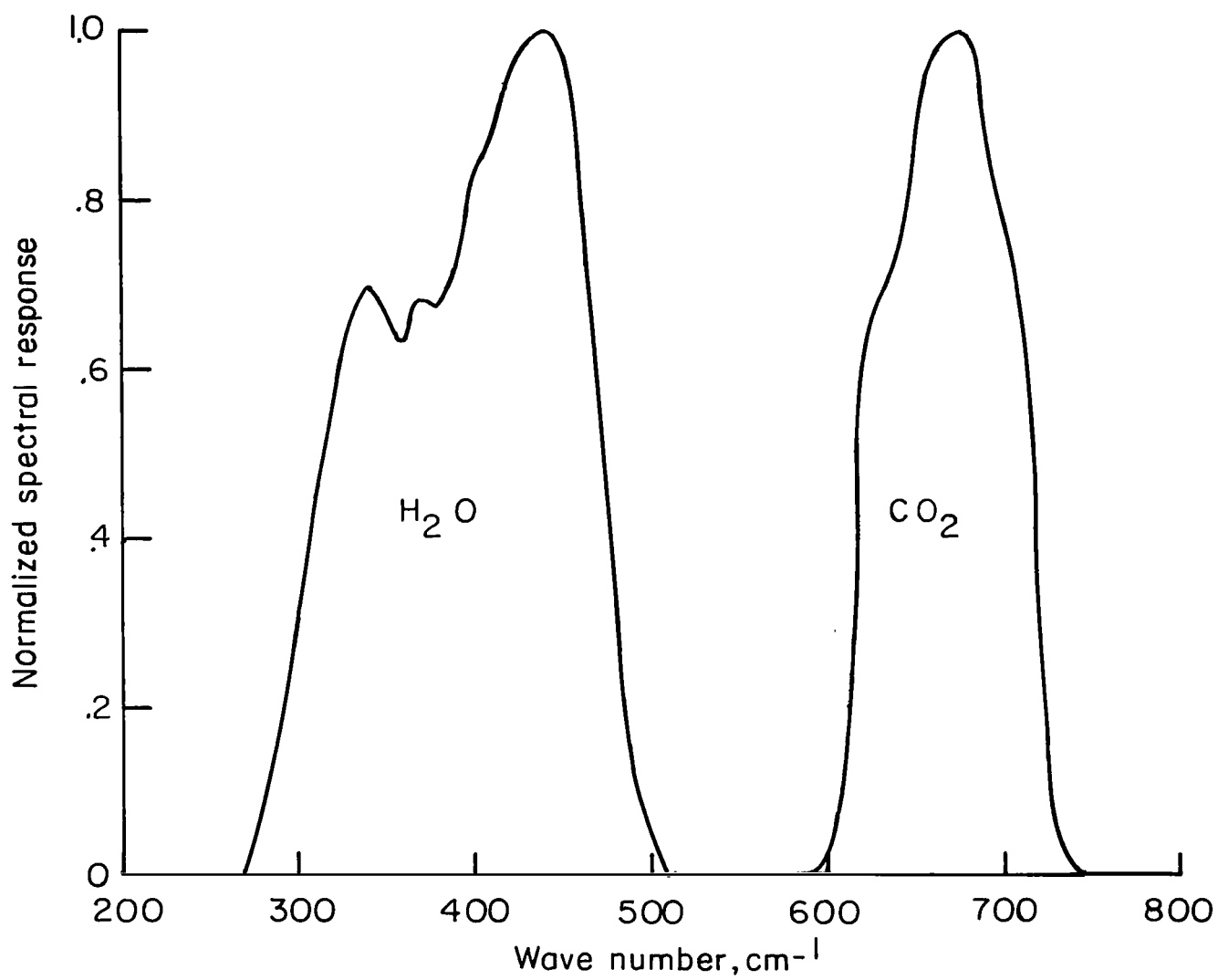
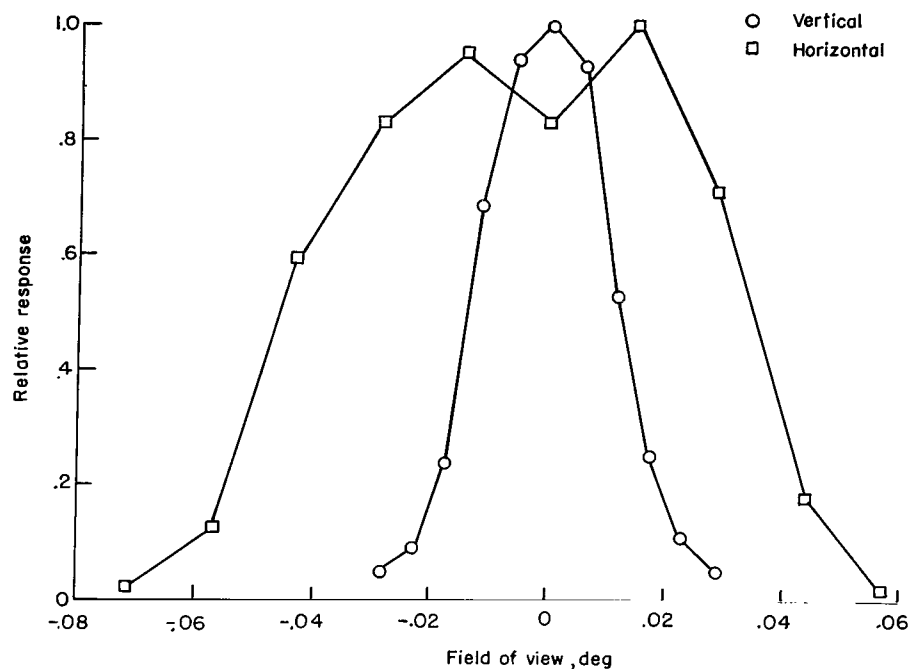
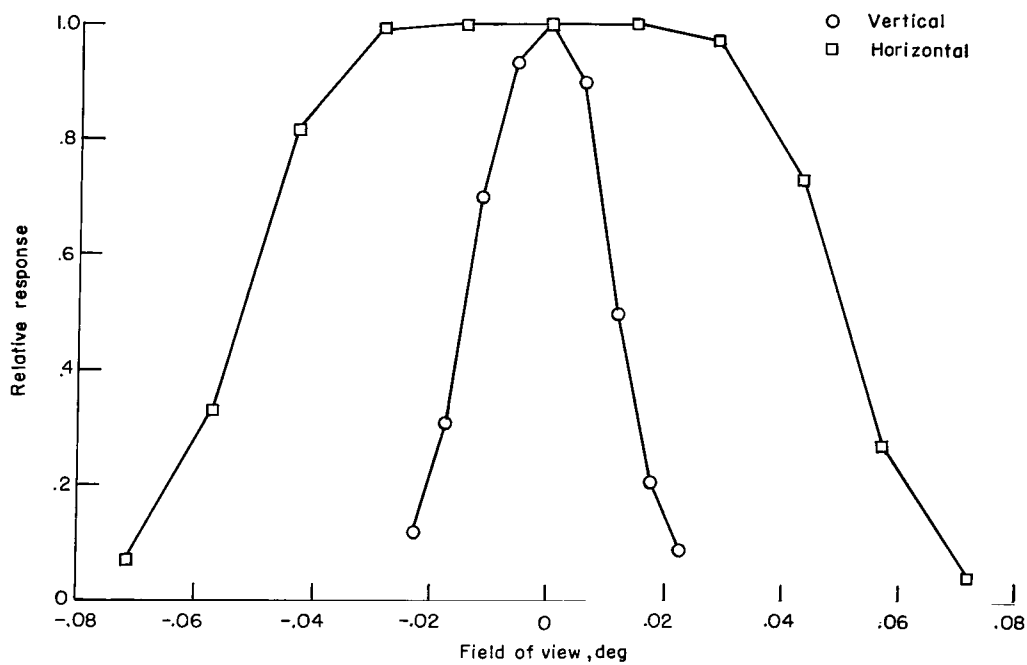


Figure 15.- Normalized spectral response of dual radiometer.

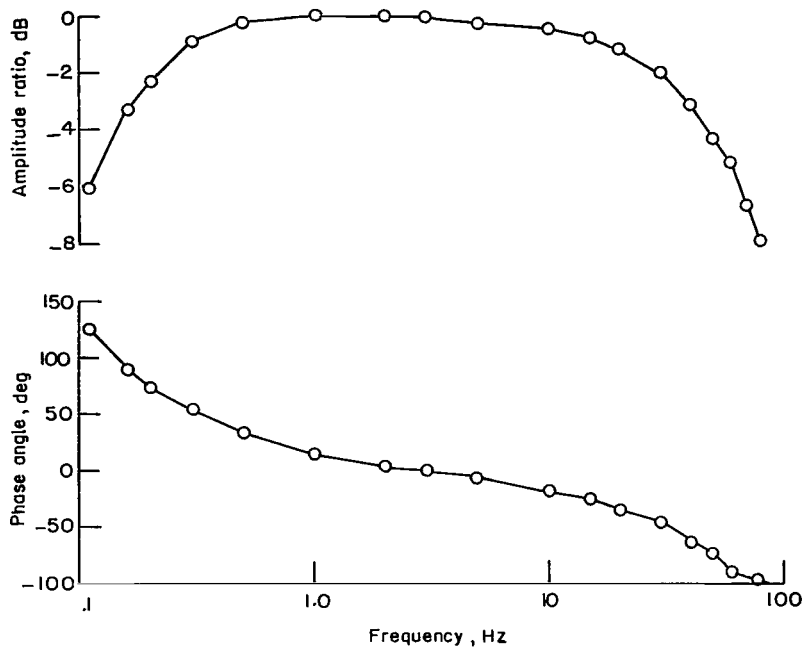


(a) 615 cm<sup>-1</sup> to 715 cm<sup>-1</sup> (CO<sub>2</sub>).

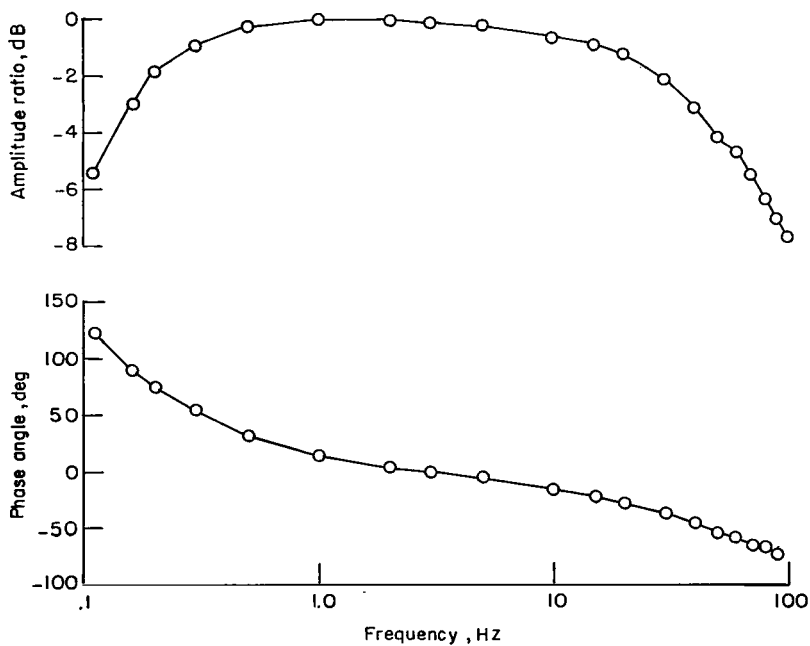


(b) 315 cm<sup>-1</sup> to 475 cm<sup>-1</sup> (H<sub>2</sub>O).

Figure 16.- Typical elemental field-of-view contours for dual radiometer.



(a)  $615\text{ cm}^{-1}$  to  $715\text{ cm}^{-1}$  ( $\text{CO}_2$ ).



(b)  $315\text{ cm}^{-1}$  to  $475\text{ cm}^{-1}$  ( $\text{H}_2\text{O}$ ).

Figure 17.- Typical phase and amplitude responses for dual radiometer.

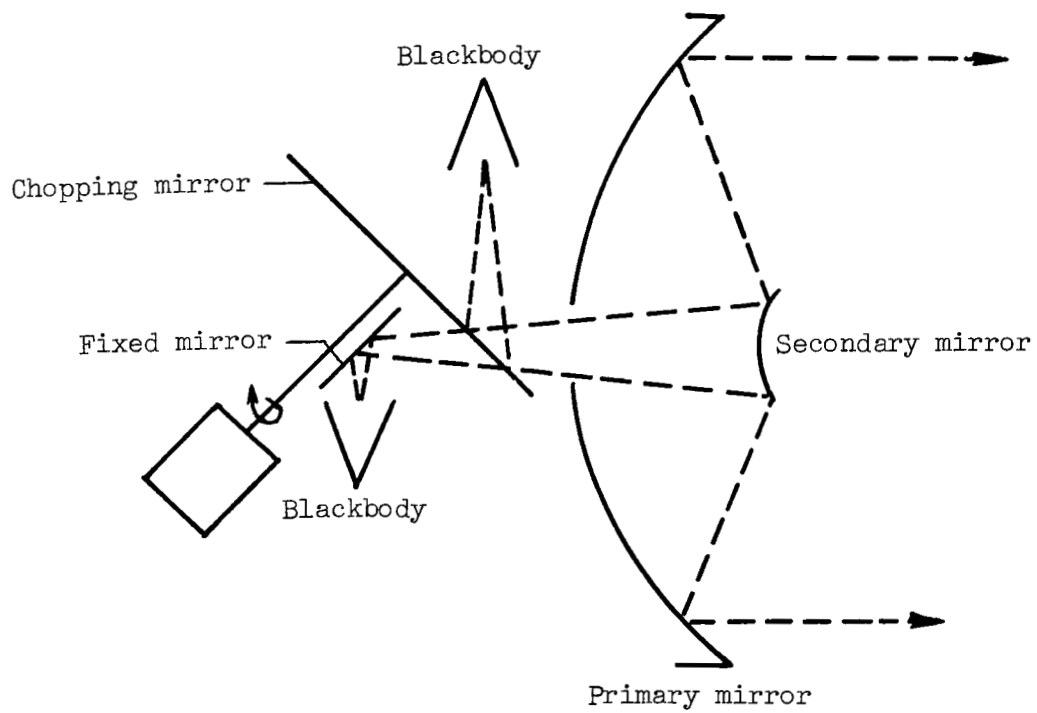


Figure 18.- Schematic of calibration optical system.

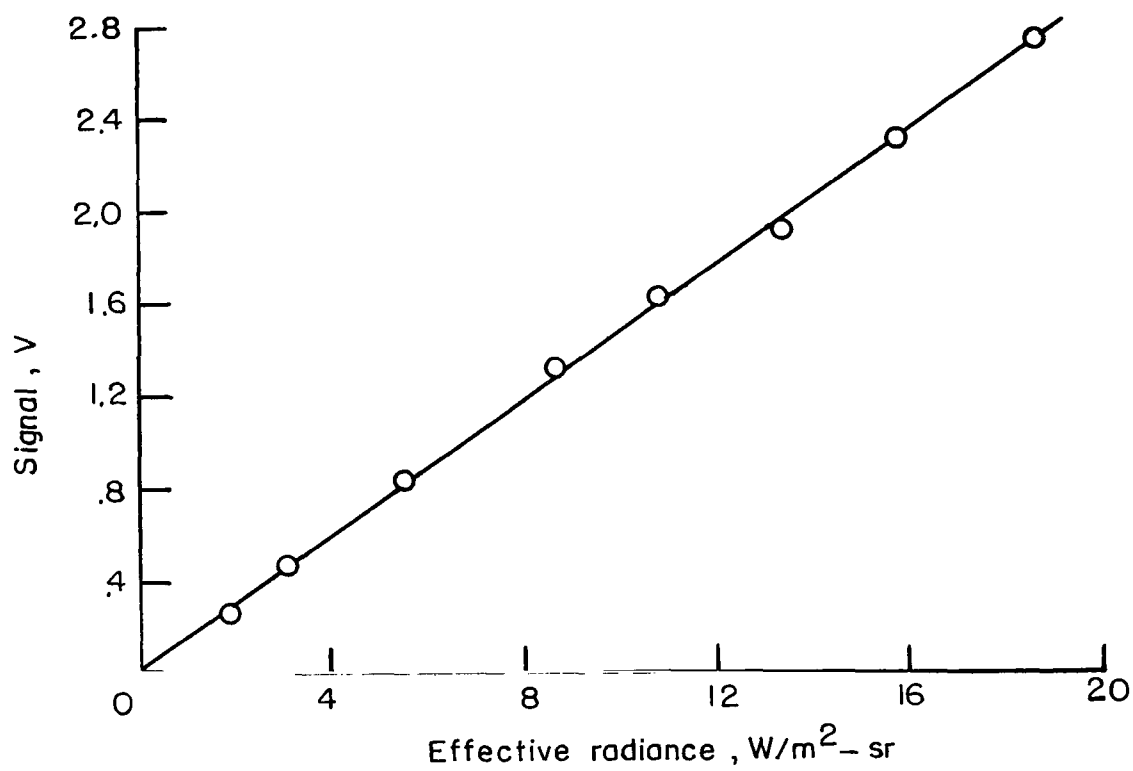


Figure 19.- Typical radiometer calibration curve.

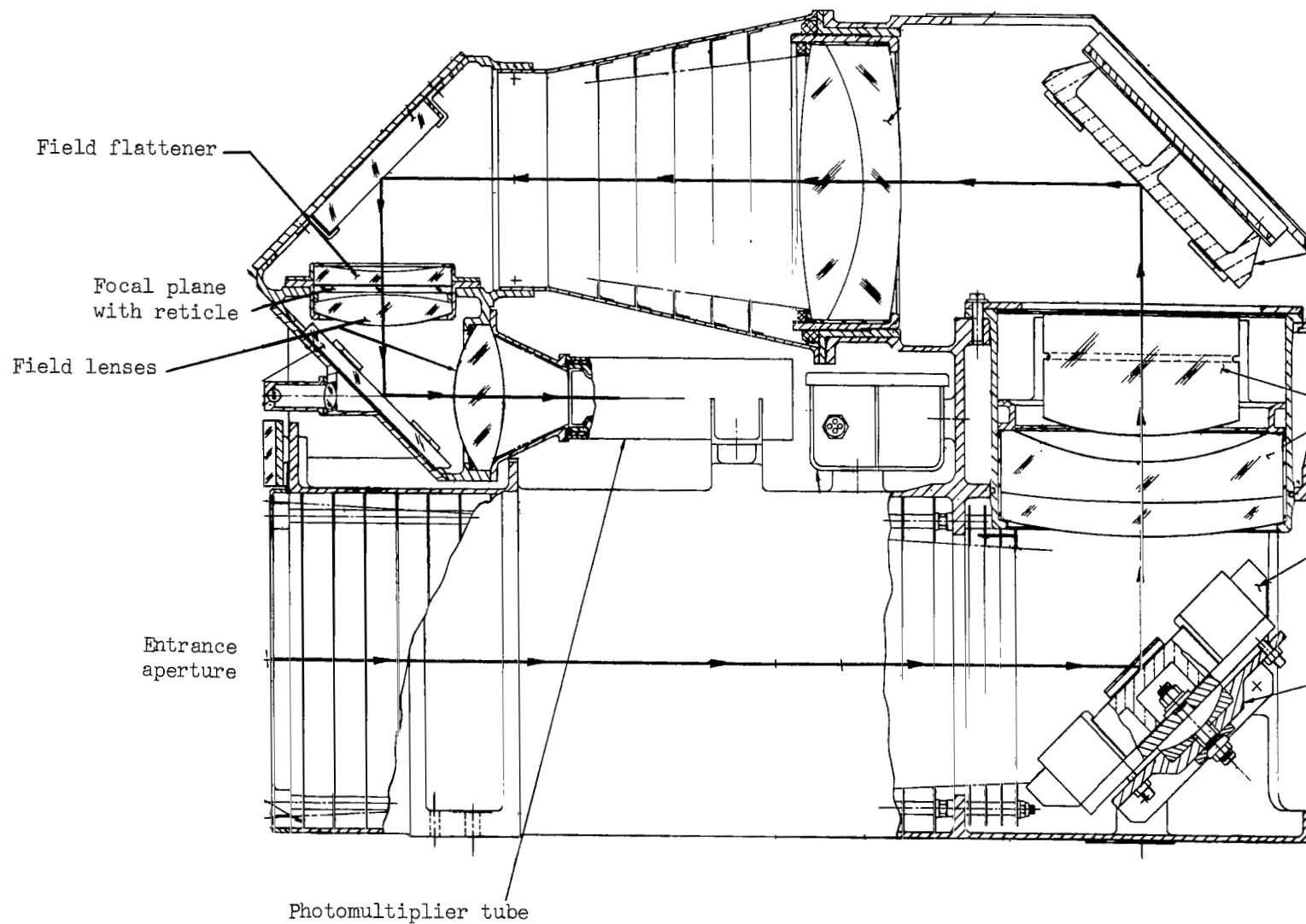
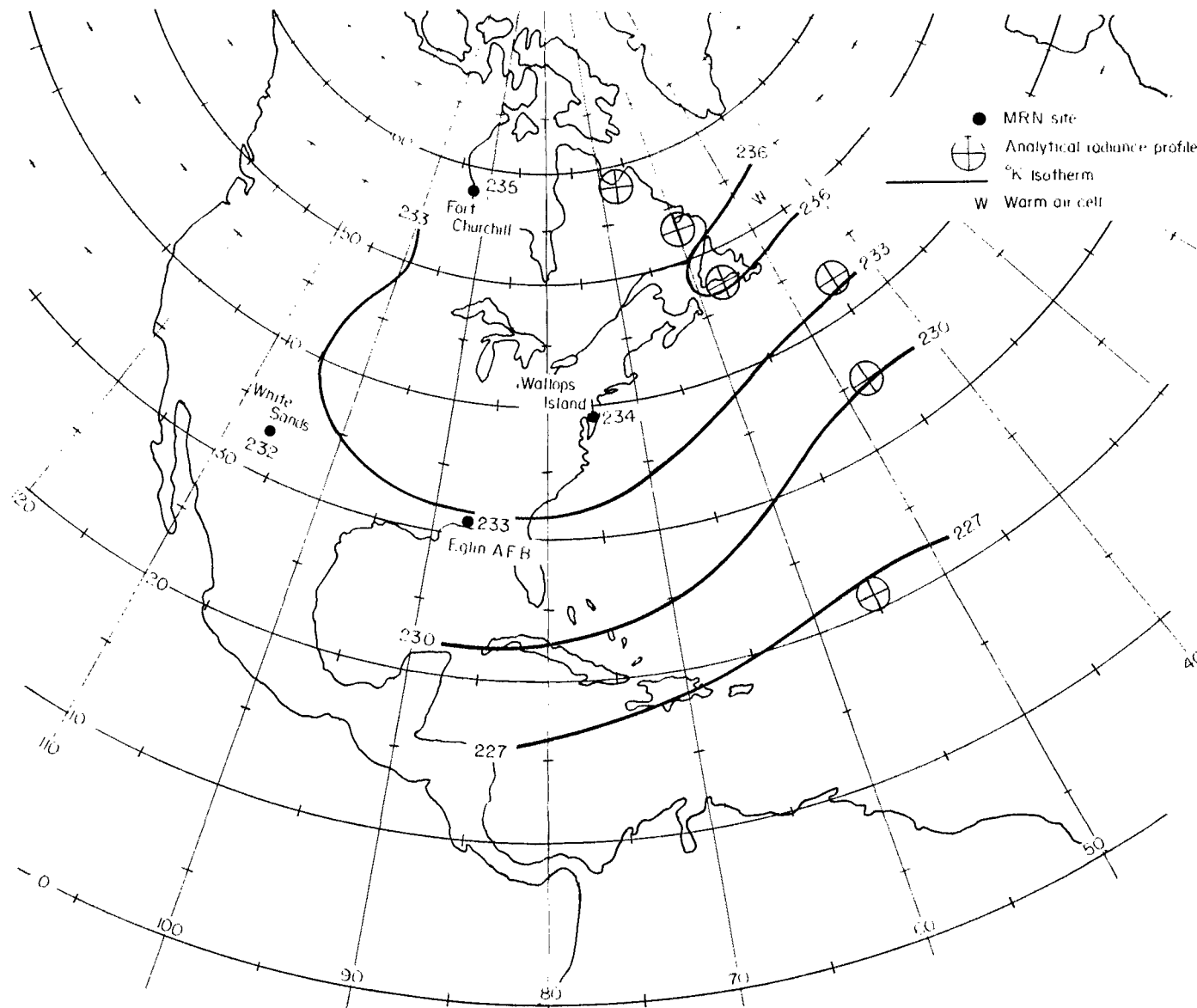
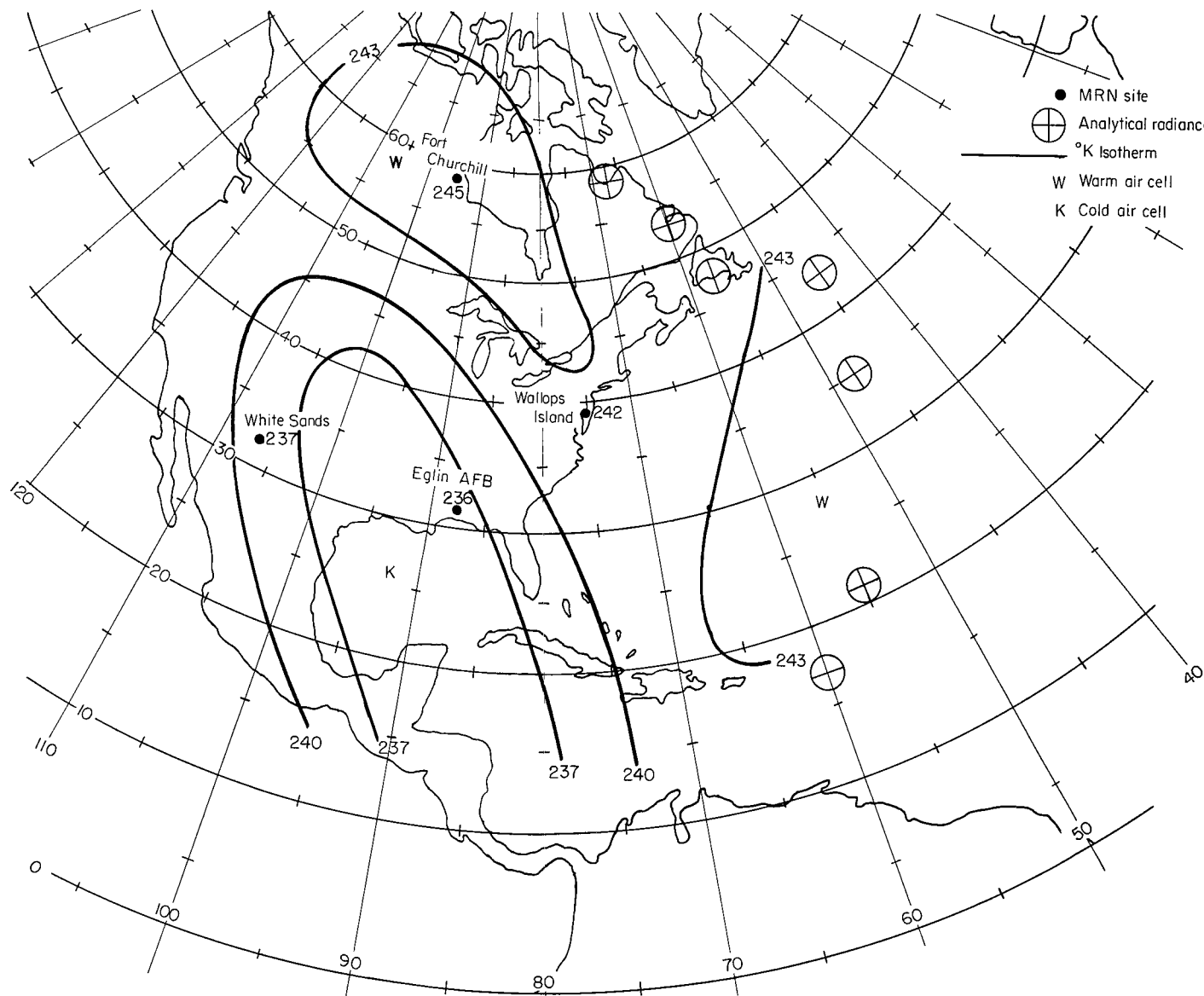


Figure 20.- Sketch of star mapper.



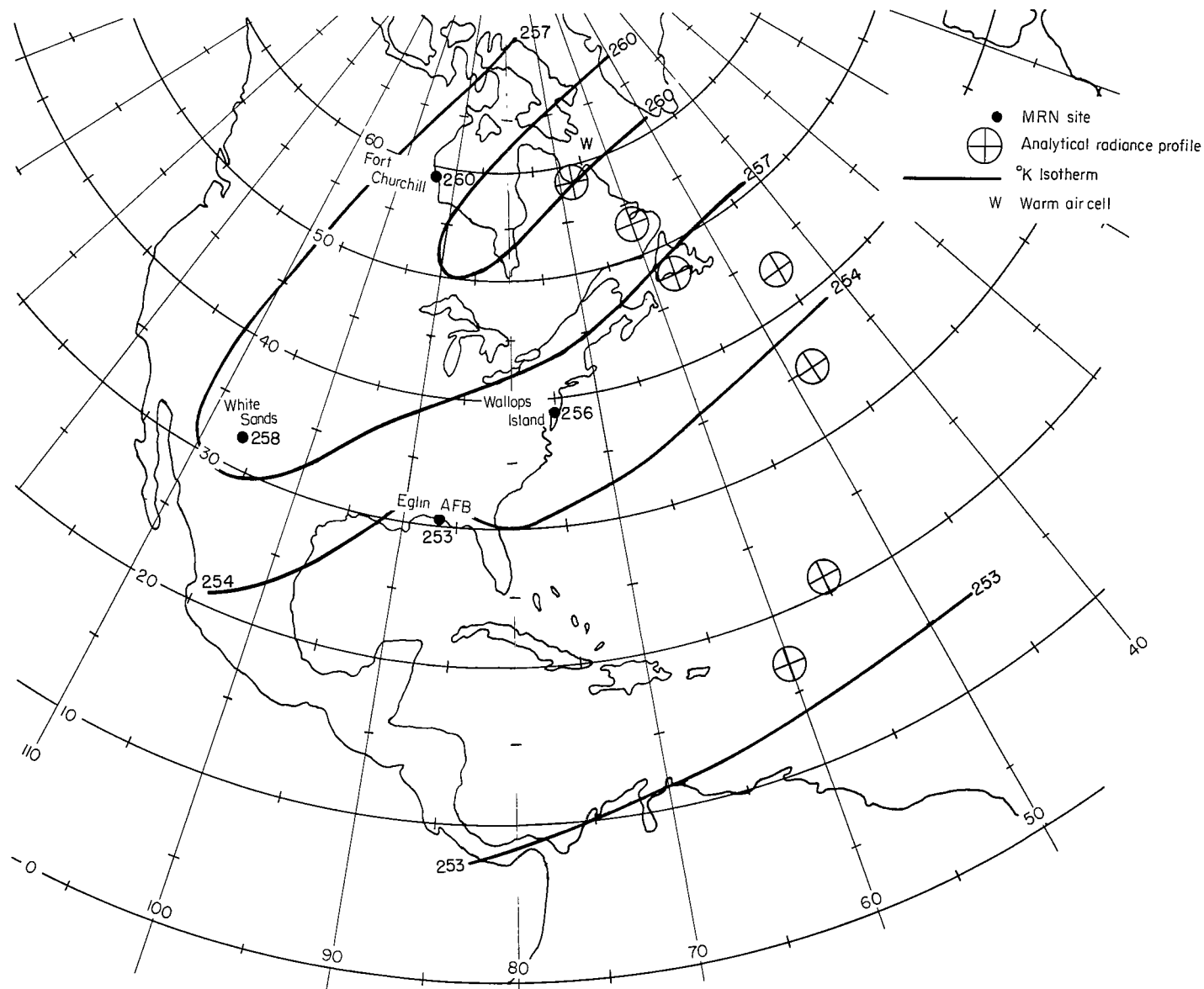
(a)  $h = 30$  km.

Figure 21.- Temperature analyses.



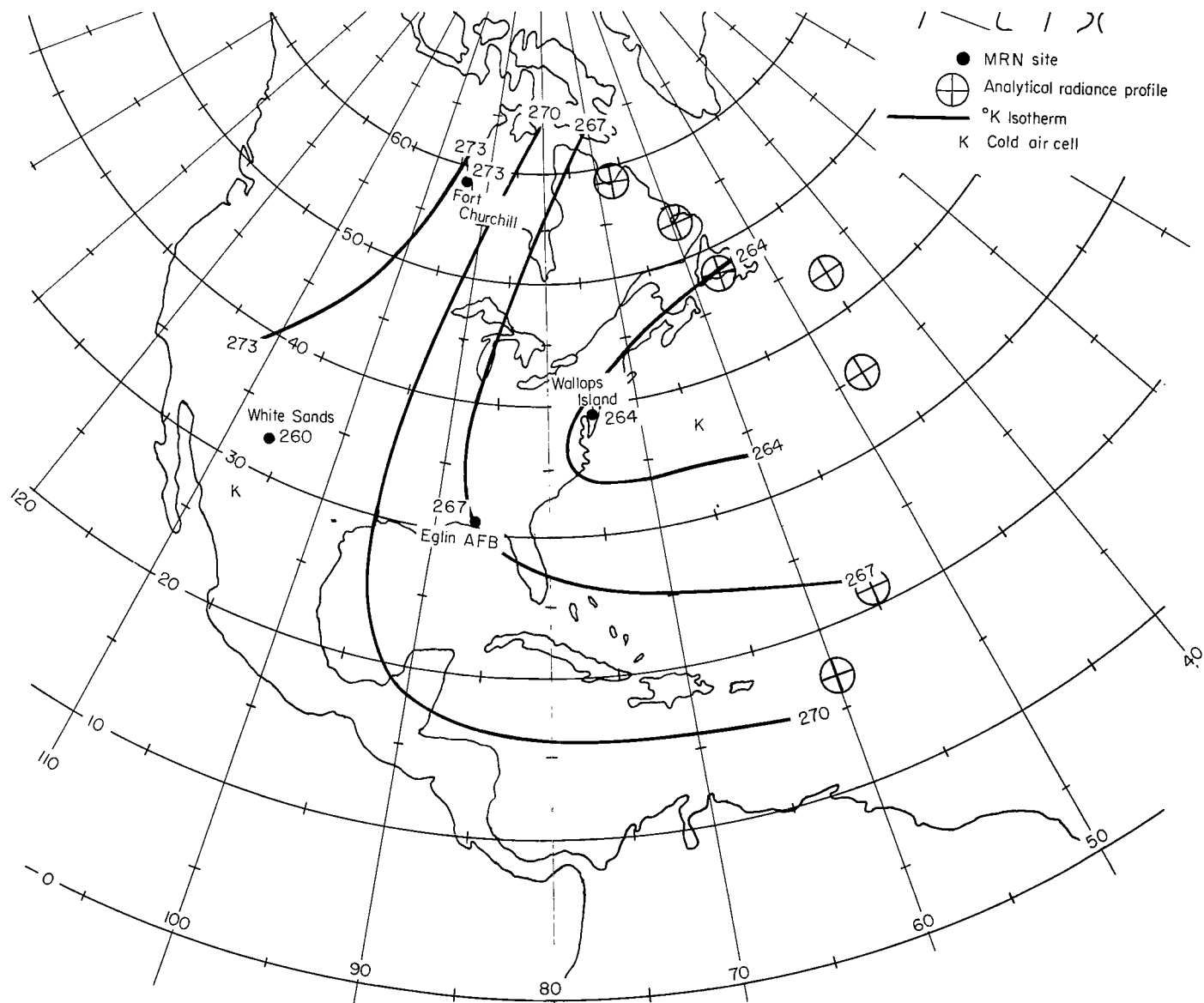
(b)  $h = 35$  km.

Figure 21.- Continued.



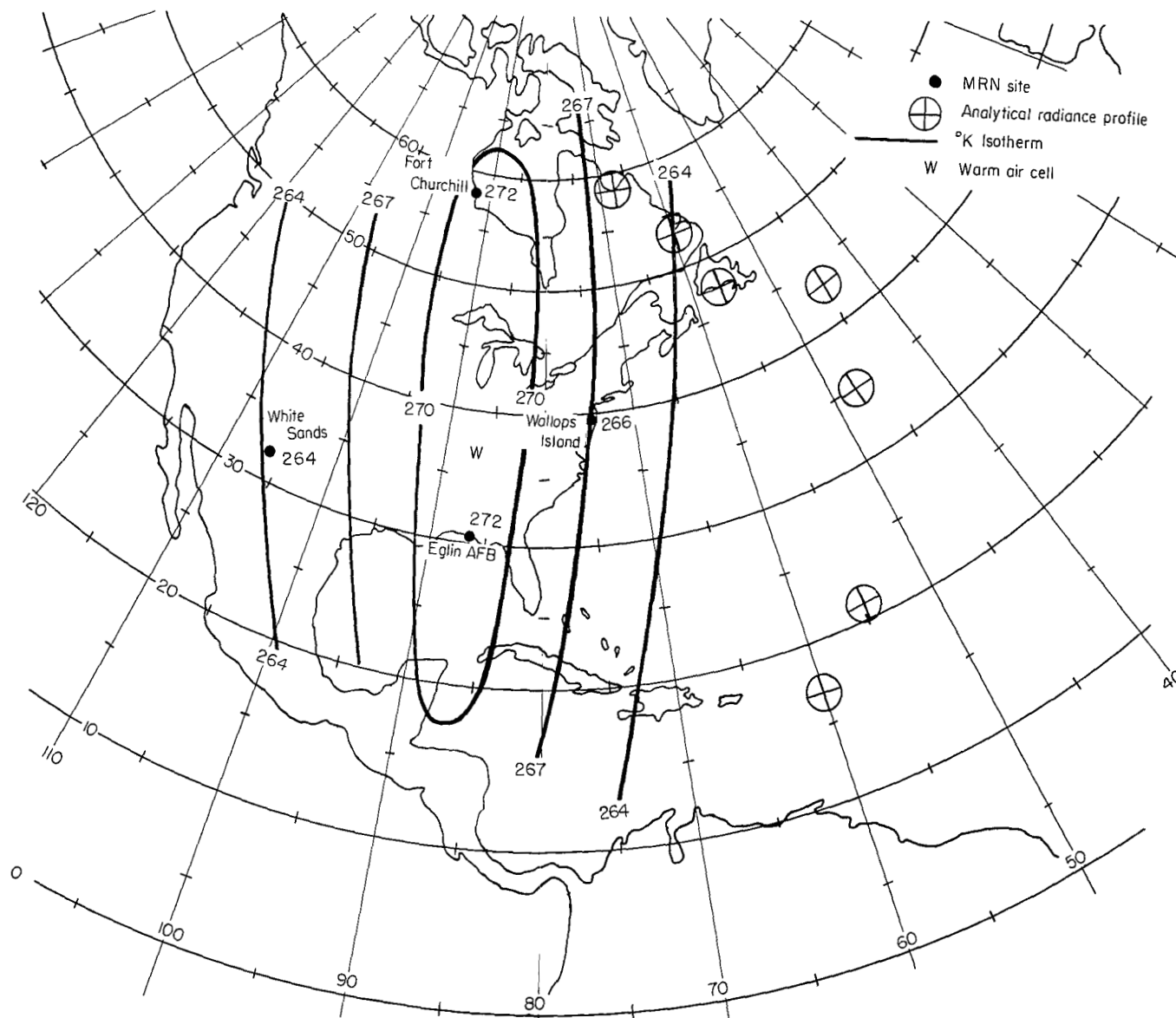
(c)  $h = 40$  km.

Figure 21.- Continued.



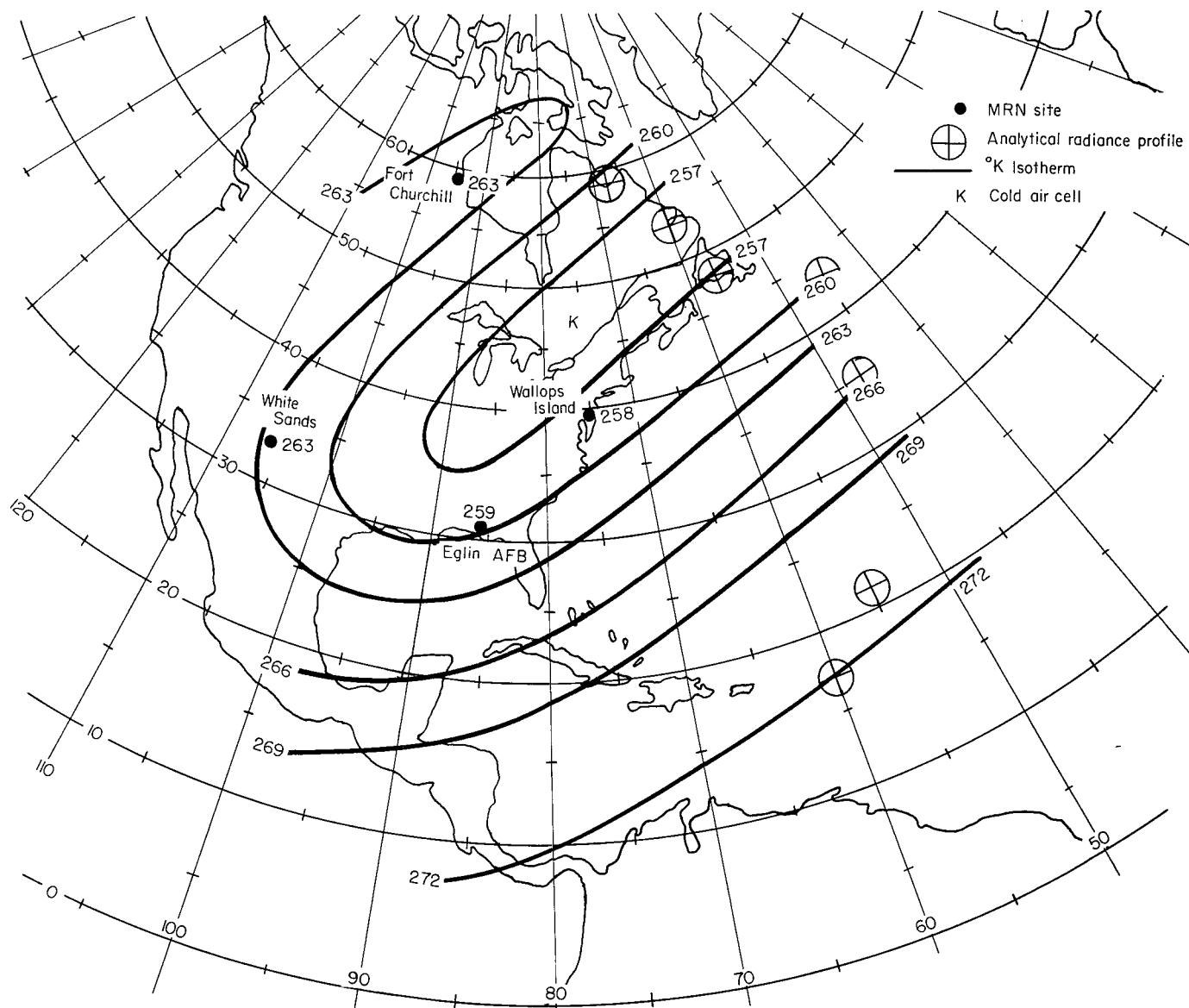
(d)  $h = 45$  km.

Figure 21.- Continued.



(e)  $h = 50$  km.

Figure 21.- Continued.



(f)  $h = 55$  km.

Figure 21.- Concluded.

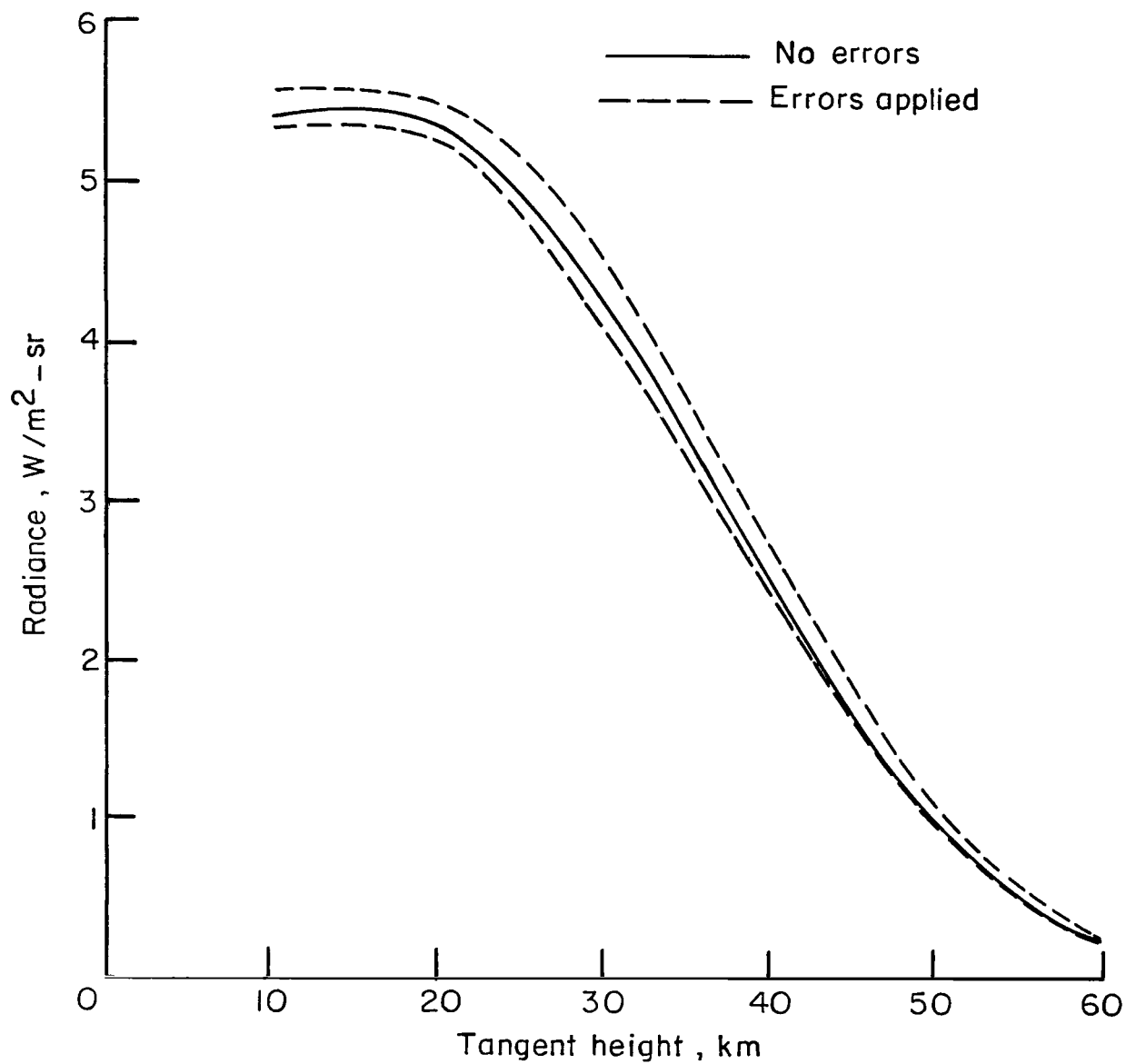


Figure 22.- Error analysis for meteorological data for  $615\text{ cm}^{-1}$  to  $715\text{ cm}^{-1}$  spectral band.

POSTMASTER: If Undeliverable (Section 158  
Postal Manual) Do Not Return

*"The aeronautical and space activities of the United States shall be conducted so as to contribute . . . to the expansion of human knowledge of phenomena in the atmosphere and space. The Administration shall provide for the widest practicable and appropriate dissemination of information concerning its activities and the results thereof."*

—NATIONAL AERONAUTICS AND SPACE ACT OF 1958

## NASA SCIENTIFIC AND TECHNICAL PUBLICATIONS

**TECHNICAL REPORTS:** Scientific and technical information considered important, complete, and a lasting contribution to existing knowledge.

**TECHNICAL NOTES:** Information less broad in scope but nevertheless of importance as a contribution to existing knowledge.

**TECHNICAL MEMORANDUMS:** Information receiving limited distribution because of preliminary data, security classification, or other reasons.

**CONTRACTOR REPORTS:** Scientific and technical information generated under a NASA contract or grant and considered an important contribution to existing knowledge.

**TECHNICAL TRANSLATIONS:** Information published in a foreign language considered to merit NASA distribution in English.

**SPECIAL PUBLICATIONS:** Information derived from or of value to NASA activities. Publications include conference proceedings, monographs, data compilations, handbooks, sourcebooks, and special bibliographies.

**TECHNOLOGY UTILIZATION PUBLICATIONS:** Information on technology used by NASA that may be of particular interest in commercial and other non-aerospace applications. Publications include Tech Briefs, Technology Utilization Reports and Notes, and Technology Surveys.

*Details on the availability of these publications may be obtained from:*

SCIENTIFIC AND TECHNICAL INFORMATION DIVISION  
NATIONAL AERONAUTICS AND SPACE ADMINISTRATION  
Washington, D.C. 20546